

THE EFFECT OF CATALYST ACTIVITY ON  
STABILITY LIMITED PACKED BED REACTORS

by 45

KERRY FRED WILLIAMS

B. S., Kansas State University, 1966

---

A MASTER'S THESIS

submitted in partial fulfillment of the

requirements for the degree

MASTER OF SCIENCE

Department of Chemical Engineering

KANSAS STATE UNIVERSITY  
Manhattan, Kansas

1969

Approved by:

  
Major Professor

2668  
74  
1969  
4538

## TABLE OF CONTENTS

	<u>Page</u>
I. Introduction	1
I.1 Stability Studies	1
I.2 Stability - Reactor Runaway, Multiple Steady-States and Parametric Sensitivity	2
I.3 Catalyst Activity	4
I.4 Catalyst Poisoning	6
I.5 Purpose and Concepts	7
I.6 Typical Assumptions	8
I.7 Runaway Stability Criteria	13
I.7.1 Wilson's Criterion	13
I.7.2 Gee et al. Criterion	13
I.7.3 Hoelscher's Criterion	15
I.7.4 Harriott's Criterion	19
I.7.5 Barkelew's Criterion	21
I.7.6 Froment's Comparison	28
I.7.7 Marek and Hlaváček's Criterion and Comparison	29
I.7.8 Fraser's Comparison	34
I.8 Multiple Steady-State Stability	36
I.9 Parametric Sensitivity	40
I.10 Selection of a Stability Criterion	41
II. The Development of the Study	44
II.1 The Model and Assumptions	44
II.2 Activity Profiles	46
II.3 Equations for Developing the Stability Criterion	47

II.4 Application of the Equations	49
II.5 Example Reactor System	61
III. Uniform Activity Profiles	65
III.1 Results for Uniform Activity Profiles	65
IV. Negative Sloped Activity Profiles	93
IV.1 Results for Negative Sloped Activity Profiles	93
V. Positive Sloped Activity Profiles	113
V.1 Results for Positive Sloped Activity Profiles	113
VI. Discussion of the Results	136
VII. Conclusions	141
VIII. Nomenclature	142
IX. Acknowledgments	146
X. Bibliography	147
XI. Appendix	150
XI.1 Derivation of the Equations for the Modified Stability Criterion	150
XI.2 Equation for Determining the Stability Limited Inlet Temperature and Concentration	156
XI.3 Derivation of the Equations for the Example Reactor System	159
XI.4 Derivation of the Stability Criterion Equations for Linear Catalyst Activity Profiles	166

## LIST OF TABLES

<u>Title</u>	<u>Page</u>
1. Commonly used assumptions in packed tubular reactor analysis	9
2. Kinetic parameter values for Barkelew's stability criterion	25
3. Kinetic and parameter values for the example reactor system	62

## LIST OF FIGURES

<u>Title</u>	<u>Page</u>
1. Hoelscher's stability diagram	18
2. Barkelew's stability envelope	27
3.a. Unique operating points	38
3.b. Multiple operating points	38
4. Activity profiles	48
5. Locus of the maximum dimensionless temperature for $a=1.0$	50
6. Locus of the maximum dimensionless temperature for $a=0.70$	51
7. Locus of the maximum dimensionless temperature for $N/S=2.00$	53
8. Locus of the maximum dimensionless temperature for $N/S=1.00$	54
9. Typical dimensionless temperature and length profiles as a function of the conversion	56
10. Typical dimensionless temperature and length profiles as a function of the conversion	57
11. Stability envelope for $a=0.70$	59
12. Semi-log plot of the stability envelope for $a=0.70$	60
13. Outline of graphical results	66
14. Stability envelope for $a=1.0$	67
15. Stability envelope for $a=0.70$	68
16. Stability envelope for $a=0.30$	69
17. Stability envelope for $a = 0.10$	70
18. Stability envelope for uniform activity profiles	71
19. Critical inlet temperature operating policy for $a = 1.0$	73
20. Critical inlet temperature operating policy for $a = 0.70$	74
21. Critical inlet temperature operating policy for $a = 0.30$	75

<u>Title</u>	<u>Page</u>
22. Critical inlet temperature operating policy for $a = 0.10$	76
23. Effect of activity on the critical inlet temperature for $-\Delta H = 25,000$ cal/mole	77
24. Effect of activity on the critical inlet temperature for $-\Delta H = 50,000$ cal/mole	78
25. Effect of activity on the critical inlet temperature for $-\Delta H = 100,000$ cal/mole	79
26. Semi-log plot of the critical inlet temperature as a function of the activity for $-\Delta H = 50,000$ cal/mole	80
27. Typical temperature and conversion profiles for $-\Delta H = 25,000$ cal/mole	81
28. Typical temperature and conversion profiles for $-\Delta H = 50,000$ cal/mole	82
29. Typical temperature and conversion profiles for $-\Delta H = 100,000$ cal/mole	83
30. Effect of activity on the conversion of $z=L$ for $-\Delta H = 25,000$ cal/mole	85
31. Effect of activity on the conversion at $z=L$ for $-\Delta H = 50,000$ cal/mole	86
32. Effect of activity on the conversion at $z=L$ for $-\Delta H = 100,000$ cal/mole	87
33. Sensitivity of the conversion to graphical error for $-\Delta H = 25,000$ cal/mole	89
34. Sensitivity of the conversion to graphical error for $-\Delta H = 50,000$ cal/mole	90

<u>Title</u>	<u>Page</u>
35. Sensitivity of the conversion to graphical error for $-\Delta H = 100,000 \text{ cal/mole}$	91
36. An example of reactor runaway for $T_{\text{crit}} + 5.0^{\circ}\text{C}$	92
37. Stability envelope for $B = 1.00$	96
38. Stability envelopes for negative sloped activity profiles	97
39. Critical inlet temperature operating policy for $B = 1.00$	98
40. Critical inlet temperature operating policy for $B = 3.00$	99
41. Critical inlet temperature versus $B_{\text{act}}$ and $B_{\text{calc}}$	100
42. Effect of the exit activity condition on the critical inlet temperature for $-\Delta H = 25,000 \text{ cal/mole}$	101
43. Effect of the exit activity condition on the critical inlet , temperature for $-\Delta H = 50,000 \text{ cal/mole}$	103
44. Effect of the exit activity condition on the critical inlet temperature for $-\Delta H = 100,000 \text{ cal/mole}$	104
45. Typical temperature and conversion profiles for an exit activity of 0.90	105
46. Typical temperature and conversion profiles for an exit activity of 0.50	106
47. Typical temperature and conversion profiles for an exit activity of 0.10	107
48. Effect of the exit activity condition on the conversion at $z=L$ for $-\Delta H = 25,000 \text{ cal/mole}$	108
49. Effect of the exit activity condition on the conversion at $z=L$ for $-\Delta H = 50,000 \text{ cal/mole}$	109
50. Effect of the exit activity condition on the conversion at $z=L$ for $-\Delta H = 100,000 \text{ cal/mole}$ ,	110

<u>Title</u>	<u>Page</u>
51. An example of reactor runaway for $T_{O_{crit}} + 5.0^{\circ}\text{C}$	112
52. Stability envelope for $B = -2.00$ and $a_o = 0.30$	115
53. Stability envelope for $B = -4.00$ and $a_o = 0.30$	116
54. $\zeta$ at the point of $\tau_{max}$ for $B = -2.00$ and $a_o = 0.30$	117
55. Stability envelope for positive sloped activity profiles with $a_o = 0.30$	119
56. Critical inlet temperature operating policy for $B = -2.00$ and $a_o = 0.30$	120
57. Critical inlet temperature operating policy for $B = -4.00$ and $a_o = 0.30$	122
58. Critical inlet temperature versus $B_{act}$ and $B_{calc}$ for $a_o = 0.30$	123
59. Effect of the inlet activity condition on the critical inlet temperature for $-\Delta H = 25,000$ cal/mole	124
60. Effect of the inlet activity condition on the critical inlet temperature for $-\Delta H = 50,000$ cal/mole	125
61. Effect of the inlet activity condition on the critical inlet temperature for $-\Delta H = 100,000$ cal/mole	126
62. Typical temperature and conversion profiles for $a_o = 0.30$	128
63. Typical temperature and conversion profiles for $a_o = 0.70$	129
64. Typical temperature and conversion profiles for $a_o = 0.10$	130
65. An example of reactor runaway for $T_{O_{crit}} + 10.0^{\circ}\text{C}$	132
66. Effect of the inlet activity condition on the conversion at $z=L$ for $-\Delta H = 25,000$ cal/mole	133
67. Effect of the inlet activity condition on the conversion at $z=L$ for $-\Delta H = 50,000$ cal/mole	134



<u>Title</u>	<u>Page</u>
68. Effect of the inlet activity condition on the conversion at $z=L$ for $-\Delta H = 100,000$ cal/mole	135
69. Effect of the activity profile shape on the operating policy	137
70. Computer flow sheet for calculating the stability envelopes	153
71. Computer flow sheet for calculating the critical values of $T_0$ and $x_{A_0}$	157
72. Computer flow sheet for the example reactor system	163
73. Computer flow sheet for determining the value of the parameter B	169

## I. Introduction

The investigations completed in this thesis are concerned with packed tubular reactors having catalyst beds of reduced activity operating near the stability limit imposed by reactor runaway. This section of the thesis contains the basic definitions and explanations of stability, catalyst activity and poisoning and how they are associated with this work. It also includes the purpose of the thesis, a description of many of the assumptions used in modeling packed tubular reactors, and a review of the criteria of stability developed during the past twenty-five years. The last part of the section presents the requirements which were felt necessary for an acceptable stability criterion and finally the choice of one of the available stability criteria for use in the investigation.

### I.1 Stability Studies

The study of operational stability and control of packed tubular reactors has attracted an increasing number of researchers in recent years. With the advent of modern computing techniques and numerical methods many new approaches to the basic problems of stability and control have been developed. Because the equations describing tubular reactors are nonlinear and coupled, analytical solutions are generally not possible and only with the use of modern computers has it been possible to expand the investigation of operational stability and control over a large range of operating parameters and conditions.

Industrial competition has greatly increased the economic importance of operating reactors at maximum production levels. This often entails operation in regimes where the reactor is extremely sensitive to any change of parameters or operating conditions, that is, near the limit of stable

operation. The economic factors coupled with the availability of computers has generated considerable interest in the area of stability.

## I.2 Stability - Reactor Runaway, Multiple Steady-States, and Parametric Sensitivity

There are three broad classifications under which stability is normally studied, reactor runaway, multiple steady-states, and parametric sensitivity. These classifications are not precise and there is considerable overlap, but they can be looked upon as a means to help clarify a portion of the confusion associated with what reactor stability or instability really means.

Reactor runaway is generally connected with exothermic reactions occurring in tubular heat exchange type vessels containing a catalyst. In such reactors the axial temperature profile generally rises from the inlet of the reactor, goes through a point of maximum temperature, and then decreases until the exit is reached. The point at which the temperature profile reaches its maximum is commonly called the hot-spot temperature. Considerable importance is centered around the hot-spot temperature, its magnitude, its axial position in the reactor, and, most closely related to stability, its response to fluctuations in the operating conditions. Reactor runaway is said to occur when the fluctuations cause the hot-spot temperature to rise out of control. The excessively high temperatures may cause severe damage to the catalyst and reactor and in extreme cases result in explosions. This type of stability then is characterized by the complete loss of temperature control within the reactor system resulting in excessively high temperatures.

The existence of multiple steady-states was first brought to the attention of chemical engineers by Van Heerden (3) who showed that under given conditions of operation a stirred-tank reactor may possess three possible

steady-state operating points. Two of these steady-state operating points are stable while the third is unstable, i.e., small fluctuations of the operating variables cause the reactor to switch to one or the other of the two stable steady-state operations. This type of stability investigation has since been extended to packed tubular reactors, primarily by Amundson et al. (15, 16, 17, 18, 19), where it has been shown that under certain conditions depending on the initial temperature conditions of the catalyst bed there exist three steady-state operations. Again two of these are stable and the third is unstable in the same sense as described above. To characterize this type of stability, one is not necessarily concerned with excessive temperatures which may damage the catalyst and reactor, but with the temperature regions in which the reactor must be operated in order to achieve the desired stable steady-state operation.

Parametric sensitivity, as a third broad classification of stability, is very closely connected with both of the previously described stability classifications, but at the same time encompasses a great deal of stability considerations that are not contained in the other two. In any reactor operation it is desirable to know what the effects of changes in the operating variables and parameters will be. The effect of the reactor diameter, catalyst particle diameter, wall temperature, flow rate, heat transfer coefficient, etc., all determine the final product leaving the reactor and it is essential not only from the point of view of reactor runaway or the existence of multiple steady-states that these effects be clearly understood so that the reactor can be operated in an efficient and economical manner. These effects clearly must be considered a part of any stability analysis and classification.

### I.3 Catalyst Activity

Catalyst activity is a common term, the meaning of which is often misinterpreted. It is used in the literature with several different meanings (9, 22, 26, 30, 31, 32, 33, 34). It is, therefore, advantageous to give a brief description of catalyst activity and define what aspect of catalyst activity is being considered in the investigation which follows.

The basic definition of catalyst activity can be given in terms of the rate of the catalytic reaction in one of two ways. It can be described as the rate of reaction in moles per unit time per unit area of catalyst surface (30). It can also be defined as the amount of product produced per unit time per unit mass of catalyst (26). The two descriptions above are related through the surface area and the mass of the catalyst so that they both describe the same phenomena, but with a slightly different dependence.

Generally the activity of a catalyst will not be directly proportional to the surface area as some interior pore surface area may be inaccessible for reaction. Thus when comparing different catalysts for a given reaction, their activities cannot be compared on the basis of their surface areas alone. However, when comparing the activities of different batches of the same catalyst, as when checking the extent of poisoning, the surface area can be used to give an effective comparison.

Another method which can be employed in comparing catalyst activities is the use of catalyst-activity factors (33). These factors can be used to account for catalyst deactivation due to poisoning or sintering and also for comparing the activities of different catalysts. The catalyst-activity factor is a constant which appears in the rate equation and is a multiplier in any integrated form of the rate equation. In order to compare the activities of two sets of catalysts for the same reaction it is necessary to specify

one as an arbitrary standard with a catalyst-activity factor of 1.0. Then for the same degree of conversion for both, the space velocities required to achieve the conversion must be different. The comparison of the activities is then given by the ratio of the activity factors:

$$\frac{a_I}{a_{II}} = \left[ \frac{(W/F)_{II}}{(W/F)_I} \right]_{\text{conv.}}$$

where

$W/F$  is the space velocity

$W$  is the mass of catalyst in the reactor

$F$  is the feed rate in moles/unit time

$a$  is the catalyst activity factor

A third method (33) of comparing activities consists of comparing the ratio of the conversions obtained using a standardized testing condition. Again it is necessary to specify a catalyst as a standard against which others may be compared.

The description of catalyst activity given above is necessarily brief and by no means does it include all the descriptions used in the literature. However, it is thought that the descriptions given are the ones most often used.

In the investigations of this thesis the activity and change of activity of the catalyst in the packed bed will be described by a relative activity which can be defined as follows:

$$\text{relative activity, } a = \frac{\left( \begin{array}{l} \text{rate of reaction per unit volume} \\ \text{of catalyst} \end{array} \right)}{\left( \begin{array}{l} \text{rate of reaction per unit volume} \\ \text{of catalyst when the catalyst} \\ \text{has experienced no deactivation} \\ \text{or modification} \end{array} \right)}.$$

The reaction rates in the above ratio must be determined under identical operating conditions, i.e., temperature, etc. Using the relative activity provides a simple way of accounting for catalyst deactivation or for the addition of inert particles in place of a portion of the catalyst particles. This description corresponds to the third method listed above and its general form is commonly used in the literature.

#### I.4 Catalyst Poisoning

Commercial catalysts experience a decline in activity during reactor operation because of two principal causes, poisoning and sintering. Poisoning is the more common of these two and will be briefly discussed here.

A poison can be defined as a substance, either in the reactants stream or produced by a side reaction, which causes a decrease of the catalyst activity (26). Classifications of specific poisons are numerous in the literature (26, 30, 31). Carbon is a common fouling agent and has been frequently investigated because of its occurrence in commercially important hydrocarbon reactions. Poisons such as this are classified as deposited poisons. Sulfur is another frequently occurring poison. Unlike carbon, this poison is chemisorbed on metallic catalysts and hence is called a chemisorbed poison. Other typical poisons in this class include zinc, mercury, lead and iron oxides.

Poisons may also be classified according to their influence on the selectivity of the catalyst. The heavy metals are frequently classified in this manner.

As the complete phenomena of catalyst activity and poisoning is not fully understood, the literature in this area contains a number of models which have been used to approximate the poisoning phenomena. There are

two basic approaches. In one the catalyst is assumed to be poisoned as a function only of the operating time (36, 37). This model approximates reactors in which poisoning occurs uniformly throughout the catalyst bed. The second approach considers the rate of formation of the fouling compounds as a side reaction in conjunction with primary product forming reaction (34). In this approach the catalyst fouling is not uniform throughout the catalyst bed and an activity profile will exist. Predicted conversion, selectivity, and temperature distributions may thus be dramatically different from those based on the first approach.

### 1.5 Purpose and Concepts

This thesis, whose subject matter lies within the framework of a reactor runaway stability analysis, has a twofold purpose. First, it makes it possible to formulate for existing reactors a general procedure for determining an operating policy near the stability limit for the reactant inlet temperature when the catalyst is experiencing poisoning. Second, the investigation is the starting point for a future study to increase the level of conversion, while operating the reactor near the stability limit, by developing an optimum catalyst activity profile for the catalyst bed.

When the catalyst bed of a reactor experiences deactivation, the reactant inlet temperature must be raised to maintain the same level of conversion (20, 22). The permissible temperature increase is limited, however, by three considerations. In some cases the catalyst will experience damage by sintering if the temperature in the reactor is increased excessively. In other cases, an increased operation temperature may cause a detrimental effect in the selectivity of the catalyst. The third consideration is that an increase of the inlet temperature may cause the reactor to run away. This thesis is



concerned with reactors limited by stability considerations.

Froment (2) suggested that the only way to increase conversion and yields from packed tubular reactors operating near the stability limit was to realize a different type of temperature profile than normally associated with heat-exchange reactors. One way of doing this is to vary the catalyst activity. If, while preserving reactor stability, a decrease of catalyst activity allows an increase of the inlet temperature which more than offsets the activity decrease, an increased level of conversion is realized. It is felt by this author that this possibility exists. It is then one of the purposes of this thesis to obtain the basic information necessary for developing this type of optimum activity profile.

As a more immediate result, however, the investigations supplied a procedure for determining an operating policy for the inlet temperature under the conditions discussed above.

Three types of activity profiles were investigated; uniform profiles, positively sloped profiles, and negatively sloped profiles. These types roughly approximate uniform poisoning, poisoning by a parallel mechanism, and poisoning by a consecutive mechanism. In addition to approximating the possible poisoning mechanisms, they were the simplest geometrical forms available which would not unduly complicate the investigation.

## I.6 Typical Assumptions

There are a number of assumptions generally made in order to simplify the mathematical description of reactor operation. The most common assumptions are listed in Table 1 and will be discussed in a general nature.

The first four assumptions are generally made in any investigation of a packed tubular reactor. Homogeneity of the catalyst bed is an inherent

Table 1. Commonly used assumptions in packed tubular reactor analysis

1. Homogeneity of the catalyst bed.
2. Fluid properties unaffected by temperature and reaction.
3. Negligible axial heat- and mass-transfer by conduction and diffusion.
4. Negligible heat transfer by radiation.
5. Flat velocity profile.
6. A specific heat generation form.
7. The rate of heat generation is a function of temperature, reactant concentration, catalyst activity, and for certain cases of the time of contact.
8. The temperature dependence of the rate coefficient can be linearized.
9. The fluid temperature at any cross section follows the solid temperature with a constant difference between them.
10. The fluid temperature and catalyst temperature are identical.
11. The temperature at all points in the catalyst are constant with respect to time.
12. There are no radial concentration gradients in the reactor.
13. There is no radial temperature profile, the resistance to heat transfer through the bed in the radial direction is small compared with the resistance at the tube wall.
14. There is no pressure drop through the reactor.
15. Idealized reactor operation--adiabatic, isothermal, constant wall temperature, constant heat flux through reactor wall, etc.

assumption, its validity coming under question only when the catalyst particle diameter is very large as compared with the reactor diameter (9, 23). The use of average fluid properties is an assumption common to all engineering processes. Axial heat and mass transfer is normally neglected as their effect in industrial operation is small and only at low flow rates of material through the reactor do they contribute any sizable effect (2, 23, 26). The heat transfer by radiation is also normally neglected although at high temperatures and with large catalyst particles this form of heat transfer should be included in the investigation (9, 27, 28, 29). The influence of velocity gradients in packed tubular reactors is considered unimportant by Denbigh (24) thus suggesting the use of the assumption of a flat velocity profile without causing any serious distortion of results of an investigation. Beek (23), however, points out that radial velocity gradients are present, but that more experimental work in this area needs to be done.

Assumption six is sometimes used in order to by-pass the necessity of using a reaction rate expression and thus eliminating the need for a mass balance equation. The use of this assumption is limited, however, and the results obtained will generally not be representative of a great many reaction situations (1, 5).

Assumption seven is generally used in place of the previous assumption. Using a heat generation function of this form is a much more realistic approach. It uses the actual reaction rate expression in conjunction with material and energy balances to achieve the rate of heat generation. Any dependence on catalyst activity can be included in the reaction rate expression in a number of suitable forms (2, 4, 9, 24, 34). The objection to using this form appears in the nonlinear coupling of the material and energy

balances which results. The following assumption overcomes a part of this objection.

Assumption eight is similar to seven except that the temperature dependence as expressed in the Arrhenius equation is replaced by a linearized expression. Froment (2) presented a comparison of the two forms for a single case with good agreement for low temperature values. The use of this assumption should be considered separately in each individual case with the operating conditions of the reactor determining its usefulness.

The next two assumptions, nine and ten, are the commonly used simplifications in many situations. For a transient analysis of a packed reactor neither of the two generally represent the actual phenomena which occurs, and the effect of mass and heat transfer rates may play an important part in the transient behavior of the reactor. However, their use does greatly simplify the analysis by reducing the number of equations needed to describe the reactor's operation. The utility of results from an analysis using such an assumption is necessarily limited to specific cases (1, 17, 18, 19). In a steady-state analysis, however, the mass and heat-transfer rates remain constant at any axial position and the validity of the results in the above sense are not dependent on the use of the assumption.

Closely related to assumptions nine and ten is the assumption of no temperature gradients in the catalyst particles. Denbigh (24) and several other authors have presented in considerable detail discussions concerning the existence of such temperature gradients and their effect on the reaction taking place.

Assumptions 12 and 13 are often used in order that an investigator may work with a one-dimensional model. There is no justification for assuming

the absence of a temperature gradient in the radial direction other than the simplicity it allows. In using such assumptions average temperatures and concentrations result from the investigation and no information can be obtained concerning the extreme temperatures which are known to exist at the axis of the reactor (1, 2, 5, 23, 24). In many situations, however, the average temperature and concentration profiles which result represent a good approximation to the more valid two-dimensional results obtained by not making such assumptions (2). The purpose and accuracy required of the results and the effort which must be expended to obtain them will normally determine whether or not these two assumptions are made.

Assumption 14 is that the pressure over the reactor's length remains constant. This assumption is generally used in one-dimensional models although in actual fact the pressure in a packed bed reactor may vary considerably. Even so, the pressure drop often may not significantly affect the kinetic results. Sufficient work in this area has been done so that methods of predicting the pressure drop are readily available (23, 24).

The final assumption in Table 1 concerns the various types of idealized operations of a reactor. These types of operation are generally not the actual operating conditions which are incurred, but many times may be closely approximated.

Table 1 is certainly not a complete list of the assumptions that are used in a reactor's analysis, but it does include those assumptions most often made. As has been expounded upon by a great many authors, the use of any or a number of these assumptions is entirely dependent upon the purpose of the analysis and the time and resources available for the analysis, and the results obtained must be viewed with consideration of the assumptions made.

## I.7 Runaway Stability Criteria

There exist at the present time a number of stability criteria that have been developed over the period of the last 25 years which fall under the three categories of stability discussed. Some of these criteria will be considered individually with those pertaining to reactor runaway being discussed first.

### I.7.1 Wilson's Criterion

One of the first to put forth a stability criterion was Wilson (9). Using a steady-state analysis, he assumed there was no resistance to heat or mass transfer in the radial direction, no axial transfer of heat and mass other than by bulk flow, no radiation effects, and the catalyst particle temperature was the same as that of the fluid temperature. The reaction rate was assumed to be of the following general form:

$$- \frac{dc}{dt} = K_a f(c) \cdot F(T) \quad 1.1$$

where the reaction rate can be considered to be dependent only upon the concentration of one reactant and the temperature. The temperature dependence can be expressed by the well known Arrhenius form. The corresponding heat balance over a differential volume of the reactor is:

$$- \frac{dc}{dt} = \frac{4U}{HD\phi} (T - T_o) + \frac{VS}{H} \cdot \frac{dT}{dx} \quad 1.2$$

where

$c$  = reactant concentration

$U$  = overall heat transfer coefficient of the wall

$H$  = heat of reaction

$D$  = reactor diameter

$\phi$  = void fraction

$T$  = fluid temperature

$T_o$  = coolant temperature

$V$  = linear velocity of fluid

$t$  = time

$x$  = axial direction

$a$  = catalyst activity

$S$  = volume heat capacity

$A$  = activation energy/gas law constant

$K$  = reaction velocity constant

By substituting equation 1.1 into equation 1.2, the equation describing the reactor becomes:

$$Kaf(c)e^{-A/T} = \frac{4U}{HD\phi} (T - T_o) + \frac{VS}{H} \cdot \frac{dT}{dx} \quad 1.3$$

where the temperature dependence of the reaction rate is the familiar Arrhenius expression. Differentiation of equation 1.3 with respect to  $c$  and resubstituting the result back into equation 1.3 gives:

$$\frac{dT}{dc} = \frac{T^2 \left( VS \frac{d}{dc} \left( \frac{dT}{dx} \right) - Kae^{-A/T} f'(c) \right)}{\frac{4U}{HD\phi} (A(T - T_o) - T^2) + \frac{AVS}{H} \frac{dT}{dx}} \quad 1.4$$

Wilson used this equation to establish his criterion by noting that when the denominator approaches zero the temperature in the reactor is extremely sensitive to small fluctuations of  $c$ . The criterion for instability was then:

$$T^2 - A(T - T_o) = \frac{AVSD\phi}{4U} \frac{dT}{dx} \quad 1.5$$

or in the usual form presented in the literature,

$$\frac{T - T_o}{T} > \frac{R'T}{E} \quad 1.6$$

where the temperatures are expressed in absolute degrees and their position of occurrence is at the hot-spot of the reactor, that is, the point where  $\frac{dT}{dx} = 0$ . From the inequality 1.6 it is then possible to determine an upper temperature limit for the hot-spot temperature in the reactor. It is of interest to note that Wilson developed his criterion entirely from an analysis of the equation used to describe the reactor. No solution for the temperature and concentration profiles in the reactor was necessary.

### I.7.2 Gee et al. Criterion

With the advent of digital computers another approach to establishing stability criteria became available. Gee et al. (13) used a steady-state one-dimensional reactor model to simulate an actual reactor. By repeatedly solving the model's equations for a large range of parameter values, they were able to determine the regions of instability for the particular reactor model and the values of the parameters at which the reactor would become unstable. In this way, they were able to considerably improve the actual reactor's operation while establishing a criterion for stable operation.

### I.7.3 Hoelscher's Criterion

Hoelscher (5) attempted to establish a general criterion based on a time-dependent analysis of a two-dimensional energy balance equation. By assuming a form for the heat generation function,  $\beta_1(\tau)$ , that is the energy liberated by chemical reaction, he was able to eliminate the coupling of the mass and energy equations which normally exist and was able to describe the reactor by the following equation.

$$-\frac{\partial \tau}{\partial \theta} + u \frac{\partial \tau}{\partial x} = \frac{K}{R^2} \left( \frac{\partial^2 \tau}{\partial \rho^2} + \frac{1}{\rho} \frac{\partial \tau}{\partial \rho} \right) + \beta_1(\tau) \quad 1.7$$



In this equation

$\tau$  = dimensionless temperature

$\theta$  = time

$u$  = linear velocity

$x$  = axial distance

$K$  = thermal diffusivity

$R$  = reactor radius

$\rho$  = dimensionless radial position

$A$  = cross sectional area

In addition to the assumption of a form for the heat generation function, it was also assumed the gas phase temperature and solid surface temperature were equal at all times, heat transfer in the axial direction by conduction could be neglected, and that the temperature profiles along the reactor were similar and varied only by a constant scale factor. The temperature profile was chosen to be of the form:

$$\tau(\theta, x, \rho) = \tau_m(\theta, x) \cdot f(\rho) \quad 1.8$$

By noting that

$$\frac{\int_A f(\rho) dA}{A} = \gamma = \text{constant} \quad 1.9$$

Hoelscher was able to integrate equation 1.7 and arrive at

$$\frac{\partial \tau_m}{\partial \theta} + u \frac{\partial \tau_m}{\partial x} = \frac{K \tau_m \lambda}{\gamma R^2} + \frac{\int_A \beta_1(\tau) dA}{A} \quad 1.10$$

where

$$\frac{\int_A \beta_1(\tau) dA}{A} = h_m \quad 1.11$$

is defined to be the instability integral. The subscript  $m$  refers to the axial temperature.

Equation 1.10 defines a time-temperature-axial position surface in space. To complete the analytical solution it was then necessary to establish a form for both the temperature profile and the heat generation function. By assuming the reactor to be adiabatic and

$$\tau = \frac{T - T_w}{T_w} = \tau_m (\theta, x) f(\rho) \quad 1.12$$

with

$$f(\rho) = A + B\rho + C\rho^2 + D\rho^3 \quad 1.13$$

and using the boundary conditions at the reactor's axis and wall, the temperature profile was found to be:

$$\tau = \tau_m (1 - 3\rho^2 + 2\rho^3) \quad 1.14$$

A heat generation function was then chosen as:

$$\beta(T) = \alpha e^{-E/R'T} \quad 1.15a$$

or

$$\beta(\tau) = \frac{\alpha}{T_w} \exp \left[ -\frac{E}{R'T_w} \cdot \frac{1}{\tau+1} \right] \quad 1.15b$$

This function corresponds to a zeroth-order reaction. An exact solution of the instability integral, equation 1.11, was not possible but an approximate solution was obtained. A time-temperature relationship resulting from equation 1.7 is given by:

$$\theta = \int_{\tau_m}^{\tau_m} \frac{d\tau_m}{h(\tau_m)} \quad 1.16$$

Using the approximate solution of the instability integral in equation 1.16 another approximate solution for the  $\theta - \tau_m$  relationship was obtained. Typical results for this relationship are shown in Figure 1 for three sets of parameters. The stability criterion then becomes: if  $\alpha$  is large the

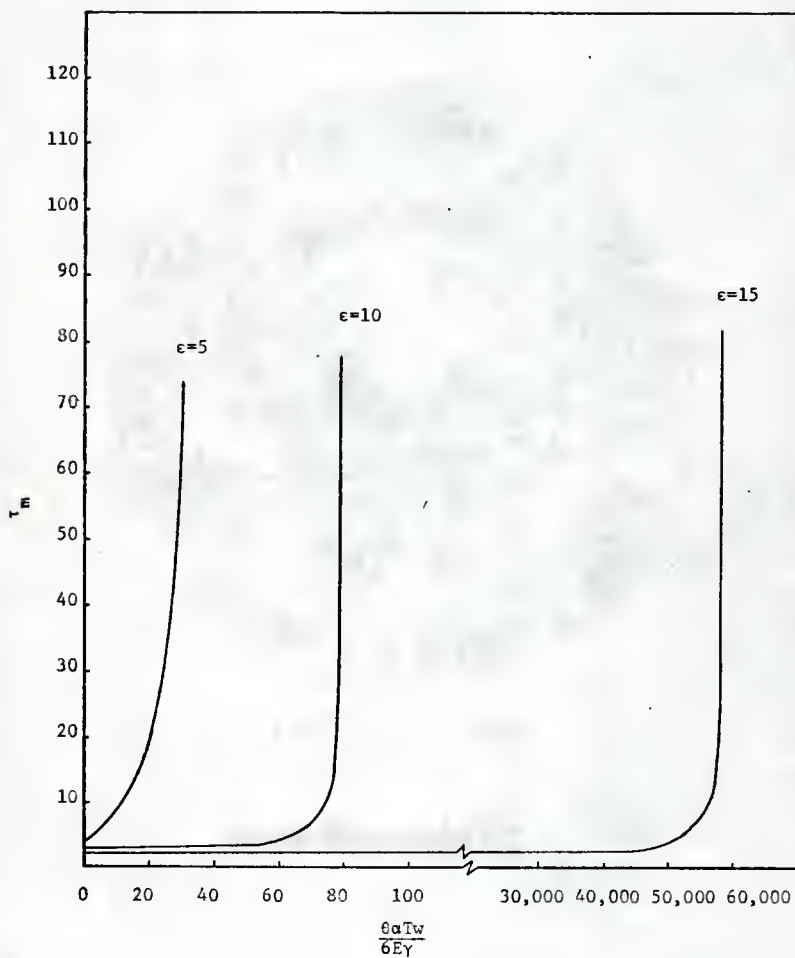


Fig. 1. Hoelscher's stability diagram

operation is likely to be unstable, that is, the time required to reach undesirable temperatures is short, if  $\alpha$  is small then the reactor will likely be stable, that is, considerable operation time is required before undesirable temperatures are incurred.

The general nature of Hoelscher's criterion makes it possible to consider more complex heat generation functions and reactor wall conditions, but the solutions for such cases become considerably more difficult. The usefulness of this criteria is very limited. It has little significance beyond zero-order reactions because of its inability to give either quantitative or qualitative information concerning reactor stability. Even in the case of zero-order reactions the heat generation function does not adequately take into account the reactant concentration. This is apparent in the infinite increase of heat generation even though the reactant concentration may have become zero.

#### 1.7.4 Harriott's Criterion

Another method which can be used to predict when a reactor will be stable was presented by Harriott (14). This method is based on a two-dimensional steady-state model for the reactor which assumes axial heat conduction can be neglected and the temperature difference between the fluid and catalyst particles is small and thus has no effect on the reaction. The reactor is also assumed to operate with a constant wall temperature,  $T_w$ .

For given kinetic and heat-transfer data the suggested method can be applied to determine whether a reactor with a specified diameter can be operated without the danger of reactor runaway. The analysis is focused at the axial hot-spot in the reactor. An additional simplifying assumption can be made in cases where radial temperature gradients are not extremely large.

For such cases it is possible to represent the reaction rate at the hot-spot as a function only of the temperature at the axis of the reactor. With this assumption, Harriott made a heat balance on an annular element where the hot-spot temperature occurs. The heat balance is given by

$$k_e \left[ \frac{d^2 T}{dr^2} + \frac{1}{r} \left( \frac{dT}{dr} \right) \right] + \alpha H = 0 \quad 1.17$$

where

$r$  = radius

$R$  = radius of the reactor

$k_e$  = effective thermal conductivity

$H$  = heat of reaction

$T$  = temperature of fluid

$\alpha$  = reaction rate at the axial hot-spot temperature

Integration of equation 1.17 over the reactor radius then gives

$$R^2 = \frac{4k_e}{\alpha H} (T_c - T_r) \quad 1.18$$

where

$T_c$  = axial hot-spot temperature

$T_r$  = fluid temperature at the wall

A heat balance at the wall then results in the following equation

$$\pi R^2 \alpha H = 2\pi R h_w (T_r - T_w) \quad 1.19$$

where

$T_w$  = wall temperature of the reactor

$h_w$  = wall heat transfer coefficient

If in equation 1.18 the temperature difference  $(T_c - T_r)$  is small then the use of  $\alpha$  as a function only of the axial hot-spot temperature is justified and reasonable results can be expected from the following criterion of

stability. Equations 1.18 and 1.19 can be used to eliminate  $T_r$  which is unknown and to calculate a value for  $T_w$ . To check the stability of the reactor the above process is repeated assuming a slightly higher value for  $T_c$  and calculating a new value of  $T_w$ . The reactor will then be stable if the new wall temperature is higher than the previous value calculated. Physically, this means that the rate of heat removal is greater than the rate of heat generation and the reactor will thus be stable to small fluctuations in the operating conditions.

Some further mention of the expression used for the reaction rate is necessary. Obviously, sufficient kinetic data must be available to account for the temperature and concentration dependence of the reaction before any stability analysis can be made.

Assuming this is available, the form assumed for  $\alpha$  will be dependent upon the physical situation existing in the reactor. If  $(T_c - T_r)$  is large the assumption of  $\alpha$  as a constant is not justified and some other form must be used to account for the temperature gradient in the radial direction. However, as pointed out by Harriott, because of the simplicity injected into the calculations by assuming  $\alpha$  a constant it is always the form to assume first. Even with large  $(T_c - T_r)$  differences it may supply enough information to predict stability.

#### 1.7.5 Barkelew's Criterion

Probably the most general method available for predicting packed bed reactor runaway stability was developed by Barkelew (1). Using a one-dimensional model Barkelew made use of a linearized Arrhenius expression in order to develop dimensionless parameters which could describe steady state reactor stability in terms of the dimensionless parameters rather than

definite values of the variables used in forming the parameters. In this way a general stability criterion resulted which could be used for designing stable reactors.

Barkelew's analysis includes the following assumptions.

1. Transport of heat and mass in the axial direction other than by bulk flow can be neglected.
2. Resistance to heat transfer in the radial direction is insignificant compared to the resistance at the tube wall.
3. The reaction rate is a unique function of the fluid properties.
4. The dependence of the reaction rate on composition is expressible in terms of the concentration of a single component.
5. The temperature of the fluid and the catalyst are the same.

The fourth assumption restricts the analysis to single reactions, a point which definitely limits the criterion's use but does not effect its validity for the general case of single reactions.

The steady state equations for the reactor are:

$$(-\Delta H)R - AU(T - T_w) - C_p G \frac{dT}{dz} = 0 \quad 1.20$$

$$R + G \frac{dc}{dz} = 0 \quad 1.21$$

where the wall temperature is assumed constant over the reactor's length. The nomenclature in this work corresponds to that found in the appendix of this thesis. For convenience the reaction rate expression was represented by

$$R = kf(c)e^{\gamma T} \quad 1.22$$

with

$$\gamma = \frac{E}{R'T_w^2} \quad 1.23$$

$$k = k_o e^{-2\gamma T_w} \quad 1.24$$

instead of the usual Arrhenius form

$$R = k_o f(c) e^{-E/R'T} \quad 1.25$$

Barkelew suggests that the form given by equation 1.22 can be fitted to the reaction-rate data nearly as well as the Arrhenius form. As will be seen, the use of equation 1.22 greatly simplified later analysis and its use does not severely limit or alter the stability analysis.

The following transformations can then be used to make equations 1.20 and 1.21 dimensionless.

$$C = C_o (1-X) \quad 1.26$$

$$R = x_o k_o e^{\gamma T_w} (1-X) g(X) e^{\tau} \quad 1.27$$

$$T = T_w + \frac{\tau}{\gamma} \quad 1.28$$

$$z = \frac{G}{k_o e^{\gamma T_w}} \zeta \quad 1.29$$

$$N = \frac{2U}{r C_p k_o e^{\gamma T_w}} \quad 1.30$$

$$S = \frac{(-\Delta H) x_o \gamma}{C_p} \quad 1.31$$

where

$$A = \frac{2}{r} \quad 1.32$$

$$R = x_o k_o e^{\gamma T_w} \text{ for } X = 0, T = T_w \quad 1.33$$



The jacket temperature,  $T_w$ , has been assumed to be constant in this work. The function  $g(X)$  was introduced to allow for reaction-rates other than first-order. Barkelew considers two forms for  $g(X)$  as follows:

$$g(X) = (1+\alpha X) \quad 1.34a$$

$$g(X) = (1+\beta X)^{-1} \quad 1.34b$$

where  $\alpha=\beta=0$  for first-order reactions. The following table presents the various values of  $\alpha$  and  $\beta$ .

Equations 1.20 and 1.21 in dimensionless form are:

$$\frac{d\tau}{d\zeta} = S(1-X) g(X) e^{\tau} - N\tau \quad 1.35$$

$$\frac{dX}{d\zeta} = (1-X) g(X) e^{\tau} \quad 1.36$$

Further manipulation of these equations results in the following equations:

$$\frac{d\tau}{dX} = S - \frac{N\tau e^{-\tau}}{(1-X)g(X)} \quad 1.37$$

$$\frac{d\zeta}{dX} = \frac{e^{-\tau}}{(1-X)g(X)} \quad 1.38$$

Equation 1.37 alone can now be used to investigate the thermal stability of the reaction system as the length dependence has been eliminated by the manipulations. The variables,  $\tau$ ,  $X$ , and  $\zeta$ , and the dimensionless parameters  $N$  and  $S$  in the above equations can be identified with the following physical meanings as pointed out by Barkelew.

1.  $\tau$  is a dimensionless temperature whose scale is determined by the temperature dependence of the reaction rate. It is zero when  $T = T_w$  and a unit increase of  $\tau$  increases the reaction rate by a factor  $e$ .

2.  $X$  is the dimensionless conversion, zero at the inlet and unity when all the reactant is converted.

Table 2. Kinetic parameter values for Barkelew's stability criterion

Reaction	$\alpha$	$\beta$
First-order	0	0
Second-order	$-1 \leq \alpha < 0$	0
Autocatalyzed	$\alpha > 0$	0
Product-inhibited	0	$\beta > 0$
Reactant-inhibited	0	$-1 < \beta < 0$
Fractional-order <sup>#</sup>	0	$-\frac{1}{\text{reaction order}}$

<sup>#</sup> Special consideration must be given to cases of fractional-order reactions as pointed out by Barkelew (1).

3.  $\zeta$  is the dimensionless length defined as the ratio of the reaction rate per unit volume at  $X = 0$ ,  $\tau = 0$  to the space velocity, i.e., ratio of mass velocity to length.

4.  $S$  is a parameter which gives the value  $\tau$  would reach if the inlet temperature were the same as the jacket temperature and if the reactor was operated adiabatically.

5.  $N/S$  is a parameter which expresses the ratio of the rate of heat transfer per unit volume at  $\tau = 1$  to the rate of heat generation per unit volume at  $\tau = 0$ ,  $X = 0$ .

Barkelew numerically integrated equations 1.37 and 1.38 over an extensive set of parameter values, varying  $N$ ,  $S$ ,  $\tau_0$ ,  $\alpha$ , and  $\beta$ . A typical set of results is shown in the following figure where  $\tau_0 = 0$ ,  $\beta = \alpha = 0$ .

Contained in this figure is the basis of the stability criterion developed by Barkelew. The solid curves for the various values of  $S$  form an envelope which is shown as the dashed curve drawn tangent to the "knee" of the  $S$  curves. No curve can penetrate below this envelope and it can thus be used to define stability. The physical significance of the envelope shows that above the tangent to the envelope  $\tau_{\max}$  is extremely sensitive to small changes of  $N/S$  while below the tangent  $\tau_{\max}$  is relatively insensitive. The envelope then separates the range of parameter values where stable thermal operation occurs from the corresponding unstable range. This fact led Barkelew to suggest the following stability criterion.

"A reactor is stable with respect to small fluctuations if its maximum temperature is below the value at the tangent to the envelope described." As Barkelew pointed out, the choice of the model, the reaction rate expression, and the nature of the envelope construction all tend to make this a conservative criterion.

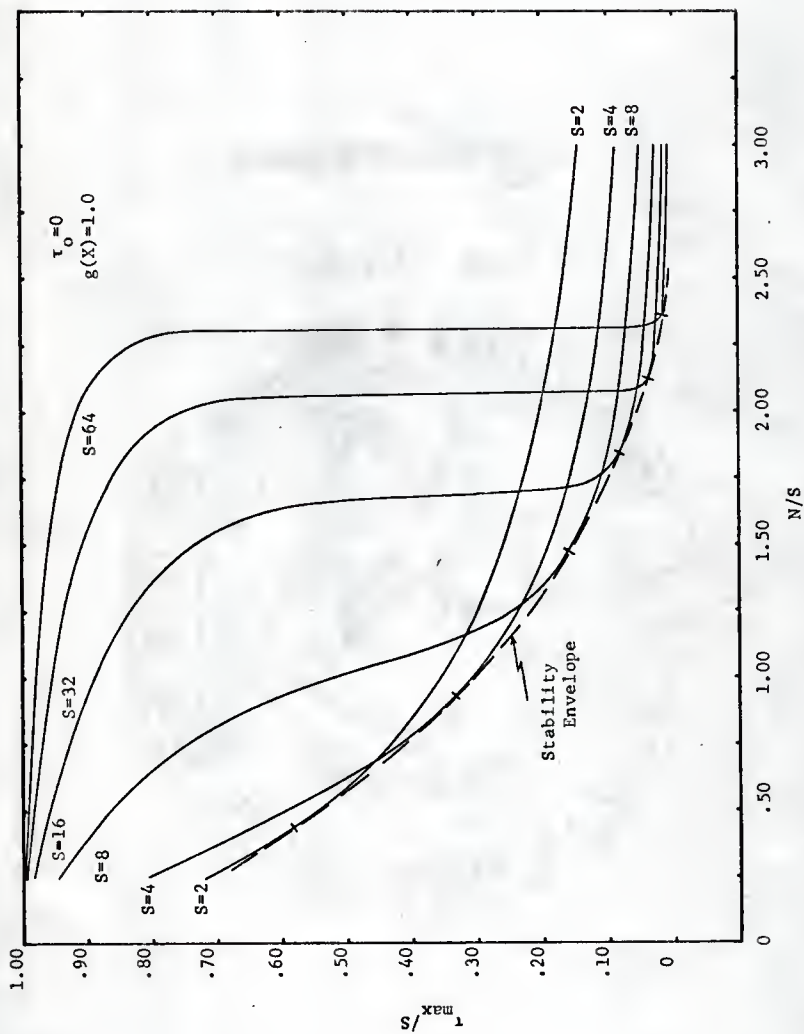


Fig. 2. Barkelew's stability envelope

Once the stability envelope has been drawn it is then possible to determine the physical parameter values which can be safely used in reactor design for an actual set of conditions. For example, an acceptable reactor diameter can be determined when the activation energy, heat of reaction, flow rate, etc., are given.

Even with its limitations and conservative nature, the generality of this stability criterion allows it to be used for a large variety of specific cases. This is a feature not common to the previously discussed criteria.

#### I.7.6 Froment's Comparison

The stability criteria which have been discussed all contain a number of assumptions. A question of considerable importance then is how much and in what way do the assumptions made concerning the reactor model effect the results of the analyses? A more specific question to which a great number of researchers have sought the answer is, how accurately does a one-dimensional model represent the physical situation as compared with a two-dimensional representation? Several recent publications have considered this question and its importance to a stability analysis of reactor runaway. Froment (2) noted that Barkelew's (1) one-dimensional steady-state stability criterion is conservative for the reasons stated previously, i.e., the criterion is based on the construction of an envelope and the reaction rate expression used was forced into a convenient form. Froment then considered a complex oxidation process using both one- and two-dimensional models. For a given reactor design and inlet reactant concentration, the value of the inlet temperature which caused reactor runaway was then calculated by repeated numerical integrations of the heat and mass balance equations, incrementing the inlet temperature until the reactor finally experienced runaway. This trial

and error type analysis was done for both the one- and two-dimensional cases. From the results Froment was able to conclude several things. First, the one-dimensional model failed to predict the mean temperature obtained from the two-dimensional results except under "mild" conditions, and further, the one-dimensional values were always lower than the two-dimensional mean temperature for the cases of exothermic reactions. However, in spite of the temperature discrepancy the one-dimensional model predicted the inlet temperature which caused runaway within five degrees, a prediction which Froment considers excellent. A further conclusion was that the one-dimensional model can be used for initial studies of reactor design, but the final calculations should be carried out using a two-dimensional model.

#### I.7.7 Marek and Hlaváček's Criterion and Comparison

Another recent work concerned with the comparison of one- and two-dimensional models was contributed by Marek and Hlaváček (11, 12). In this work, the authors present a comprehensive study of packed tubular reactor runaway stability and parametric sensitivity for the one- and two-dimensional cases. Unlike Froment, they consider a simple  $A \rightarrow B$  first-order irreversible reaction. Although they do not use Barkelew's (1) stability criterion as a basis for defining stability they do include a comparison of the limiting values for the reactor radius determined using their one- and two-dimensional model results, Barkelew's criterion, and results from the work of Frank-Kamenecky (35).

As a basis for determining reactor stability Marek and Hlaváček use the following inequality for the one-dimensional model simulation:

$$\frac{dQ_r}{dT} > \frac{dQ_g}{dT} \quad 1.39$$

where

$Q_r$  = net rate of heat removal from reactor volume element

$Q_g$  = rate of heat generation in reactor volume element

$T$  = temperature

If the inequality holds true the reactor will not be extremely sensitive to temperature changes and hence stability will be achieved for the rate of heat removal exceeds the rate of heat generation. The form of the inequality was established by making a steady-state energy balance on an element of volume  $dV$  of the reactor. This balance can be given by

$$G c_p T_A S + r^*(-Q)dV = G c_p (T_A + dT_A)S + 2R_2 K (T_A - T_c) dL \quad 1.40$$

where

$G$  = mass velocity

$c_p$  = heat capacity

$T_A$  = temperature at the axis of the reactor

$S$  = cross-sectional area

$r^*$  = reaction rate

$Q$  = heat of reaction

$R_2$  = reactor radius

$K$  = overall heat transfer coefficient

$T_c$  = temperature of cooling medium

$L$  = axial coordinate

By differentiating equation 1.40 and modifying the authors were able to obtain for the inequality 1.39

$$(-Q) \frac{dr^*}{dT} < \frac{2K}{R_2} + G_{c_p} \frac{(d^2T_A/dL^2)}{(dT_A/dL)} \quad 1.41$$

When the reaction rate is given by

$$r^* = A (f_1/\tau) C_{A_o} \exp(-E/RT_o\tau) \quad 1.42$$

where

$A$  = frequency factor

$f_1$  = dimensionless concentration

$\tau$  = dimensionless temperature  $T/T_o$

$C_{A_o}$  = inlet value of reactant A

$\rho_o$  = density

$E$  = activation energy

$R$  = gas law constant

$T_o$  = inlet temperature

substitution of equation 1.42 into 1.41 yielded on further modification

$$\phi = \frac{R_2 C_{A_o} \rho_o (-Q) A}{2T_o K} \frac{1}{\tau} \left[ \frac{(E/RT_o)^{-\tau}}{\tau^2} f_1 + \frac{df_1/dz}{d\tau/dz} \right] \exp \left( \frac{-E}{RT_o\tau} \right) - \frac{R_2 G_{c_p} (d^2\tau/dz^2)}{2KL (d\tau/dz)} < 1 \quad 1.43$$

Equation 1.43 then gives the condition a reactor with no radial temperature gradients must fulfill in order to maintain stability.

For the two-dimensional model simulation no inequality such as 1.43 above was available to the author so stable operation had to be estimated by a slightly different method. This was accomplished by noting that when the rate of heat generation in the two-dimensional model, this inequality still defining stability, there will be no accumulation of heat at any point



in the radial direction. This fact implies that the radial temperature profiles are smooth parabolic curves which do not possess an inflection point. However, when unstable operating conditions exist in the reactor the rate of heat generation will exceed the heat removal rate at every point in the reactor except in the vicinity of the wall. Since the heat generated cannot be removed rapidly enough in the interior section of the reactor the radial temperature profile will possess an inflection point due to the heat accumulation in the center portion of the reactor. The existence of an inflection point in the radial temperature profile then indicates a high parametric sensitivity of the reactor and unstable operating conditions.

Using the two criteria to establish stable operating conditions for the one- and two-dimensional models the authors were then able to make a comparison of the results obtained from the two models. The reliability of the comparison must be questioned, however, in view of the fact that two different criteria were used to establish the stable operating conditions. For the comparisons to be completely valid would require the use of a single stability criterion to establish the operating conditions for both models. Such a flexible criteria is not yet available to the knowledge of this author, so that when viewing the results of the comparisons made by Marek and Hlaváček this fact must be taken under consideration.

The results of the comparison for the first-order reaction under stable operating conditions exhibited close agreement between the axial temperature profile for the one-dimensional model and the mean axial temperature profile obtained from the two-dimensional model. The axial concentration profiles were found to be identical and for the two-dimensional model the concentration was almost invariable in the radial direction. In an investigation to determine the limiting value of the reactor diameter based on stability

considerations the values obtained from the two models were in very close agreement. In checking the values established using Barkelew's (1) criterion and the criterion of Frank-Kamenecky (35) for the same case the authors found that Barkelew's limiting value was somewhat more conservative followed by a considerably smaller limiting value given by the method of Frank-Kamenecky. From this investigation the authors concluded that Barkelew's criterion could be used for a first approximation of the limiting reactor diameter, but that additional investigations are needed in the vicinity of this approximation to establish more accurately the parameter values which limit  $\Phi < 1$ . The final determination must be made on the basis of the two-dimensional model, however, by repeated solution decreasing the diameter until no inflection point in the radial temperature profile is observed.

The authors also investigated the effect of the inlet temperature on the comparisons of the two models. For the case studied the limiting values of the inlet temperature were found to be within two degrees Centigrade for the two models, an agreement which must be considered excellent.

Further parametric sensitivity checks of the one- and two-dimensional models lead the authors to the general conclusion that for laboratory- and production-scale reactors which are generally operated under stable conditions with a margin for safety the one-dimensional model can give sufficient results to be used for simulation purposes, but for optimization work, generally at the pilot-plant level, the two-dimensional model should be used. This conclusion does not differ significantly from the conclusions made by other workers in this area of stability, but the model comparisons made by the authors provide more justification for the use of the simpler one-dimensional model.

### I.7.8 Fraser's Comparison

A third work on the comparison of one- and two-dimensional models was recently completed by Fraser (22) in which the simulations were done with an analog computer rather than a digital computer. The reaction system used was a hydrocarbon oxidation process which was highly exothermic and whose mechanism consisted of eight primary and secondary reactions. The necessary material and energy balance equations for a one-dimensional model resulted from making the usual assumptions associated with this model, and including the additional assumption of a constant wall temperature. The one-dimensional model was then used to determine the ranges of operating variables over which the reactor behavior was sensitive and to indicate where more detailed investigations were needed.

A two-dimensional steady-state model was developed assuming a flat velocity profile, constant average molecular weight, the perfect gas law, and negligible axial heat conduction and taking into account both heat and mass transfer in the radial direction. The reactor radius was separated into four discrete sections, giving rise to a set of four partial differential equations for both the material and energy balances. Each reactor section was treated as a volume with a uniform temperature located at the center of the section with respect to the radius. The accuracy of the solution for this type of computational scheme is thus directly related to the number of discrete sections into which the radius is divided.

Having developed the one- and two-dimensional models and determined the ranges of operating conditions to investigate, Fraser then conducted a comparison between the two models varying the inlet temperature, wall temperature, and the catalyst activity. As a result of the comparison, Fraser was

able to make an adjustment of the heat transfer coefficient in the one-dimensional model so that the results more nearly equaled those of the two-dimensional model. This adjustment is essentially the same as considered by Froment (2, 6) and others who found it necessary to build up an "overall" heat transfer coefficient for one-dimensional models in order to accurately compare results with a two-dimensional model.

With this adjustment of the heat transfer coefficient Fraser found that the conversion curves from both models were practically identical. The temperature profiles from the one-dimensional case was found to be nearly the same as the mean temperature profiles from the two-dimensional model. The yield curves were also very similar for both models.

Fraser used the catalyst activity in the form of the relative activity discussed previously. He assumed that the activity of the catalyst was uniform throughout the catalyst bed and investigated relative activities of 1.0, 0.75, and 0.50. For the relative activities 0.75 and 0.50 Fraser varied the inlet temperatures in order to determine the necessary increase required in the inlet temperature to offset the decline in catalyst activity in order that the conversion remain constant. He determined that the temperature sensitivity of the lower activity cases was not as great as for the case with a relative activity of 1.0. That is, the temperature difference between the inlet temperature and the hot-spot temperature for relative activities of 0.75 and 0.50 were considerably less than for the case of a relative activity of 1.0. Physically, this means the temperature profiles are flattened out and do not possess as large an axial temperature derivative in the first sections of the reactor, thus making it less temperature sensitive and more easy to control. To this author it also suggests that for the

reduced activity cases the reactor could be operated at still higher inlet temperatures with better conversions resulting and still maintain stable operation. Fraser, however, does not consider this possibility.

Fraser concluded that the one-dimensional model could be successfully used to determine the ranges of operating conditions of importance for designing a reactor, but that the final decisions for the reactor design should be made from the results of a more exact two-dimensional model.

### 1.8 Multiple Steady-State Stability

As mentioned previously, a second type of reactor stability concerns the possible existence of multiple steady-state operating points. Although a number of papers pertaining to this field are available, the principal work in relating this type of stability consideration to packed tubular reactors can be attributed to Amundson et al. (15, 16, 17, 18, 19). The investigations made by Amundson are based on a study of the transient equations describing a packed tubular reactor. Because the transient behavior of the reactor was investigated it was necessary, in order to account for temperature differences which exist between the catalyst particles and the fluid, to include equations for describing the catalyst particle behavior in addition to the reactor material and energy balances. This lead to a set of four coupled equations, a mass and energy balance for the catalyst particle, and a mass and energy balance for the volume element of the reactor. Amundson made the following assumptions concerning the reactor model:

1. No radial transfer of either heat or mass.
2. Axial transfer other than by forced convection could be neglected.
3. Uniform velocity profile over the cross section of the reactor.
4. Temperature effects on the velocity could be neglected.

5. Heat and mass transfer resistances for the catalyst can be lumped at the surface.

The model was thus one-dimensional and the reactor was assumed to operate adiabatically (17). (Later investigations made by Amundson et al. have also considered non-adiabatic operation (18) and the effects of axial mixing on the adiabatic case (19). The procedures followed in all these investigations are similar to those used in the basic case of adiabatic operation and will thus not be considered in this review.) The equations were numerically integrated after specifying initial particle and fluid conditions and fluid inlet conditions.

In packed tubular reactors multiple steady-state operating points have been shown to exist only for individual catalyst particles. That is, a single catalyst particle under given conditions may possess three different temperatures which fulfill the steady-state operating equations of the reactor. This is not to say, however, that multiple states exist for all packed tubular reactors.

The existence or nonexistence of multiple steady-state operating points was found to have a somewhat similar relationship between steady-state heat generation and heat removal functions as that described originally by Van Heerden (3) and investigated by Amundson et al. (15, 16) for stirred tank reactors and empty tubular reactors. The only major difference between the packed tubular reactor relationship and the relationship for stirred tank reactor was that in the case of packed bed reactors the heat generation and removal terms are a function of the catalyst particle temperature rather than the fluid temperature. Figures 3.a and 3.b show the two types of steady-state relationships which can exist. The  $Q_{II}$  curve is the heat generation curve

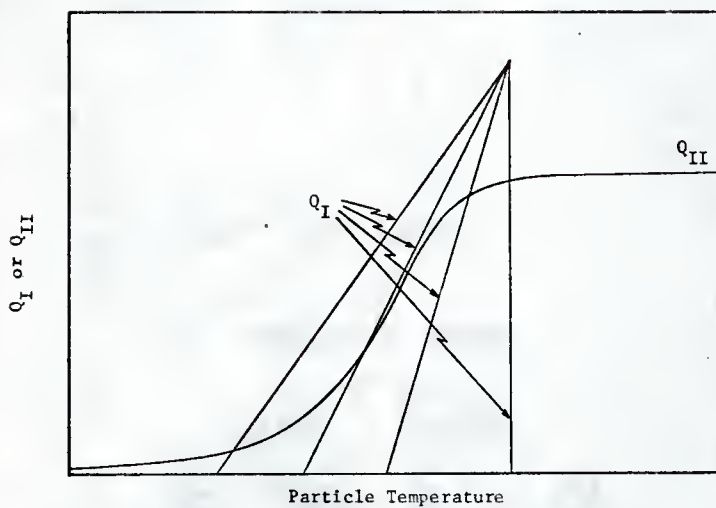


Fig. 3.a. Unique operating points

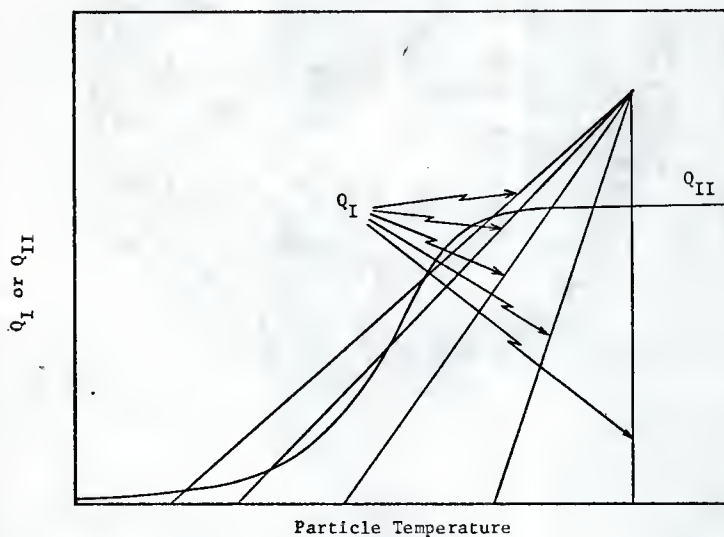


Fig. 3.b. Multiple operating points



and the  $Q_I$  curves the heat removal curves. Each  $Q_I$  line represents a constant fluid temperature. Figure 3.a represents a reactor system in which multiple steady-state points do not exist for the catalyst particles. That is, for any  $Q_I$  there is only one point of intersection with the heat generation curve,  $Q_{II}$ . This point is the steady-state temperature for the catalyst particle for the fluid temperature represented by the  $Q_I$  line. Thus, for this case the catalyst particles all have unique steady-state temperature values.

Figure 3.b represents a reactor system in which multiple steady-state points are possible for the catalyst particles. In this case some of the heat removal lines,  $Q_I$ , intersect the heat generation curve,  $Q_{II}$ , at three different points. Thus for these  $Q_I$  lines there exist three discrete temperatures for the catalyst particles which satisfy the steady-state model equations.

It is in cases such as that illustrated in Figure 3.b that the local stability of the points to small perturbations is of importance. For cases in which multiple steady-state temperatures exist for some catalyst particles, the stability of each point in the set of three possible points can be determined by the criterion set up by Amundson et al. (17). This criterion states basically that at any point of intersection in order to have local stability for that point, the slope of the heat removal line must be greater than the slope of the heat generation curve. This can be expressed as:

$$\frac{dQ_I}{dt_p} > \frac{dQ_{II}}{dt_p} \quad 1.44$$

where  $t_p$  is the particle temperature. Amundson et al. (17) have shown that the inequality is a necessary and sufficient condition for local stability.



Referring again to Figure 3.b it is obvious that for any of the  $Q_I$  lines which intersect  $Q_{II}$  in three points that the middle point of intersection is an unstable state and the two outside intersections are stable states.

The steady-state operation point which will be achieved after start-up of the reactor is dependent solely on the initial conditions of the catalyst bed. Thus the temperature profiles for both the fluid and catalyst and the conversion profile are also dependent on the initial conditions. The effect of the initial conditions on the steady-state temperature and conversion profiles can be obtained by solving the transient equations with different initial conditions.

A recent Russian publication by Boreskov and Slin'ko (10) contains a review of stability criteria in this area which has been completed by Russian authors. The work appears to be similar to that which has been completed by Amundson et al. and discussed above.

### 1.9 Parametric Sensitivity

The third area involved in stability studies is parametric sensitivity. It is apparent from the previous stability discussions that parametric sensitivity is an integral part of those stability considerations. Generally parametric sensitivity is taken to mean that there are sets of conditions where thermally the reactor is extremely sensitive to small changes in the operating conditions yet not unstable in the senses discussed previously (15, 16, 24). A typical illustration of this sensitivity was given by Amundson et al. (16). In this paper the influence of the wall temperature on the temperature profile in a tubular reactor was investigated. It was shown that for a certain range of all temperatures the axial temperature profile was extremely sensitive to any small change of that variable. Likewise there

existed a range of wall temperature values where the sensitivity was much less pronounced. A parametric sensitivity study discerns for a given parameter or parameters the ranges of values for which the reactor is thermally sensitive from those in which it is insensitive.

Numerous articles concerned with parametric sensitivity exist for packed tubular reactors (2, 12, 17, 18, 19, 22). Among the parameters most often investigated are heat transfer coefficients, inlet temperatures, wall temperatures, flow rates, reactor diameters, and catalyst particle diameters.

#### I.10 Selection of a Stability Criterion

A brief reiteration of the purpose associated with this thesis is now in order. The purpose was twofold. First it provided a procedure for determining an operational policy for the inlet temperature while operating near the limit of runaway stability when the catalyst has undergone deactivation. Second it supplied basic information which is to be used in a later study on developing an optimum catalyst activity profile for increasing the level of conversion.

In order to achieve these goals some criterion was necessary for the determination of stable and unstable conditions. There were two obvious paths which could have been followed, one being the development of such a criterion to meet the needs of the situation. As an alternative choice an already developed criterion could be selected and modified to meet the necessary demands. The latter of these possibilities was chosen in order to eliminate considerable work which would have been necessary to develop and validate a new reactor runaway stability criterion.

In making the selection of a stability criterion four properties were felt to be of principal interest from the standpoint of the purpose of the

investigation. First the criterion must be well established. Second the criterion must be of a general nature in order to accommodate the investigation of large ranges of values for the several parameters of interest. In particular it had to be adaptable for use with the relative catalyst activity as a parameter. Third the results obtained through its use must adequately and accurately represent the physical system within the limitations inherent in the choice of a reactor model. Fourth the computational efforts required by the criterion choice should be as simple as possible while remaining within the bounds set by the above considerations. Such an ideal criterion probably will never exist, but it was felt by this author that the criterion developed by Barkelew (1) came the closest to fulfilling all four of the demands. This criterion was considered to be the most general of all the criteria existing in spite of its limitation to use in single reaction systems. It was also readily adaptable for the catalyst activity study to be undertaken in this thesis. The accuracy of the results obtained by Barkelew and others (2, 12) using this criterion has been shown to be consistently conservative, yet giving a relatively good approximation of the limiting parameter values for stable reactor operation. The computational effort required by using this criterion was also considered "reasonable" as large ranges of parameter values can be investigated using a single stability envelope as opposed to the continual use of the stability criterion associated with the other available criteria. The limitation of this criterion to single reaction systems in no way hindered the intended investigation as it was felt that investigating a simple single reaction would be more beneficial in isolating the effects of changes in activation energy, heat of reaction, and catalyst activity than using a complex reaction system. To have considered a complex

reaction system involving more than one heat of reaction or activation energy would only serve to confuse the study.

## II. The Development of the Study

This section includes the assumptions and the reactor model equations which are used in the stability criterion. Following that the types of activity profiles investigated and equations describing them are presented. Then, the steps in the mathematical procedure used in developing the stability criterion are described. Finally, the equations and parameter values of the reactor model used to illustrate the investigations are presented and discussed.

### II.1 The Model and Assumptions

In line with the objectives set forth in the introduction a simple one-dimensional steady state reactor model was chosen for the investigations. The necessity for a stability criterion and the reasons for selecting Barkelew's criterion (1) were given in section I.10. However, as catalyst activity was not considered in his investigation, some additional assumptions are necessary. The assumptions Barkelew used were presented in section I.7.5 but will be repeated here.

The assumptions are:

1. Negligible axial transport of heat and mass by diffusion.
2. Resistance to radial heat transfer in the bed is small compared with the resistance at the wall.
3. The reaction rate is a unique function of fluid properties.
4. The composition dependence of the reaction rate can be expressed in terms of the concentration of a single component.

The additional assumptions necessary are:

5. The catalyst activity decay is very slow and can be considered independent of time.

6. The activity can be expressed as a factor in the reaction rate expression.

7. The maximum operating temperature is set by runaway stability. (That is catalyst damage and selectivity are assumed to be independent of temperature.)

Most of the assumptions were discussed generally in the introduction. Some additional comments can be made, however, with reference to their effect on the stability criterion. Much of the following discussion concerning the first four assumptions comes from Barkelew's work (1).

The first assumption is based on theoretical and experimental investigations (2). In addition it is a necessary assumption from a computational viewpoint. Barkelew pointed out that the numerical procedures would be too lengthy if the assumption were not made. However, under stability limited operating conditions it might be expected that axial heat and mass transfer by diffusion becomes significant. Its neglect, though, makes the stability limited conditions conservative. This can be seen by examining a typical exothermic reaction temperature profile. In the area of the hotspot temperature, if axial heat conduction were significant it would cause additional heat transfer out of this area. This would tend to smooth out the temperature profile and result in a less sensitive reactor. The assumption, therefore, leads to a conservative criterion.

The second assumption implies no radial temperature variation. It is a necessary assumption for a one-dimensional model, but hardly ever an accurate description. Even its use for obtaining the average bulk temperature has been questioned (2). Nevertheless, the stability limited values predicted by Barkelew's criterion using this assumption have been shown to be

conservative, but in "excellent" agreement with two-dimensional predictions (2, 12, 22).

Assuming the reaction rate is a unique function of the fluid properties can basically be taken to mean the catalyst particle temperature is the same as the fluid temperature. Barkelew pointed out that at steady-state this assumption is generally valid as heat conduction through direct particle contact is generally not important.

The fourth assumption does not effect the validity of the criterion but limits its use to single reaction systems.

The fifth assumption was necessary in order to make a steady-state analysis. It implies that the rate of catalyst deactivation is very much slower than the product-forming reaction. This would correspond to reactors having long operational times before shutdown for regeneration is necessary.

The sixth assumption follows readily from the previous one. It is the generally used form for the catalyst activity under steady-state conditions (9, 22).

The last assumption was discussed in section I.5. It is really more of a limitation than an assumption as it limits the nature of reaction systems which can be investigated by the model. It was necessary, however, to limit the computational effort associated with this work.

## II.2 Activity Profiles

Three types of steady-state profiles for the catalyst activity were investigated. They are:

1. Uniform Profiles
2. Negative Sloped Profiles
3. Positive Sloped Profiles

The profiles are illustrated in Figure 4. Linear profiles were assumed to facilitate the computations. As pointed out in the introduction they roughly approximate uniform poisoning, poisoning by a consecutive side reaction mechanism, and poisoning by a parallel reaction mechanism respectively.

For uniform profiles the relative activity appears as a constant in the reaction rate expression in accordance with assumption six above. The activity for the sloped profiles is given by the equation of a straight line

$$a = a_0 - mz \quad 2.1$$

$$m < 0 \quad \text{for positive slopes}$$

$$m > 0 \quad \text{for negative slopes.}$$

For the negative sloped profiles the activity at the reactor inlet,  $a_0$ , was always assumed to be unity. Likewise for the positive sloped profiles, the activity at the outlet was always assumed to be unity. The slope,  $m$ , was determined by the length of the reactor and the inlet and outlet activity conditions being investigated.

### II.3 Equations for Developing the Stability Criterion

The equations which are used to develop the stability criterion are the same as used by Barkelew (1) except that the reaction rate expression was modified to incorporate the catalyst activity in accordance with assumption six. The Appendix contains the derivations of all the principal equations used in this thesis. The final dimensionless equations are:

$$\frac{d\zeta}{dX} = \frac{e^{-\tau}}{a(1-X)g(X)} \quad 2.2$$

$$\frac{d\tau}{dX} = S - \frac{N \tau e^{-\tau}}{a(1-X)g(X)} \quad 2.3$$



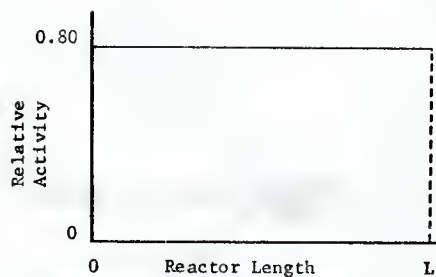


Fig. 4a. Typical Uniform Activity Profile

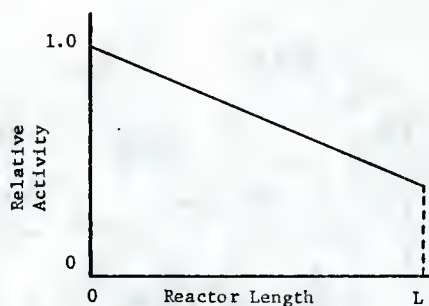


Fig. 4b. Typical Negative Sloped Activity Profile

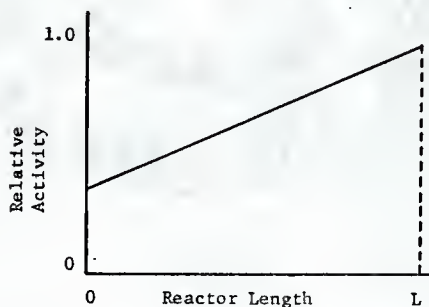


Fig. 4c. Typical Positive Sloped Activity Profile

Fig. 4. Activity profiles

The stability analysis can be made using Equation 2.3 alone while Equation 2.2 can be solved to obtain the axial length dependence if it is desired.

#### II.4 Application of the Equations

The variables in Equation 2.3 are  $\tau$  and  $X$ , the dimensionless temperature and conversion. The parameters are  $N$ ,  $S$ ,  $a$ , the reaction order (see Section I.7.5), and  $\tau_0$ , the inlet condition for  $\tau$ . Among these parameters there is a very large number of combinations which could be investigated. Barkelew (1), for example, investigated 750 combinations, none of which included the catalyst activity as a parameter. In this thesis catalyst activity was used as a parameter with the reaction rate restricted to first-order and with  $\tau_0$  assumed to be zero for all cases. This corresponds to setting  $g(X)=1$  in the reaction rate expression and setting the reactant inlet temperature equal to the reactor wall temperature. The steps followed in establishing the stability criterion for any different pair of these parameter values is exactly the same as that used here.

The procedures used in this thesis for the uniform activity profile cases are basically the same as those used by Barkelew (1). For the sloped activity profile cases a minor alteration of procedure was necessary and is discussed at a later point in the thesis.

A certain amount of qualitative information about the maximum axial temperature can be obtained from Equation 2.3 by setting  $d\tau/dX=0$ . Doing this yields the following equation

$$\tau_{\max} e^{-\tau_{\max}} = \frac{a(1-X_{\max})}{(N/S)} \quad 2.4$$

where  $g(X)=1$ . Equation 2.4 can then be used to plot the locus of the maximum temperature. Figure 5 shows the results Barkelew obtained using  $a=1$ .

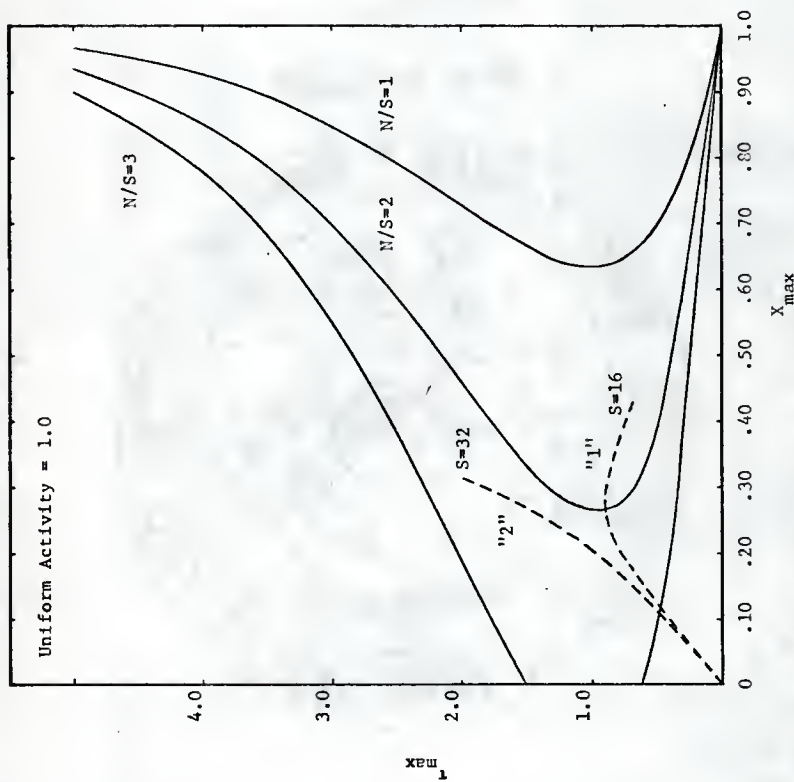


Fig. 5. Locus of the maximum dimensionless temperature for  $a = 1.0$

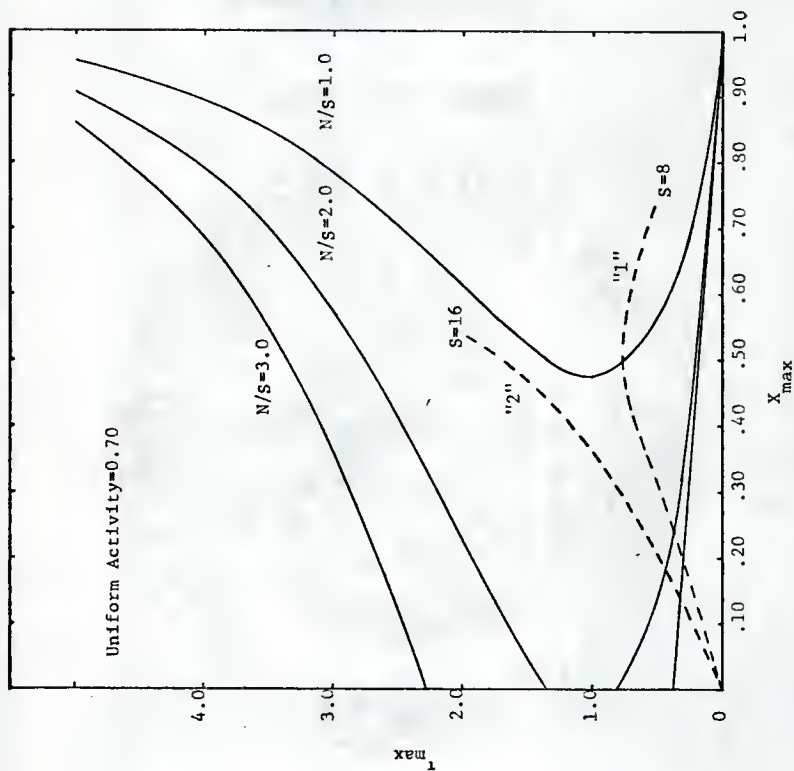


Fig. 6. Locus of the maximum dimensionless temperature for  $a = 0.70$

Figure six shows similar results with a uniform activity of  $a=0.70$ . Several points concerning these curves are of interest. First consider Figure 5 and the dashed reaction paths marked "1" and "2". The ratio of  $N/S=2.0$  is constant for both paths. Path "1" shows that the temperature increases until the path intersects the maximum temperature locus. The temperature then begins to decrease. In path "2" however, the temperature continues to increase indefinitely because the path does not intersect the maximum temperature locus. Path "2" would be considered unstable while path "1" would be considered stable. For some value of  $S$  between 16 and 32 there is thus a limiting value of  $S$  above which the reactor is unstable and below which it is stable. Figure 6 shows the same type of phenomena for  $a=0.70$  and a constant  $N/S=1$  ratio. Thus for any reaction path the temperature increases until the path intersects the corresponding  $N/S$  locus. At that point the temperature must begin to decrease.

Barkelew pointed out in Figure 5 that if  $N/S=3$  it is very unlikely for an unstable operation to occur. The only possibility is when the inlet temperature,  $\tau_0$ , is greater than the upper intersection point of the  $N/S=3$  locus with the ordinate axis. In Figure 6 the loci have been shifted further to the left than in Figure 5. As a result when  $N/S=2$  the locus shows that the only possibility for unstable operation is again an inlet temperature greater than the upper intersection point.

The effect of a lower catalyst activity is in general to increase the stability of the reactor operation. Further evidence of this can be seen in Figures 7 and 8. The loci in these figures are for constant  $N/S$  ratios with the catalyst activity as a parameter. Figure 7 shows the loci for  $N/S=2$ . There is an appreciable shift of the loci towards the left as the

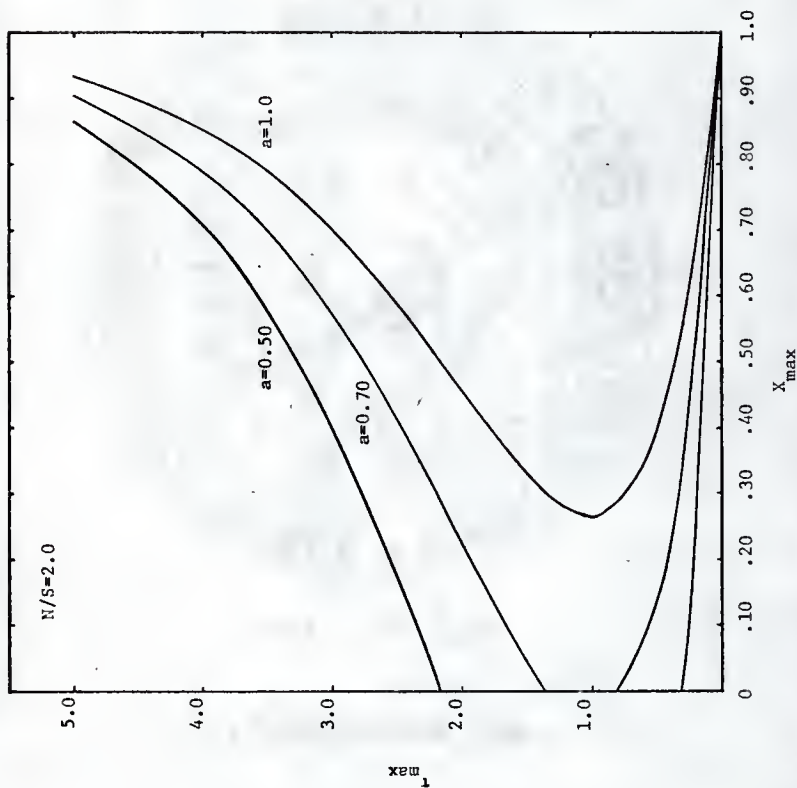


Fig. 7. Locus of the maximum dimensionless temperature for  $N/S = 2.00$

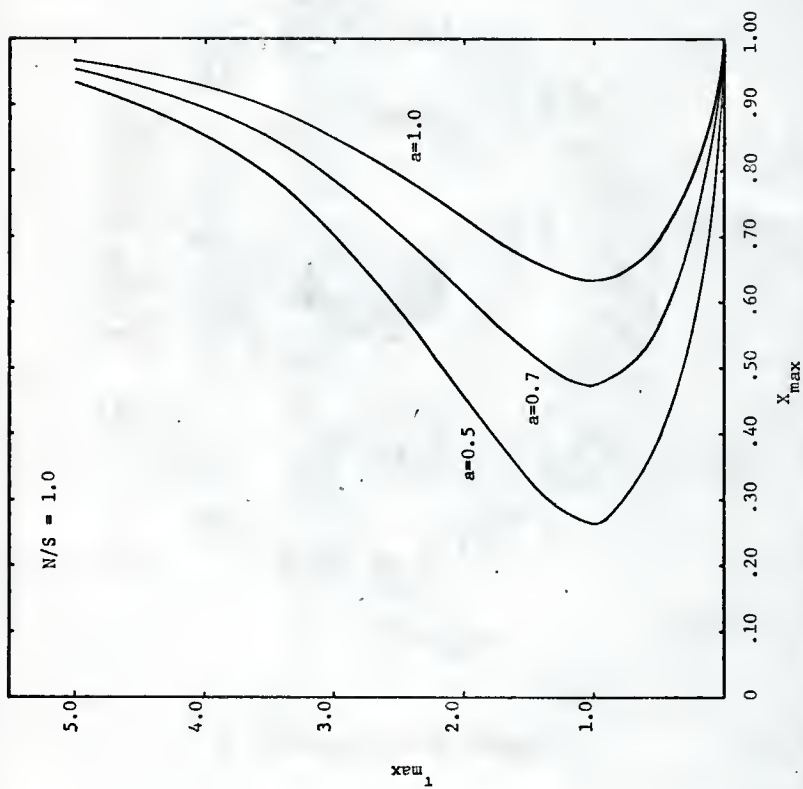


Fig. 8. Locus of the maximum dimensionless temperature for  $N/S = 1.00$

activity decreases. The figure shows that for  $\tau_0 = 0$  stable operation of the reactor always occurs if  $a \leq 0.70$ .

To establish a stability criterion, Equation 2.3 must be integrated repeatedly while varying the parameters  $N$  and  $S$ . It is evident from Figure 5 that values of  $N$  and  $S$  which result in  $N/S > 3.0$  do not need to be investigated. A criterion is valid, however, only for the form of the activity profile used in the investigations. Therefore a large number of the numerical integrations were necessary to obtain criteria for each case of catalyst activity investigated.

Typical results of the integrations are shown in Figures 9 and 10. The dimensionless length relationship in these figures was obtained by numerically integrating Equation 2.2 in conjunction with Equation 2.3. The figures show the two possible types of temperature profiles corresponding to the situation shown in Figures 5 and 6. Figure 9 shows the temperature profile going through an actual maximum. The maximum corresponds to the point of intersection with the locus of the maximum temperature for  $N/S=1.50$ ,  $S=16.0$ , and  $a=0.80$ . Figure 10 shows that when  $N/S=1.5$ ,  $S=32.0$  and  $a=0.80$  there is no real maximum in the temperature profile. The temperature continues to rise as long as there is any reactant to be converted. The value of  $\tau$  at 100 percent conversion, however, will be considered a maximum point for use in the stability criterion.

If  $\tau_{\max}/S$  is plotted versus  $N/S$  for various values of  $S$  the family of curves which result have an envelope below which no curve penetrates. This was shown by Barklelew for cases where the activity was not considered. He pointed out that since the envelope occurs very near to the "knee" of each  $S$  curve, it can be used to define a stability criterion. This principle also



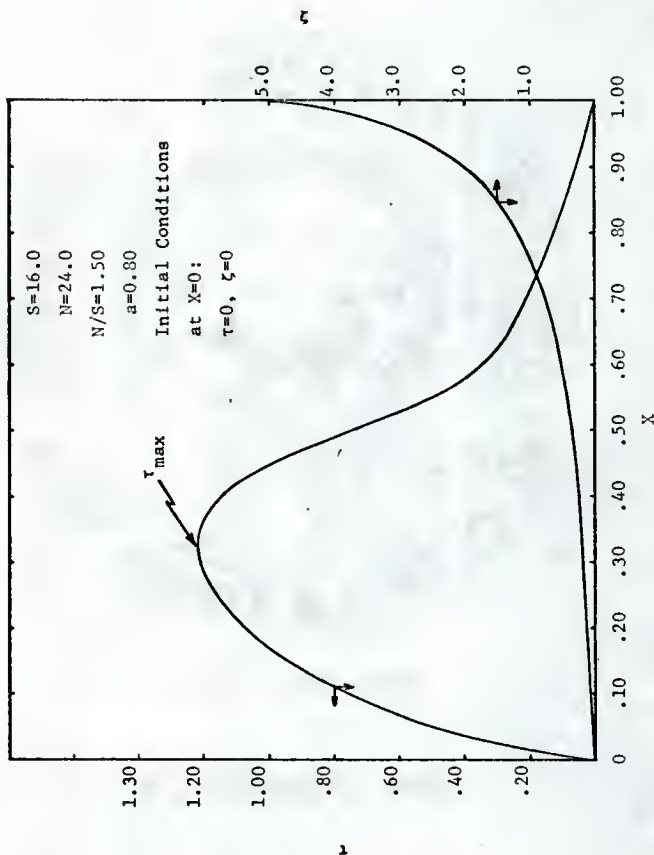


Fig. 9. Typical dimensionless temperature and length profiles as a function of the conversion

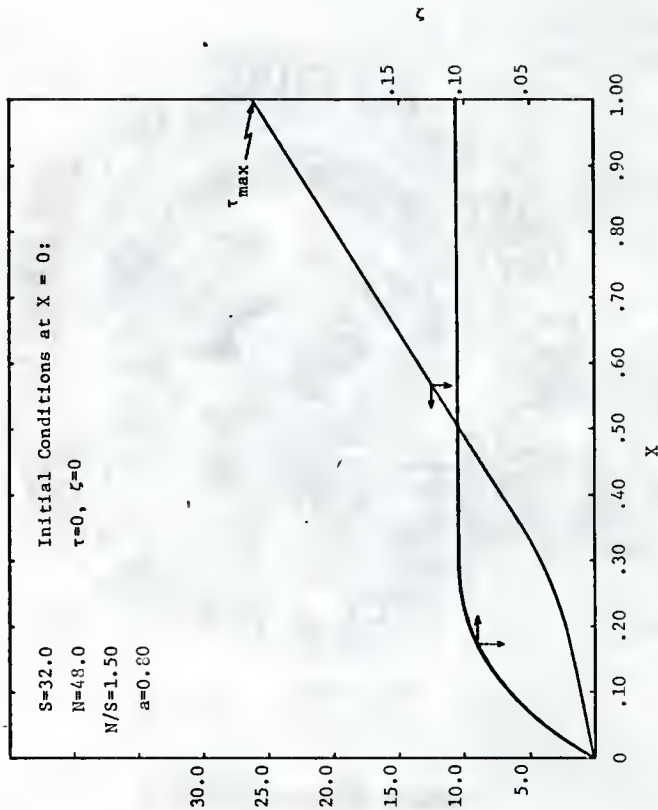
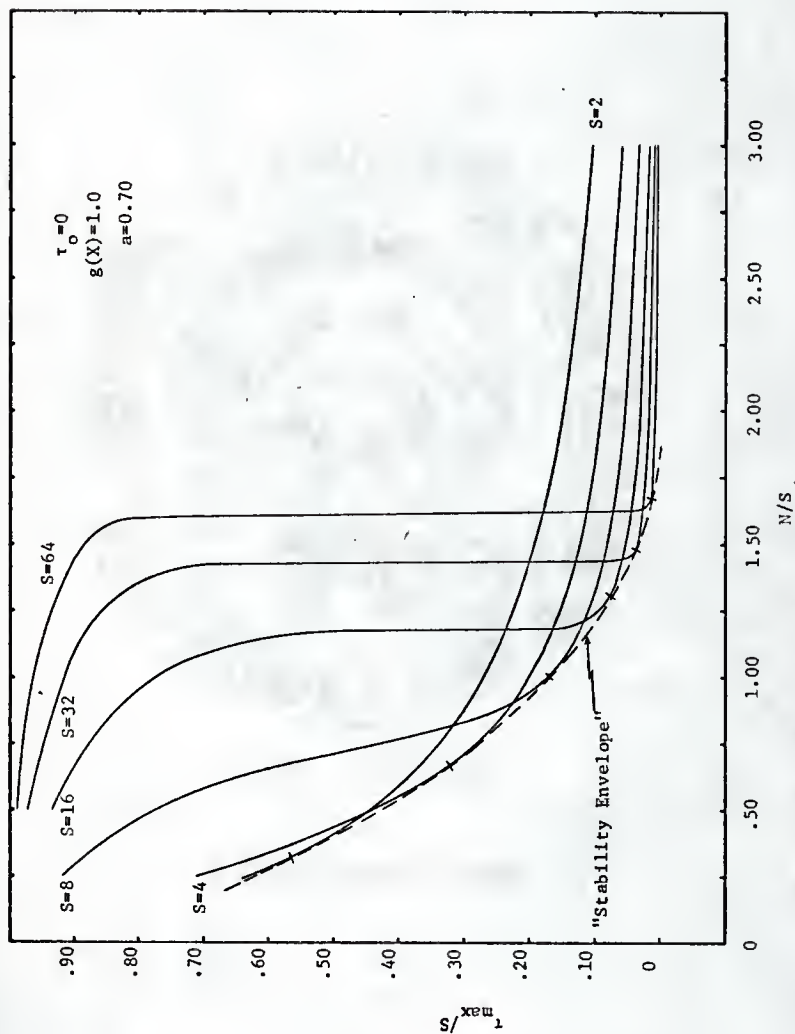


Fig. 10. Typical dimensionless temperature and length profiles as a function of the conversion

holds true when using the activity as a parameter. A typical stability envelope is shown in Figure 11. The significance of the envelope can be seen by examining the point of tangency of the envelope and one of the S curves. A value of  $\tau_{\max}$  above the value at the tangent point shows the maximum temperature to be very sensitive to small changes of N/S. For values of  $\tau_{\max}$  below the tangent value, the maximum temperature is insensitive. The points of tangency then define the regions of stability and instability. This lead Barkelew to make the following proposition: "A reactor is stable with respect to small disturbances if its maximum temperature is below the value at the point of tangency." He also noted the following points concerning the proposition. First a reactor is not necessarily unstable if the proposition is not fulfilled. Second the positioning of the envelope is arbitrary. Third the point of tangency when S is 8 or less is uncertain. However, reactors with small S values are unlikely to run away so the uncertainty becomes unimportant.

A more desirable form for the "stability envelope" is obtained by plotting the N/S values at the points of tangency versus the corresponding S values. This is illustrated in Figure 12 where S is plotted as the abscissa on a semi-log plot. Figure 12 gives a continuous curve of  $(N/S)_{\text{tang}}$  vs. S so that the stability criterion can be applied for any value of S rather than the discrete values given in Figure 11. Figure 12 is then used as a basis for determining the stability limited values for designing or operating a reactor. Figure 12 is valid only for the form of activity used in its construction and the additional restrictions of  $\tau_0=0$  and  $g(X)=1$ . For conditions other than these a stability criterion can be developed using the same procedure, but with the desired conditions.

Fig. 11. Stability envelope for  $a = 0.70$

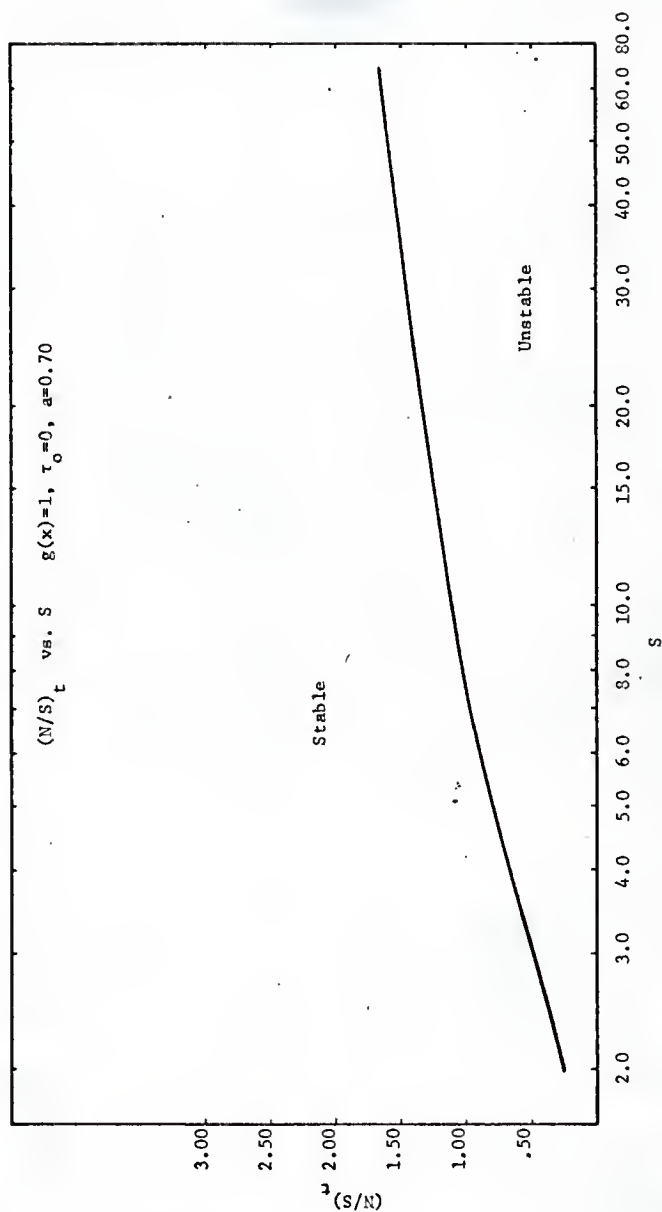


Fig. 12. Semi-log plot of the stability envelope for  $a = 0.70$

In this thesis figures such as Figure 12 were used to determine an operating policy for the inlet reactant temperature. For an already existing reactor system all the parameters which form the N and S dimensionless groups are fixed except the wall temperature and the inlet concentration of reactant. Using a family of curves similar to the curve in Figure 12, with the catalyst activity as a parameter it was possible to construct a relationship between the limiting wall temperature and the inlet concentration. Further, from the condition  $\tau_0 = 0$ , the reactant inlet temperature is equal to the wall temperature. Thus the relationship between the inlet temperature and inlet concentration at the limit of runaway stability was determined. These relationships are presented in detail in the following three sections.

The computer programs which were used in the above procedures are presented in the Appendix.

## II.5 Example Reactor System

To check the results of the above work an example reactor system was constructed. The reaction used was an irreversible first-order reaction



This simple reaction is not without industrial significance however. Oxidation of  $\text{SO}_2$  and naphthalene and the synthesis of  $\text{NH}_3$  and  $\text{CH}_3\text{OH}$  are examples of industrial reactions which can be approximated by such a form. The reaction rate constant and the parameter values that were used in the example are given in Table 3. It is felt by this author that the values are realistic and reasonable.

A one-dimensional steady-state reactor model with a constant wall temperature was used and the assumptions made previously in this section still

Table 3. Kinetic and parameter values for the example reactor system

## Reaction Mechanism:



$$k' = k'_0 \exp(-E/R'T) \text{ moles/kg cat-hr}^*$$

$$r_B = k' a_{A_0} (1-X) \text{ moles/kg cat-hr}$$

$$R' = 1.987 \text{ cal/gm-mole } ^\circ K$$

$$\ln k'_0 = 15.70$$

## Reactor Parameters:

Catalyst Activity -  $a$ Reactor Diameter -  $d_t = .036 \text{ m}$ Mean Molecular Weight -  $M_m = 29.48 \text{ gm/mole}$ Catalyst Bulk Density -  $\rho_B = 1300. \text{ kg/m}^3$ Mass Flow Rate -  $G = 7000.0 \text{ kg/m}^2\text{-hr.}$ Fluid Heat Capacity -  $c_p = 0.25 \text{ cal/gm-}^\circ C$ Overall Heat Transfer Coefficient -  $U = 73.0 \text{ kcal/m}^2\text{-hr-}^\circ K$ Catalyst Particle Diameter -  $d_p = .003 \text{ m}$ 

\* See the Appendix for explanation of the units, Section XI.3.

apply. The derivation of the material and energy balances is included in the Appendix. The final dimensionless equations for the system are:

$$\frac{dX}{dz} = B_1 r_B \quad 2.5$$

$$\frac{dt}{dz} = B_2 r_B - Ft \quad 2.6$$

where

$$B_1 = \rho_B d_p M_m / Gx_{A_0} \quad 2.7$$

$$B_2 = 1000.0(-\Delta H) d_p \rho_B / Gc_p \quad 2.8$$

$$F = 4U d_p / Gc_p d_t \quad 2.9$$

$$t = T - T_w \quad 2.10$$

$$X = \frac{C_{A_0}' - C_{A_0}}{C_{A_0}} \quad 2.11$$

$$r_B = k' x_{A_0} (1-X) \quad 2.12$$

The boundary conditions for the equations are:

$$X = 0.0 \quad @ \quad \bar{z}=0.0 \quad 2.13$$

$$t = 0.0 \quad @ \quad \bar{z}=0.0 \quad 2.14$$

The reactor wall temperature is assumed to be constant over the entire length of the reactor.

Equations 2.5 and 2.6 were numerically integrated by a Runge-Kutta scheme. The integrations were carried out using nine different combinations of the heat of reaction and activation energy. Activation energies of 10,000, 20,000 and 30,000 calories per mole and heats of reaction of 25,000, 50,000 and 100,000 calories per mole were used.



For each of the nine combinations an operational policy for the stability limited inlet temperature and concentration was determined by the methods of Section II.4. These stability limited inlet values were used in Equations 2.5 and 2.6 to obtain temperature and conversion profiles for each case. The conversion profiles were then used to determine the effect of reduced catalyst activity on the final conversion. In order to check the accuracy of the inlet temperature and concentration values obtained using the "stability envelope", Equations 2.5 and 2.6 were also integrated with a slightly higher value for the inlet temperature.

The results of these studies for the three types of activity profiles are presented in detail in the following three sections.

### III. Uniform Activity Profiles

In this section of the thesis the "stability envelopes" and the operational policy for the inlet temperature are calculated for cases where the activity is assumed uniform along the entire reactor length. The operating policy was then applied to the example reactor system and the results presented graphically.

#### III.1 Results for Uniform Activity Profiles

The activity in this part of the work was assumed constant throughout the reactor bed. Uniform activities of 1.0, 0.95, 0.90, 0.85, 0.80, 0.70, 0.50, 0.30, and 0.10 were investigated for heats of reaction of 25,000, 50,000, and 100,000 calories per mole and activation energies of 10,000, 20,000, and 30,000 calories per mole. Figure 13 gives an outline of the possible graphical results obtainable from the numerical integrations. Because of the large number of parameter combinations available only representative plots of the results will be presented here.

Figures 14, 15, 16, and 17 show the "stability envelopes" for activities of 1.0, 0.70, 0.30 and 0.10 respectively. The effect of decreasing the activity can be seen in the shift of the envelope towards the origin in these figures.

Figure 18 is a plot of the values of  $N/S$  at the points of tangency of the envelopes and the "knees" of the  $S$  curves. The point of tangency when  $S$  is 8 or less is arbitrary as discussed in Section II.4. This fact is visible in Figure 18 where irregularities appear in the curves for  $S < 6$ . The curves for  $S \geq 6$ , however, were taken to be accurate within  $\pm 0.025$  of the value of  $(N/S)_{\text{tang}}$  as will be shown at a later point in this section.

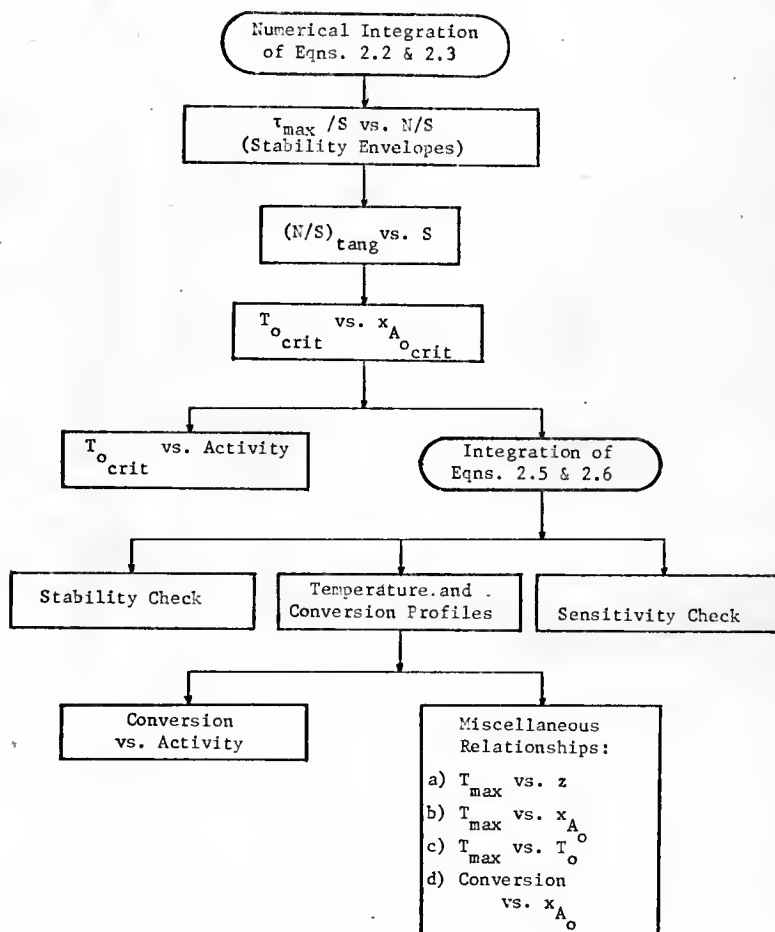
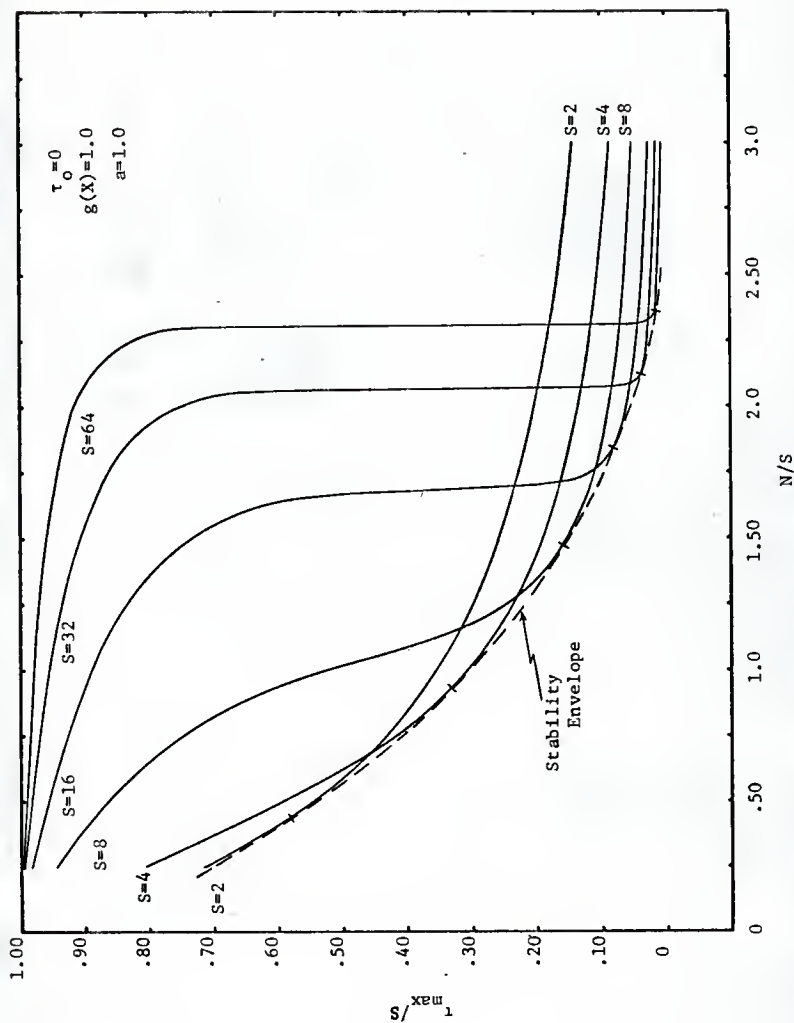
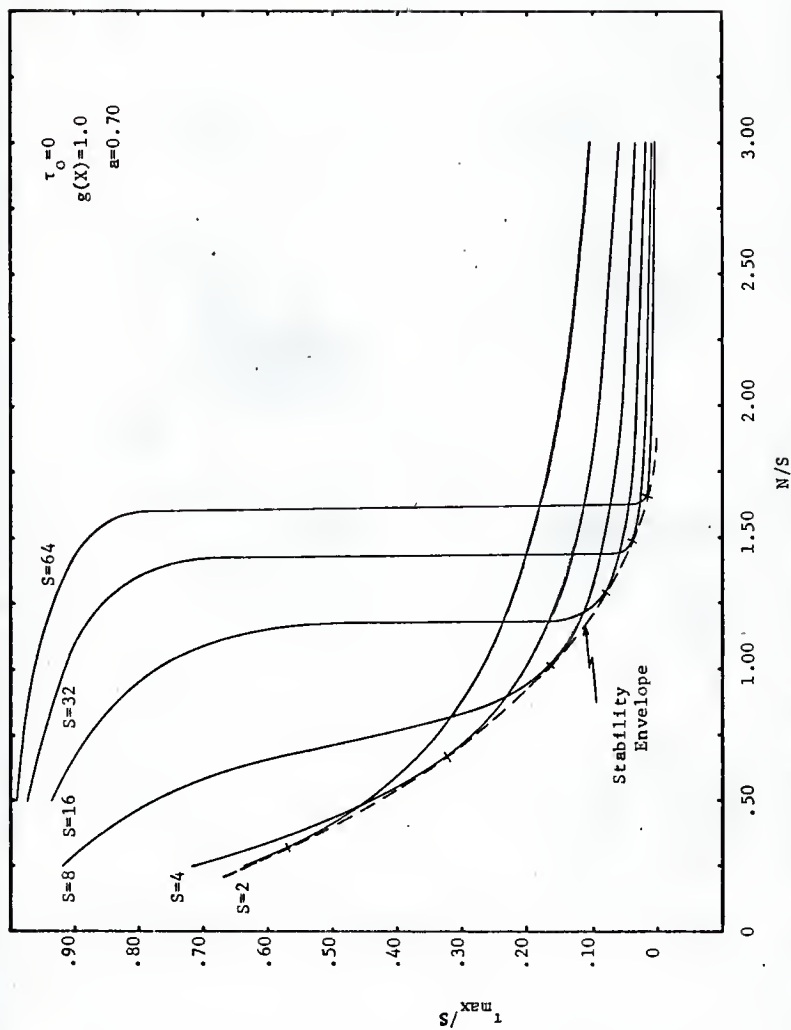
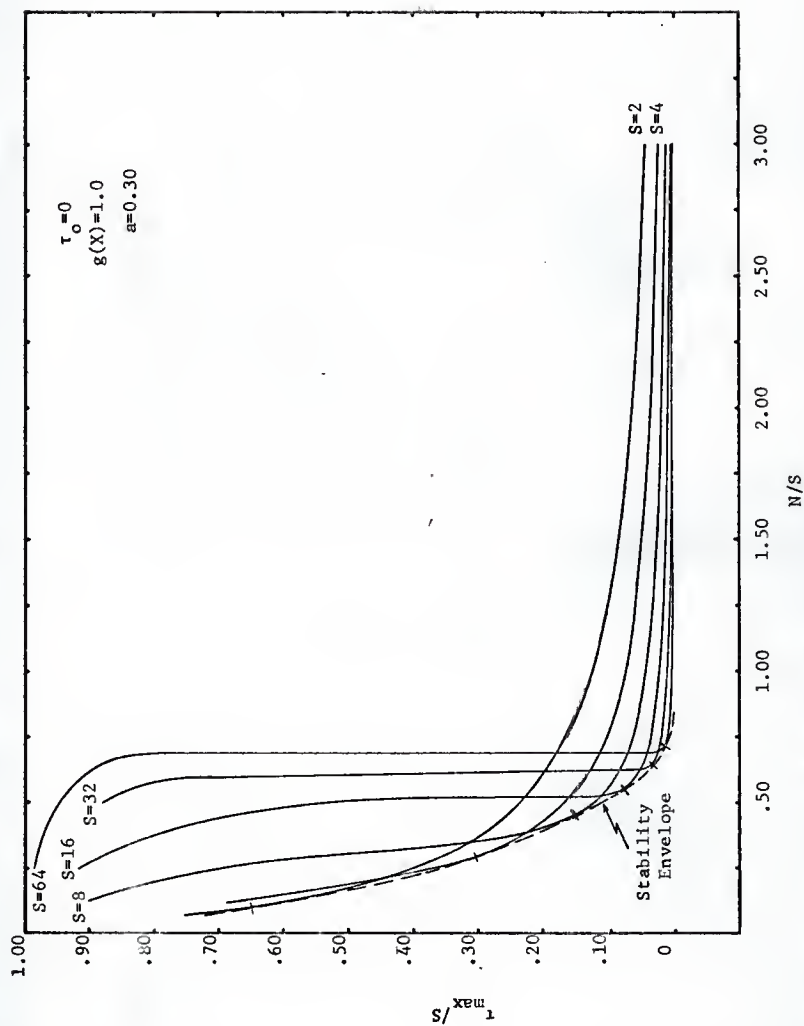
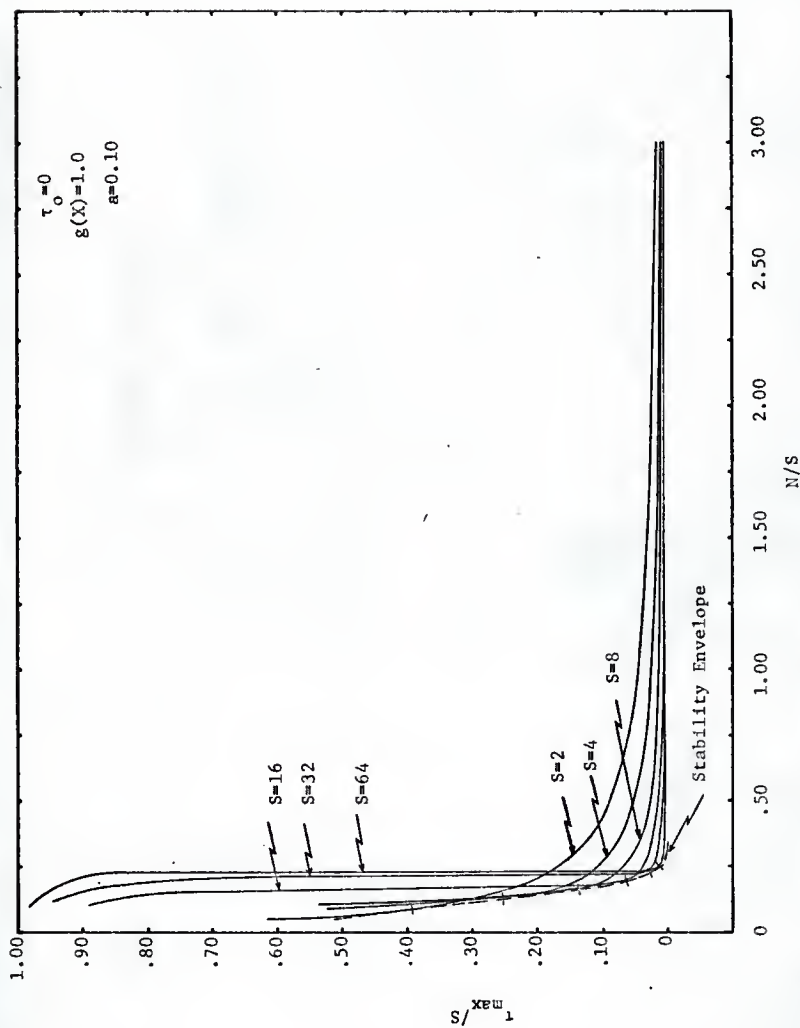


Fig. 13. Outline of graphical results

Fig. 14. Stability envelope for  $a = 1.0$

Fig. 15. Stability envelope for  $a = 0.70$

Fig. 16. Stability envelope for  $a = 0.30$


 Fig. 17. Stability envelope for  $a = 0.10$

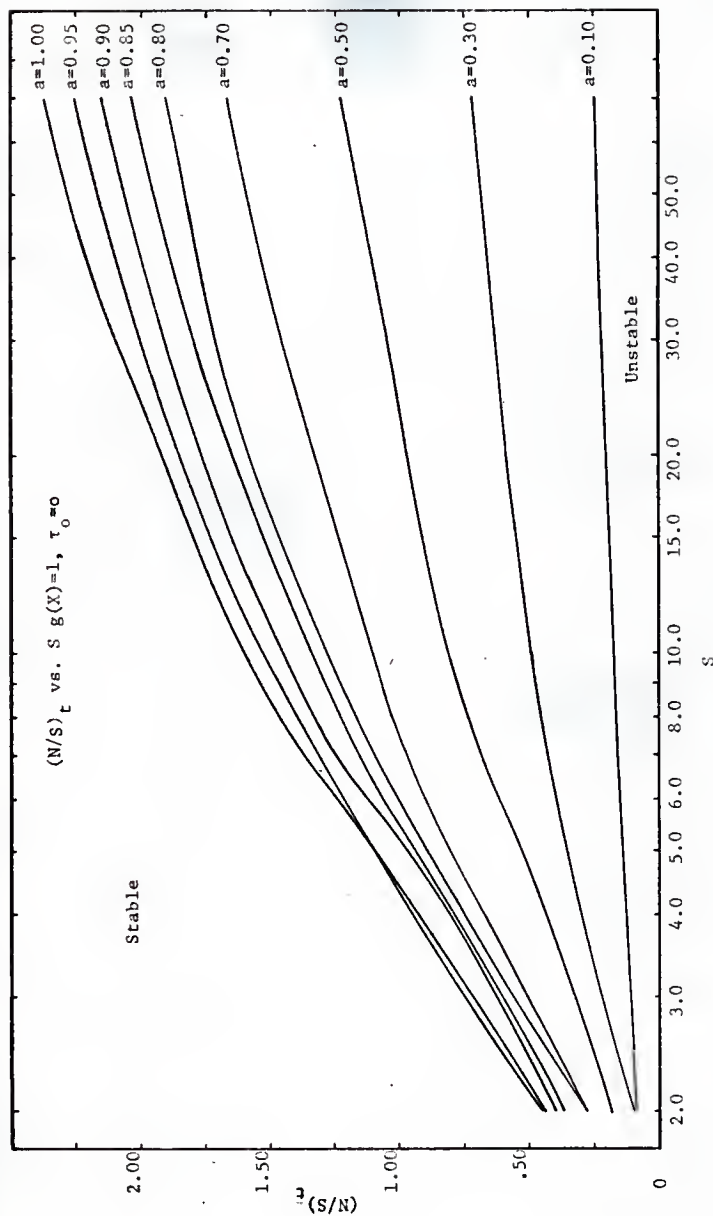


Fig. 18. Stability envelopes for uniform activity profiles



From the curves of Figure 18 the critical values of the inlet temperature and inlet mole fraction were calculated. The procedure is included in the Appendix, Section XI.2. Figures 19, 20, 21, and 22 show the results of these calculations for an activation energy of 20,000 calories per mole and relative activities of 1.0, 0.70, 0.30 and 0.10.

The effect of a decrease in the catalyst activity can be seen more easily in Figures 23, 24, and 25. In these figures the critical value of the inlet temperature has been plotted versus the activity with the inlet mole fraction held constant. The figures are for an activation energy of 20,000 calories per mole and heats of reaction of 25,000, 50,000 and 100,000 calories per mole respectively. Figure 26 is a semi-log plot of Figure 23. It shows that the critical inlet temperature approximates an exponential increase as the activity decreases.

Figures 19 through 25 thus define an operational policy for the stability limited inlet temperature as a function of the uniform catalyst activity. This policy was applied to the example reactor system discussed in Section II.5. The reactor equations, Equations 2.5 and 2.6, were numerically integrated using the critical values of the inlet temperature and inlet mole fraction. Again three values of the activation energy and three values of the heat of reaction were investigated for inlet mole fractions ranging from 0.015 to 0.200. Typical temperature and conversion profiles are shown in Figures 27, 28 and 29.

For all parameter combinations with uniform activity it was observed that the temperature profiles experienced a hotspot temperature before reaching the reactor outlet at  $\bar{z} = 600$ . This dimensionless reactor length corresponds to an actual length of 1.8 meters. For small inlet mole fractions

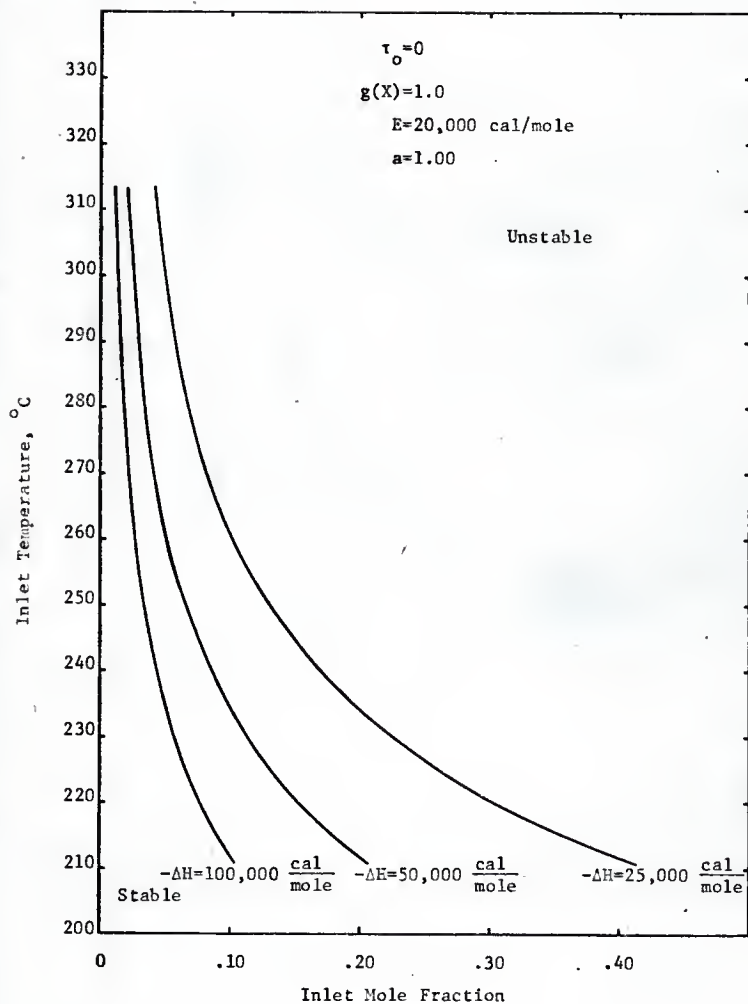


Fig. 19. Critical inlet temperature operating policy for  $a = 1.0$

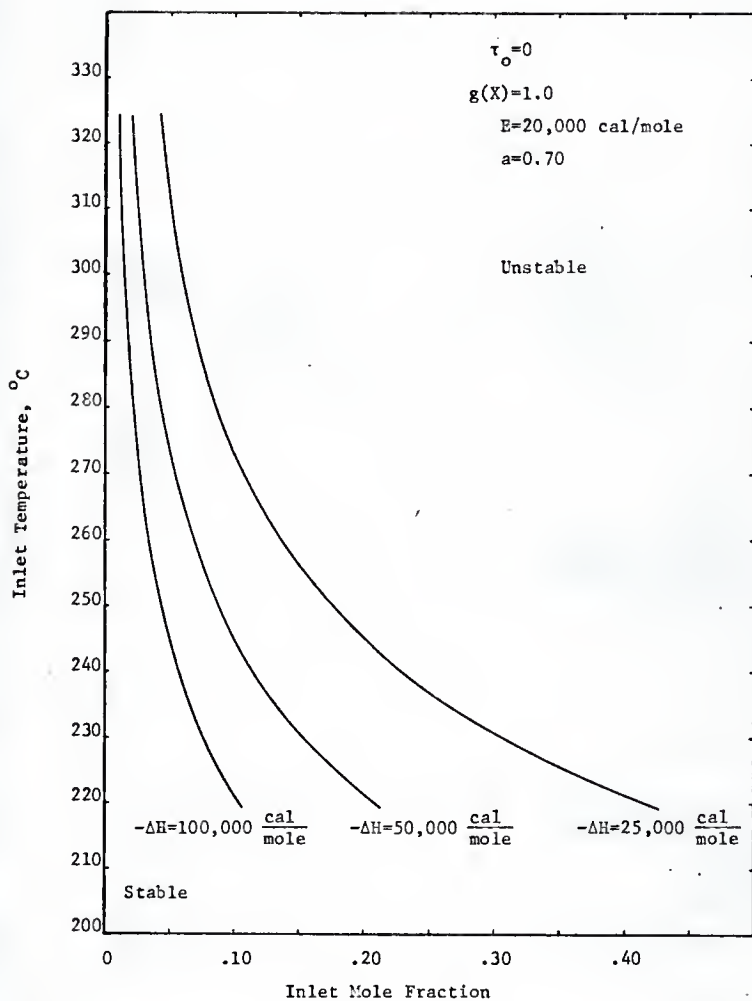


Fig. 20. Critical inlet temperature operating policy for  $a = 0.70$

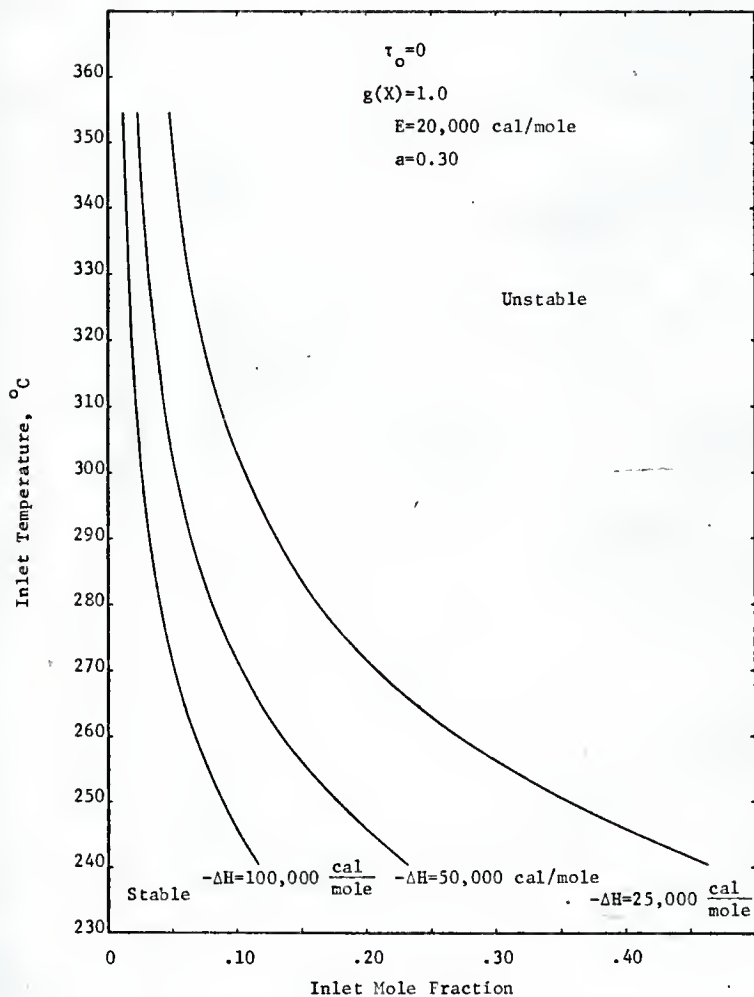


Fig. 21. Critical inlet temperature operating policy for  $a = 0.30$

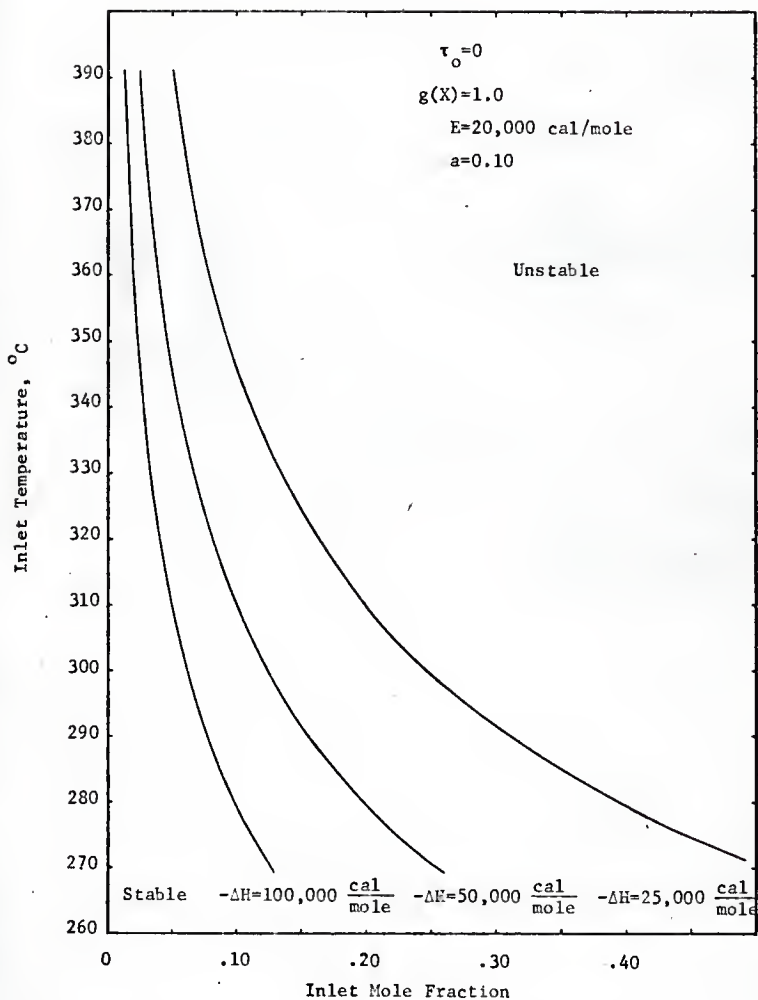


Fig. 22. Critical inlet temperature operating policy for  $a = 0.10$

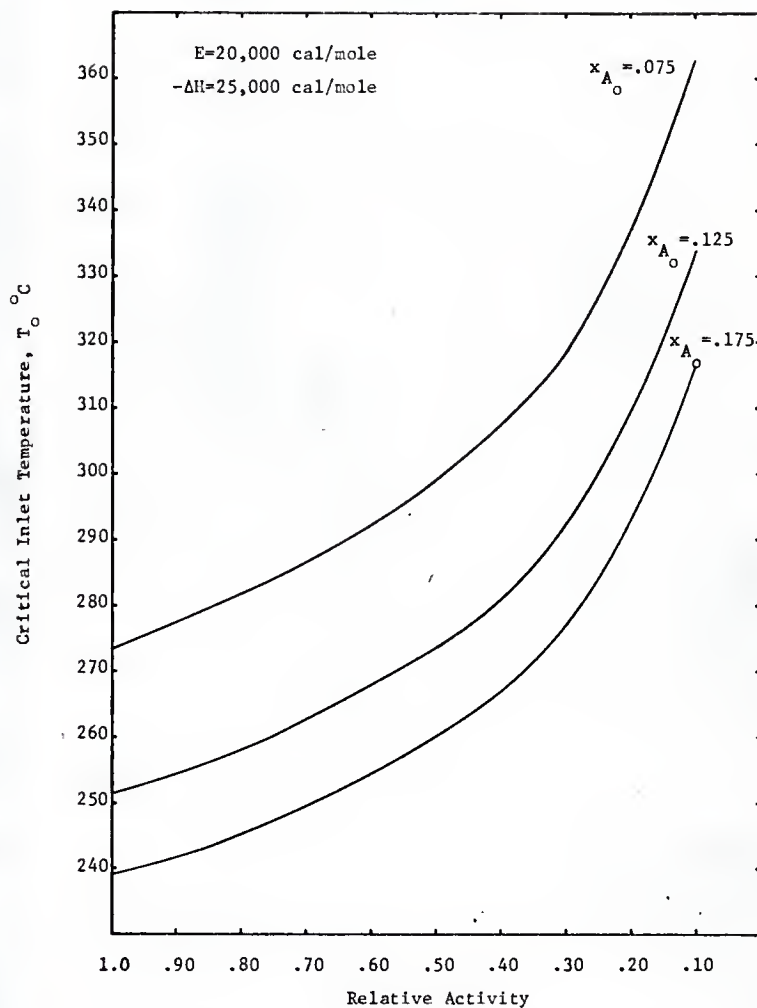


Fig. 23. Effect of activity on the critical inlet temperature for  
 $-\Delta H = 25,000$  cal/mole

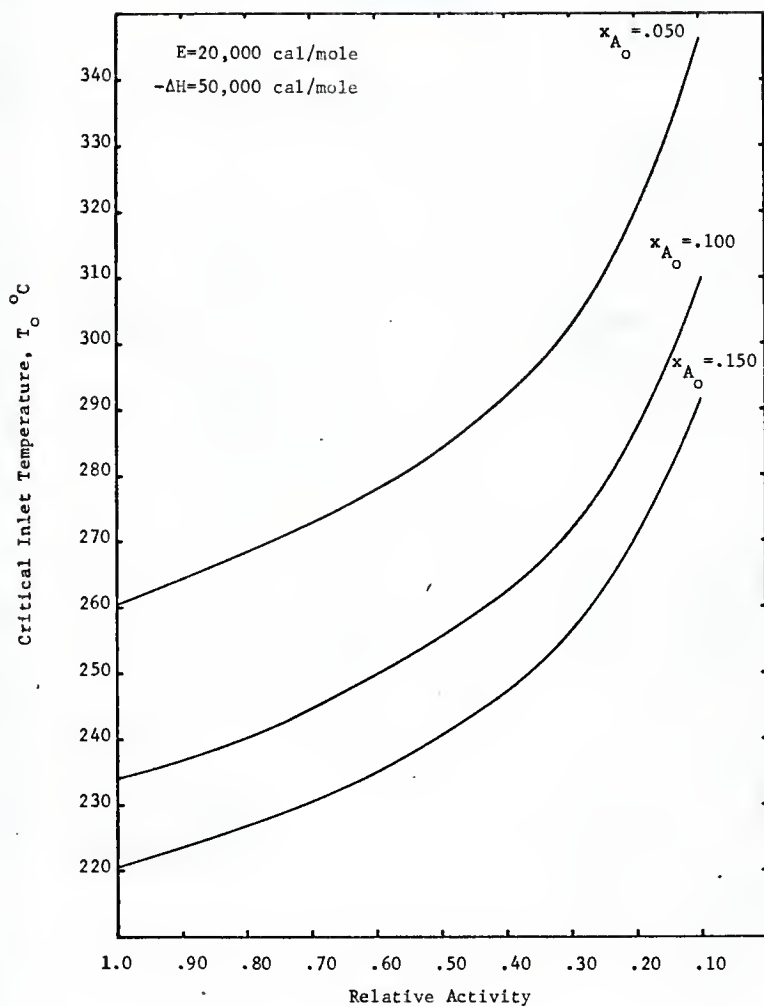


Fig. 24. Effect of activity on the critical inlet temperature for  
 $-\Delta H = 50,000$  cal/mole

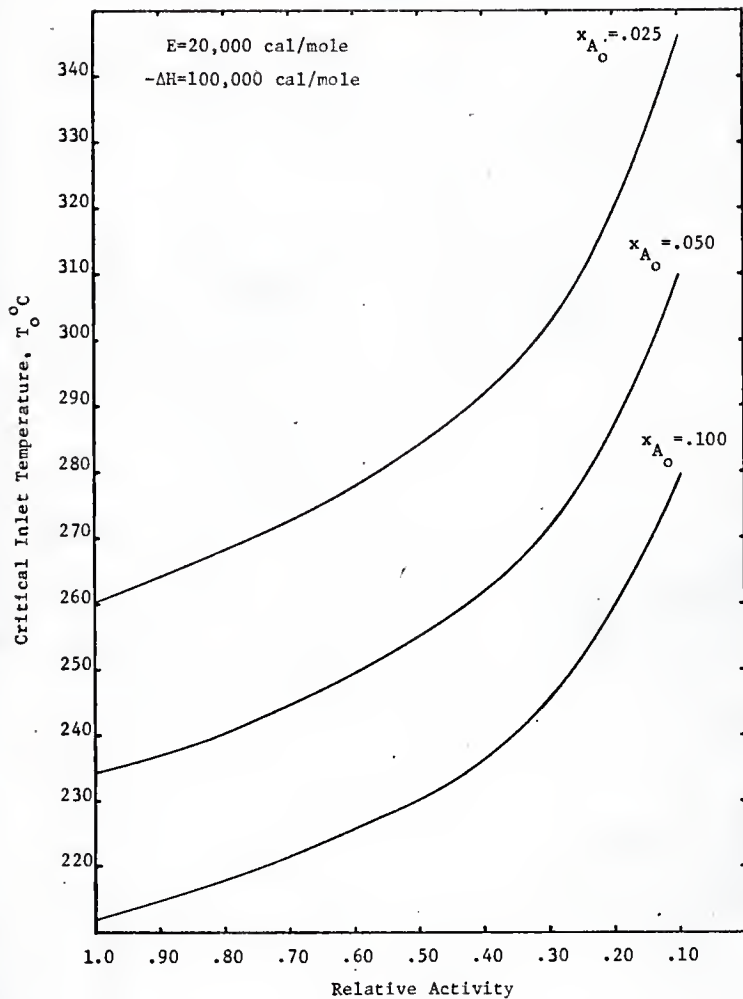


Fig. 25. Effect of activity on the critical inlet temperature for  
 $-\Delta H = 100,000 \text{ cal/mole}$



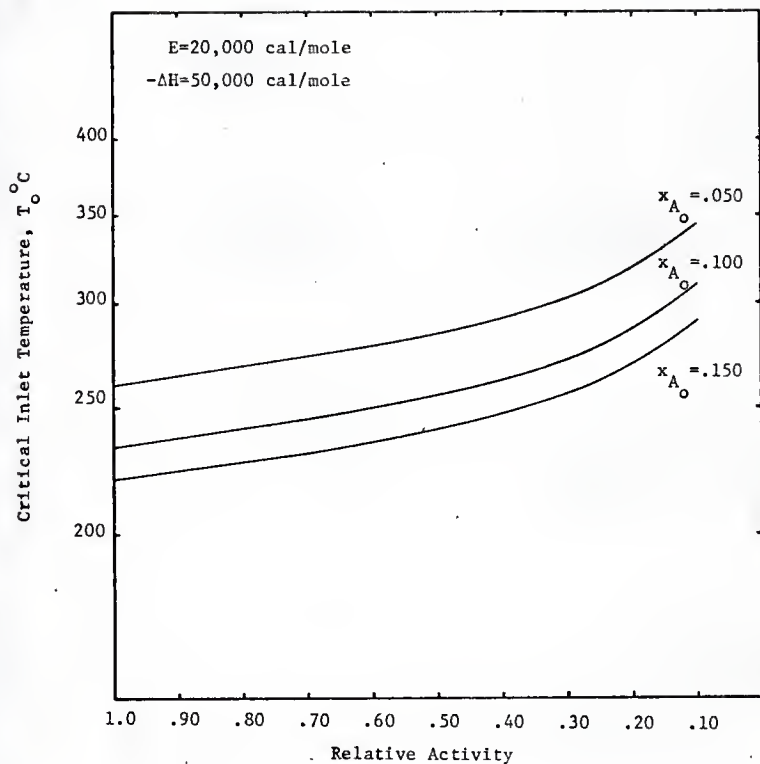


Fig. 26. Semi-log plot of the critical inlet temperature as a function of the activity for  $-\Delta H = 50,000$  cal/mole

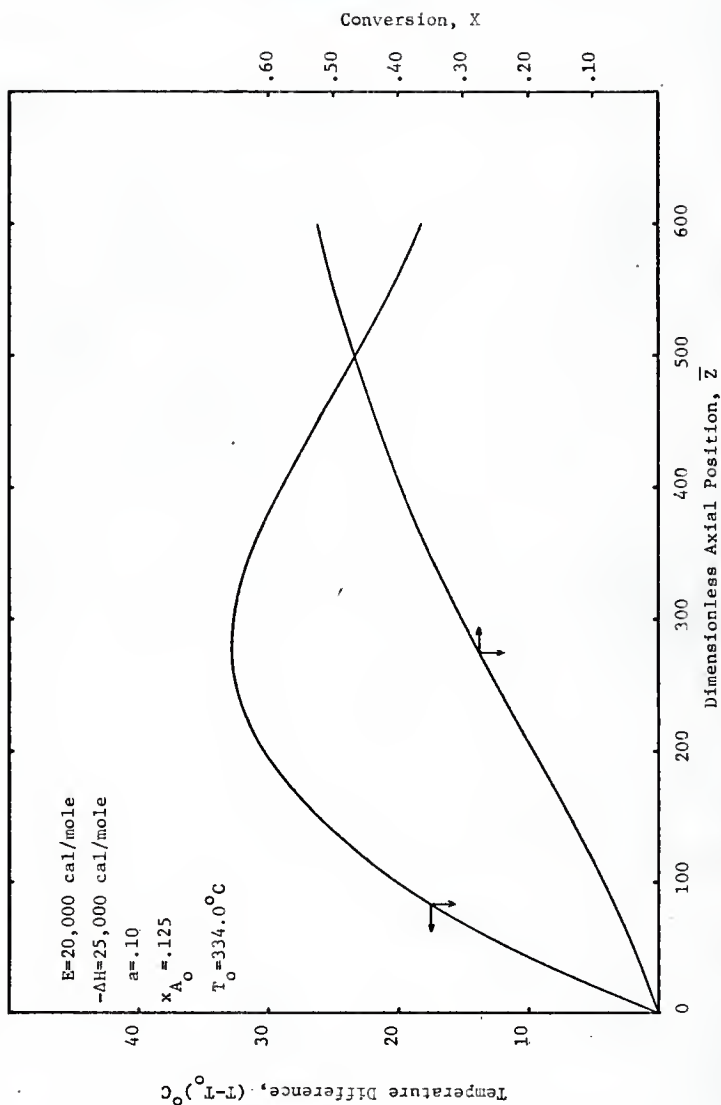


Fig. 27. Typical temperature and conversion profiles for  $-\Delta H = 25,000 \text{ cal/mole}$

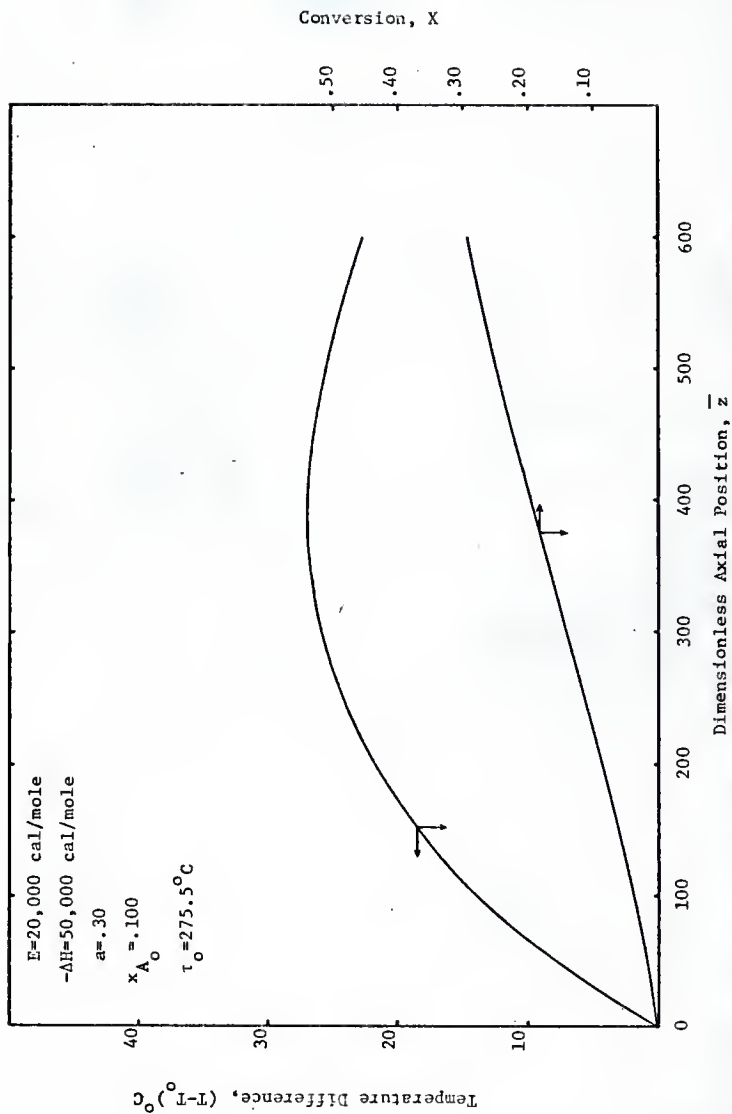


Fig. 28. Typical temperature and conversion profiles for  $-\Delta H = 50,000 \text{ cal/mole}$

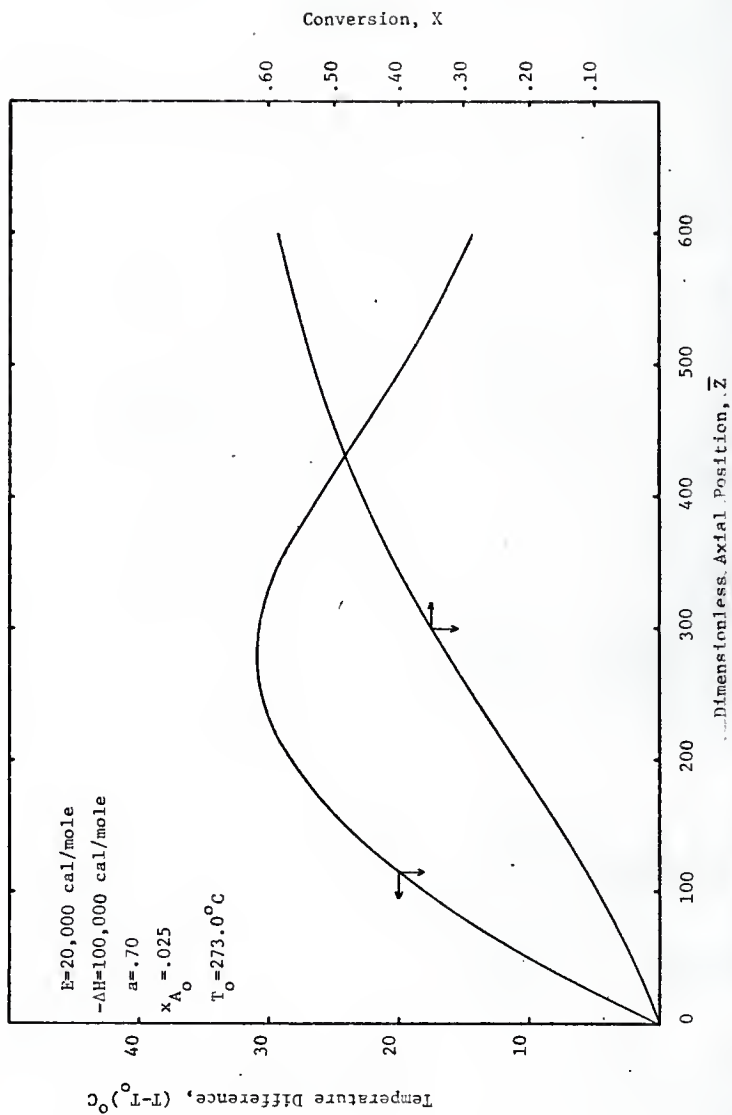


Fig. 29. Typical temperature and conversion profiles for  $-\Delta H = 100,000 \text{ cal/mole}$

of reactant the hotspot occurred in the early sections of the reactor and for the larger inlet mole fractions it occurred in the later sections. The temperature difference,  $T - T_0$ , at the hotspot for the small inlet mole fractions was generally about twice that of the large inlet mole fractions.

The effect of decreased catalyst activity on conversion for the stability limited operational policy is shown in Figures 30, 31 and 32. One point of interest in these figures is the increased conversion which was obtained with a decreased activity. In terms of the operational policy this means it is possible to offset the activity decrease by an increase of the inlet temperature and still maintain a comparable or an increased level of conversion. This would certainly be a major consideration in adopting any operating policy.

The peculiar shape of the curves in these figures is difficult to explain in a distributed system such as this. There appears to be a similarity in a trend towards a relative maximum of the conversion in most cases. However, because the activity is decreasing and the inlet temperature is increasing, it can be expected that the temperature sensitivity of the system is also changing. It is felt there is not sufficient evidence available to draw unwarranted conclusions concerning the existence of an optimum conversion because of three principal reasons. First, the graphical nature of the stability criterion introduces the possibility of graphical error into the inlet temperature operating policy. Second, the operating region being considered is extremely sensitive to small temperature changes and the effect on the conversion at the reactor exit to small temperature variations could be altered by several percent. Third, the relationship between the reaction rate and the temperature is highly complex because of

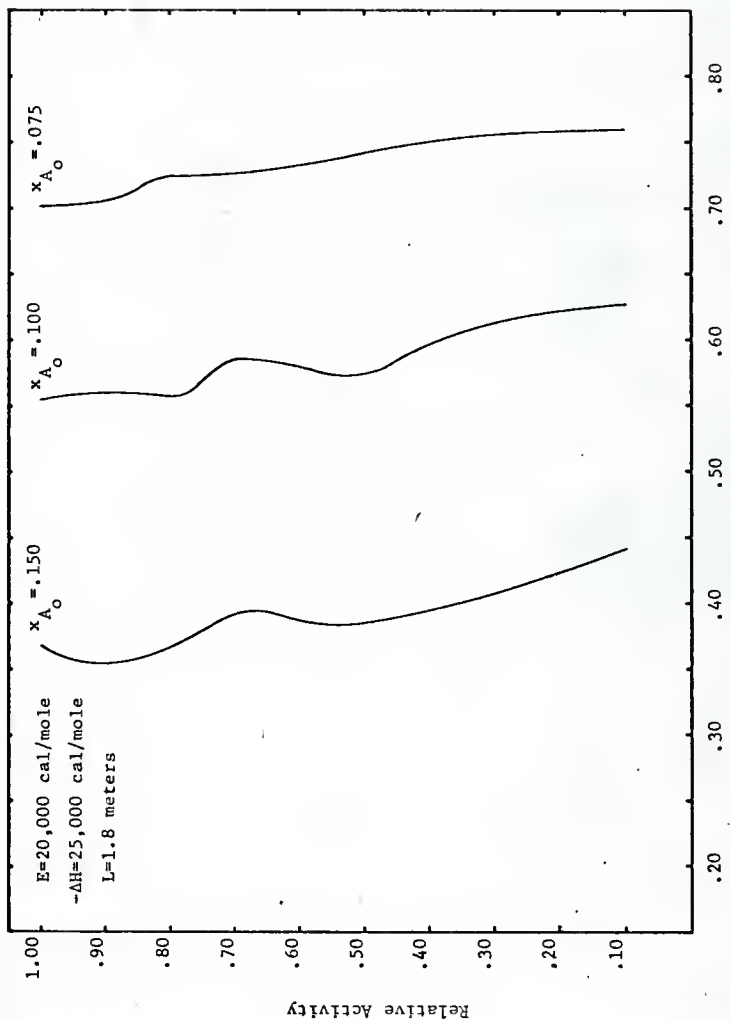


Fig. 30. Effect of activity on the conversion at  $z = L$  for  $-\Delta H = 25,000$  cal/mole

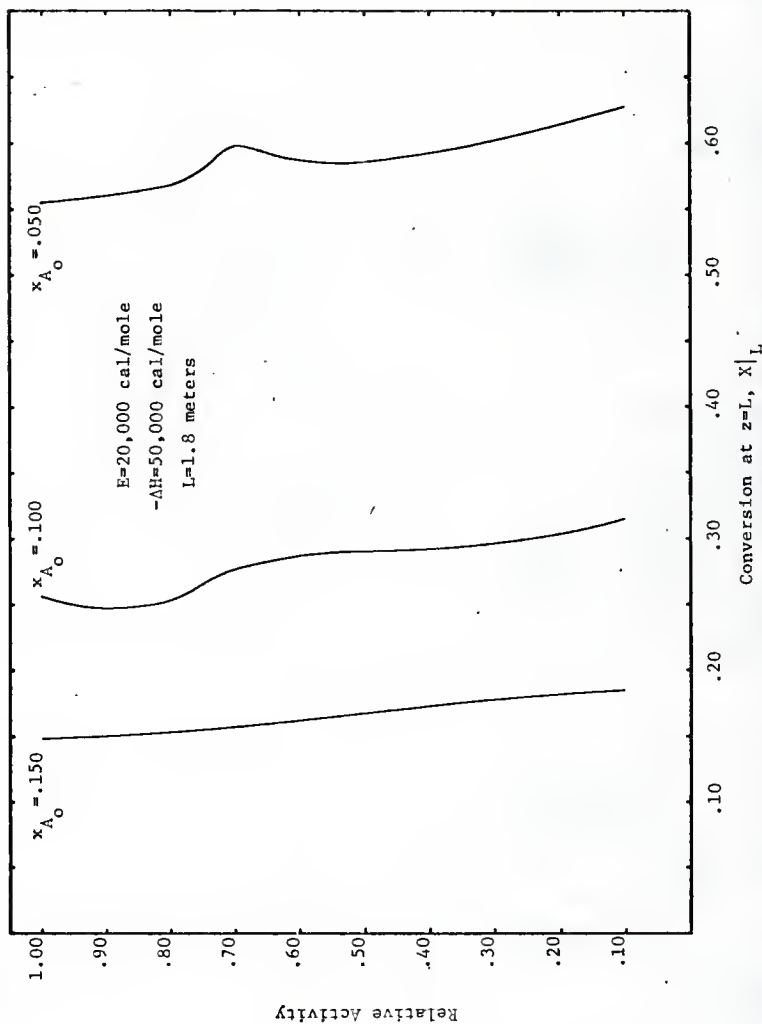


Fig. 31. Effect of activity on the conversion at  $z = L$  for  $-\Delta H = 50,000$  cal/mole

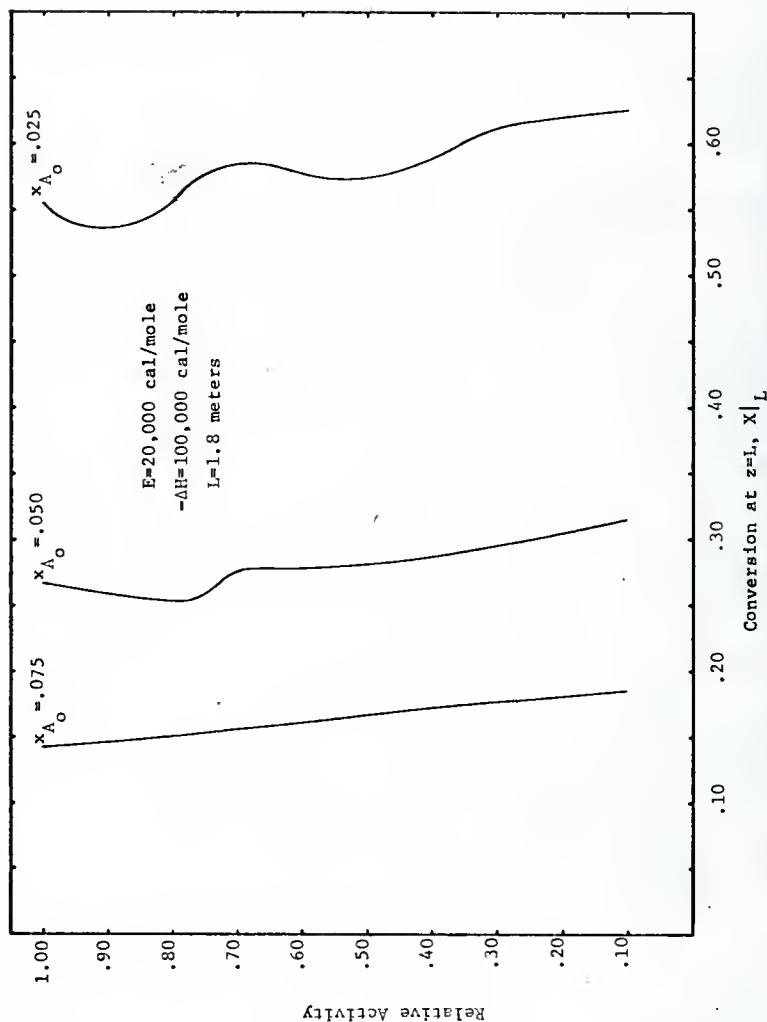


Fig. 32. Effect of activity on the conversion at  $z = L$  for  $-\Delta H = 100,000$  cal/mole



the nonlinearity introduced by the Arrhenius expression.

In order to approximate what effect graphical errors might have on the conversion, an estimate of the graphical error which might be present was made. To do this required returning to the "stability envelopes" and estimating the maximum error possible in plotting the envelope and determining the values of  $(N/S)_{\text{tang}}$ . The error in determining  $(N/S)_{\text{tang}}$  for  $S \geq 6$  was taken to be  $\pm 0.025$ . Conditions where  $S < 6$  were not used in any of the calculations. Using  $(N/S)_{\text{tang}} \pm .025$ , the corresponding critical values of  $T_0$  and  $x_{A_0}$  were calculated and plotted. The results show that this error results in a maximum error in the predicted  $T_0$  of  $\pm 0.50^\circ\text{C}$ . This error is the error which occurs with the graphical prediction of  $T_0$ . It is not the error which might exist between the predicted  $T_0$  and the actual critical inlet temperature. The effect of the  $\pm 0.50^\circ\text{C}$  error in the inlet temperature on the conversion is shown in Figures 33, 34, and 35. Increased conversion was again obtained with a reduced activity compared to the maximum conversion obtained for a relative activity of 1.0.

Although the stability criterion is known to be conservative (1, 2, 12), it was found that reactor runaway occurred in a large number of cases when  $T_0 + 5^\circ\text{C}$  was used as the inlet temperature. A typical case is shown in Figure 36. The prediction of the critical value of the inlet temperature to within a 5 to 10 degree range of the actual critical temperature must be considered a good approximation (2). It also provides a safety factor in choosing an inlet temperature so that fluctuating operating conditions will not cause instability.

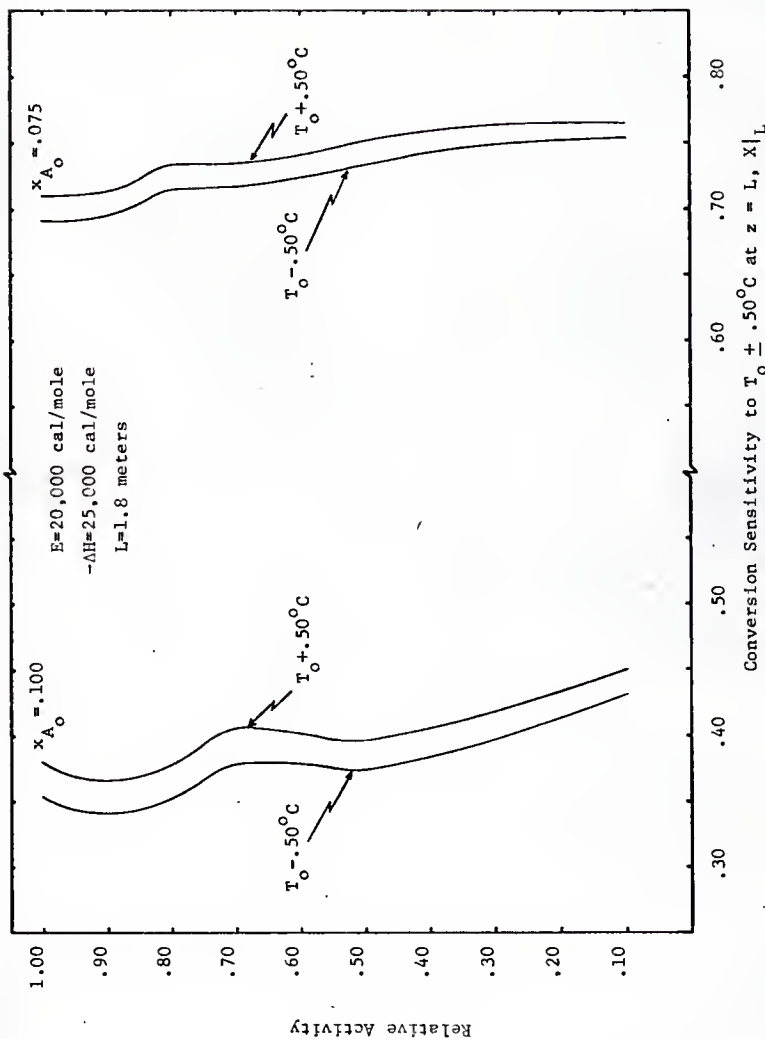


Fig. 33. Sensitivity of the conversion to graphical error for  $-\Delta H = 25,000 \text{ cal/mole}$

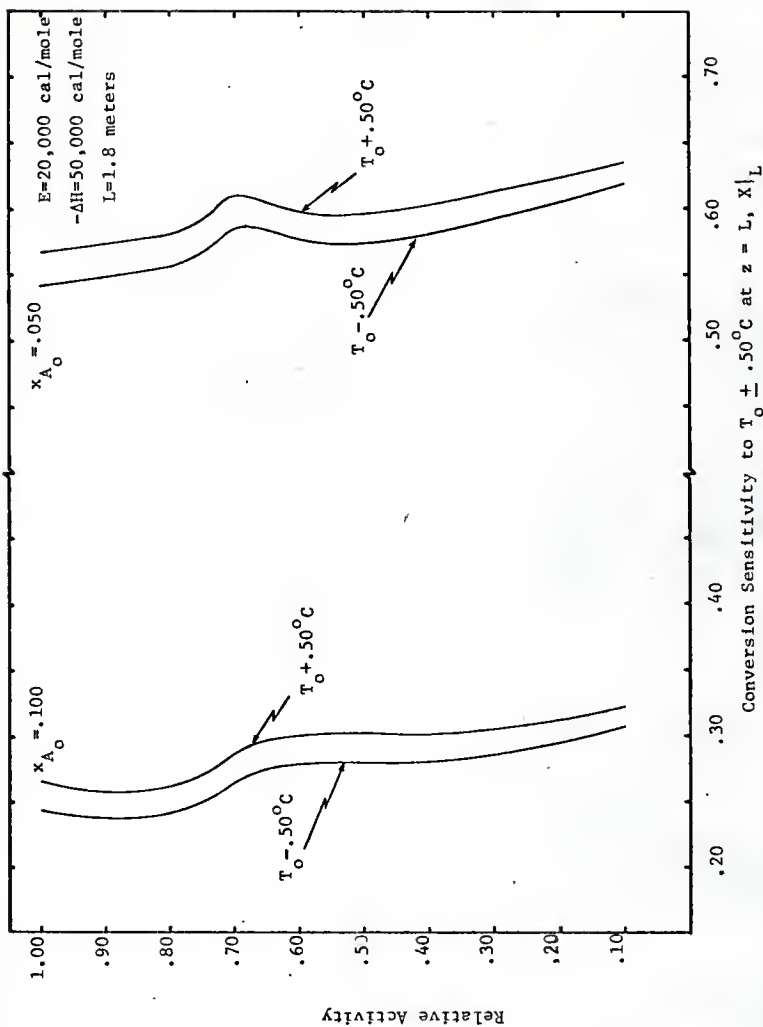


Fig. 34. Sensitivity of the conversion to graphical error for  $-\Delta H = 50,000 \text{ cal/mole}$

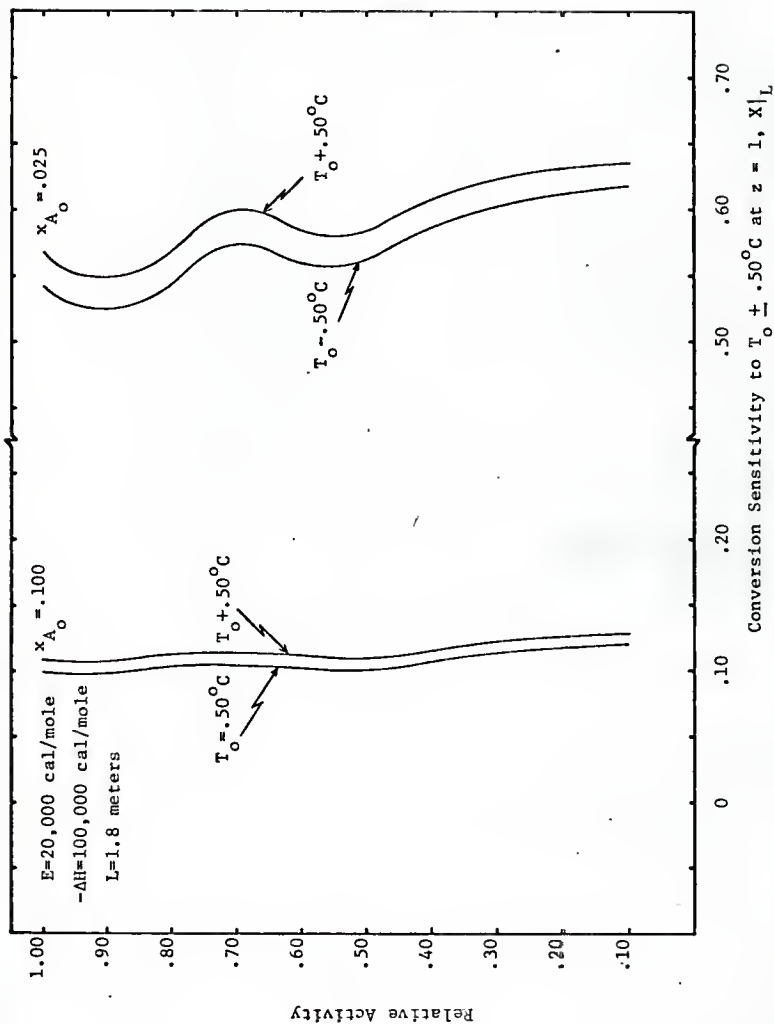


Fig. 35. Sensitivity of the conversion to graphical error for  $-\Delta H = 100,000 \text{ cal/mole}$

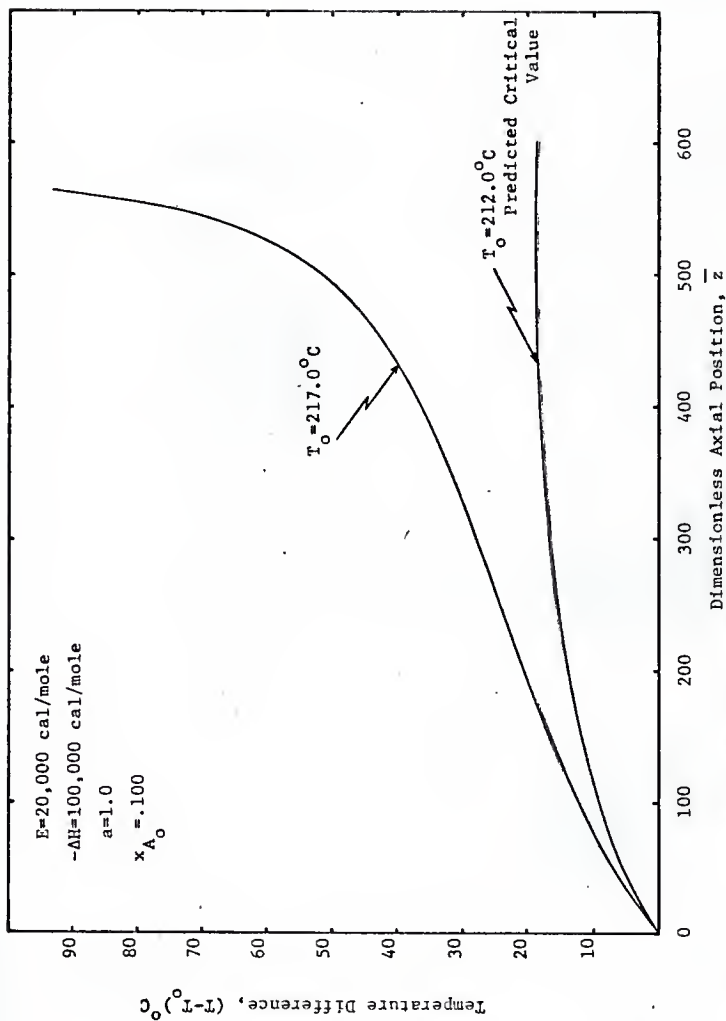


Fig. 36. An example of reactor runaway for  $T_{0\text{CRIT}} + 5.0^{\circ}\text{C}$

#### IV. Negative Sloped Activity Profiles

This section of the thesis is similar to the preceding section except that negative sloped activity profiles have replaced the uniform activity profiles. Stability envelopes are calculated and used to determine the inlet temperature operational policy for the example reactor system. The operational policy and the conversion results are presented graphically.

##### IV.1 Results for Negative Sloped Activity Profiles

In reactors where a poisoning side reaction occurs in series with the main product forming reaction, the catalyst would not be expected to experience uniform poisoning throughout the bed. Generally the catalyst will be poisoned to a greater extent near the reactor exit where the product concentration is the greatest, hence a larger poisoning reaction rate. A linear activity profile was adopted in this work to facilitate the computations. The activity at the reactor inlet was assumed to be unity for all cases of the negative sloped profiles investigated. Activity conditions at the reactor exit of 0.90, 0.70, 0.50, 0.30, and 0.10 were investigated.

To calculate the stability envelopes for the above cases a slightly altered procedure from that used for the uniform activity profiles was necessary. For the uniform activity profiles the relative activity is not a function of the reactor length and Equation 2.3 could be used to determine the stability envelopes. For sloped activity profiles however, the relative activity is a function of the reactor length as given by Equation 2.1. The introduction of the length dependence into Equation 2.3 for these cases requires the simultaneous integration of Equations 2.2 and 2.3 to account for the length dependence. For this case, Equations 2.2 and 2.3 become

$$\frac{d\zeta}{dX} = \frac{e^{-\tau}}{(1-X)(a_o - B\zeta)} \quad 4.1$$

$$\frac{d\tau}{dX} = S - \frac{N\tau e^{-\tau}}{(1-X)(a_o - B\zeta)} \quad 4.2$$

where

$$B = \frac{mG}{ke^{\gamma}T_w} \quad 4.3$$

is an additional dimensionless parameter introduced with the inclusion of the slope of the activity profile. The derivation of these equations is given in the Appendix, Section XI.4. Since B is a function of  $T_w$ , its value cannot be calculated directly until the critical value of  $T_w$  has been determined from the stability criterion. Thus it is necessary to use a trial and error procedure for determining the desired value of B and hence the correct stability envelope for a given set of activity conditions at the reactor inlet and exit. Following are the steps used in the trial and error calculations:

1. For  $a_o=1.0$ , use Equations 4.1 and 4.2 to calculate stability envelopes for various assumed values of B.
2. From the stability envelopes plot  $(N/S)_{\text{tang}}$  versus S for the various values of B.
3. With the results of Step 2, calculate and plot the critical values of  $T_o=T_w$  and  $x_{A_o}$  for each value of B.
4. Using the results of Step 3 plot  $T_o$  versus B for various  $x_{A_o}$  values.
5. Using Equation 4.3 calculate B as a function of  $T_w$  or  $T_o$  and plot the results on the plot of Step 4. The value of m in Equation 4.3 can be determined from the inlet and exit conditions of the activity and the example reactor length, L.

6. The points of intersection of the curves of Step 4 and the curve of Step 5 give the critical values of  $T_o$  for the corresponding  $x_{A_o}$  values. The above steps are illustrated in the following figures. Figure 37 is the stability envelope for  $B=1.0$ . The stability envelope for  $B=0.0$  corresponds to the stability envelope for a uniform activity profile with  $a=1.0$  and shown previously in Figure 14. Additional values of  $B$  which were used are 0.50, 1.50, 2.00, 2.50 and 3.00. These are not shown, but are similar to Figure 37.

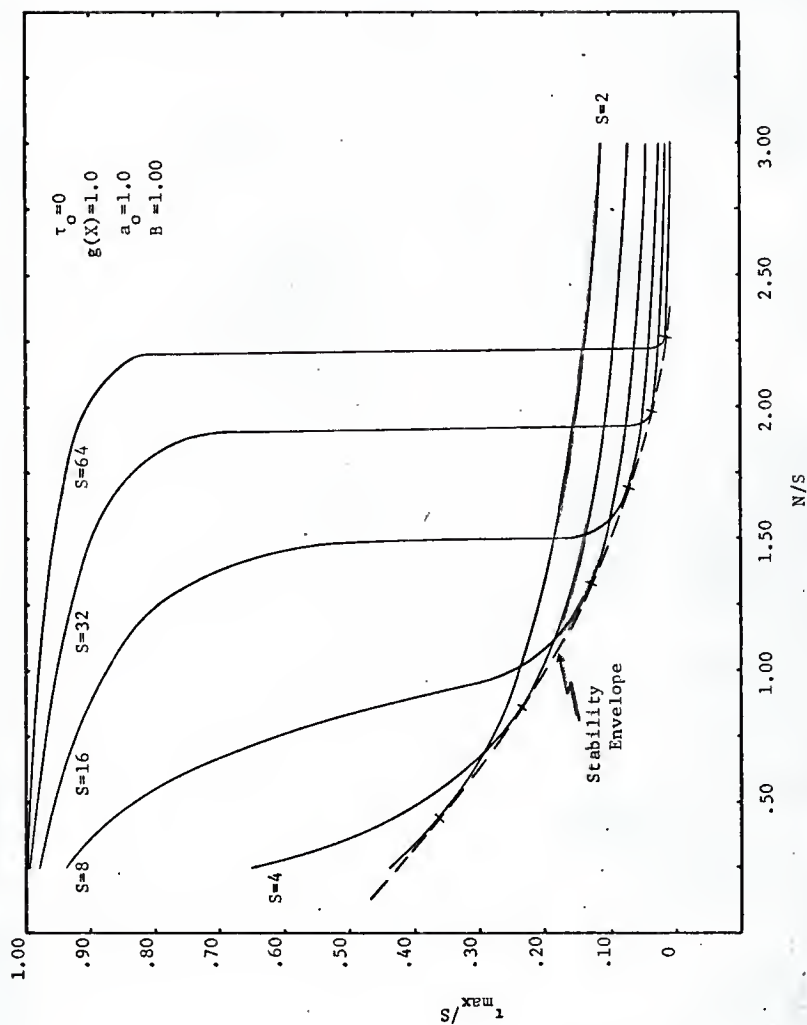
Figure 38 is the graph of the points of tangency,  $(N/S)_{\text{tang}}$ , versus the corresponding values of  $S$ . The curves for  $B=0.50$  and  $B=2.50$  are not shown in the figure but lie between  $B=0.0$  and  $1.0$  and  $B=2.0$  and  $3.0$  respectively.

With points from Figure 38 the critical values of  $T_o$  and  $x_{A_o}$  were calculated for the various values of  $B$ . The calculation procedure is explained in the Appendix, Section XI.2. Figures 39 and 40 show the typical results of this calculation for an activation energy of 20,000 calories per mole.

From the family of curves illustrated by Figures 39 and 40 the critical inlet temperature can be plotted versus  $B$  while holding the inlet mole fraction,  $x_{A_o}$ , constant. This is shown in Figure 41 by the curves labeled  $B_{\text{act}}$ .

Equation 4.3 was then used to calculate the value of  $B$  as a function of  $T_o$ , since  $T_w = T_o$ , for various values of  $m$ . These curves are labeled as  $B_{\text{calc}}$  in Figure 41. The points of intersection of the  $B_{\text{act}}$  and the  $B_{\text{calc}}$  curves are the critical values of the inlet temperature for the corresponding mole fraction. They define an operating policy for the inlet temperature for negative sloped activity profiles. Figure 42 is the operating policy for an activation energy of 20,000 calories per mole and a heat of reaction



Fig. 37. Stability envelope for  $B = 1.00$

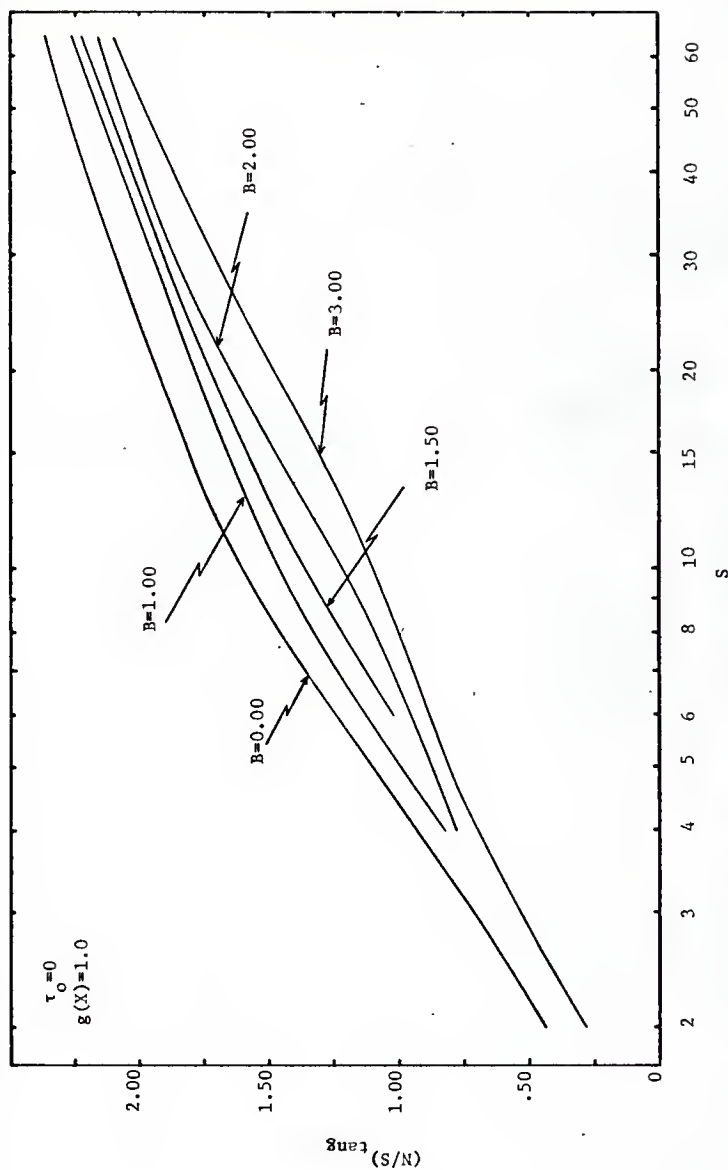


Fig. 38. Stability envelopes for negative sloped activity profiles

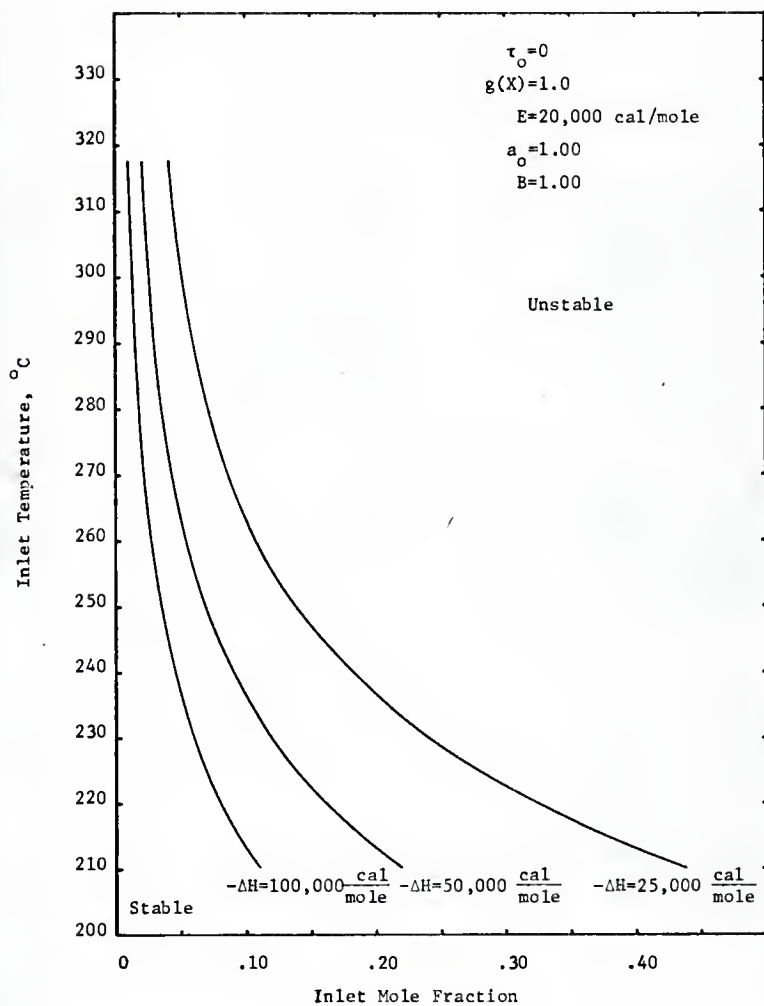


Fig. 39. Critical inlet temperature operating policy for  $B = 1.00$

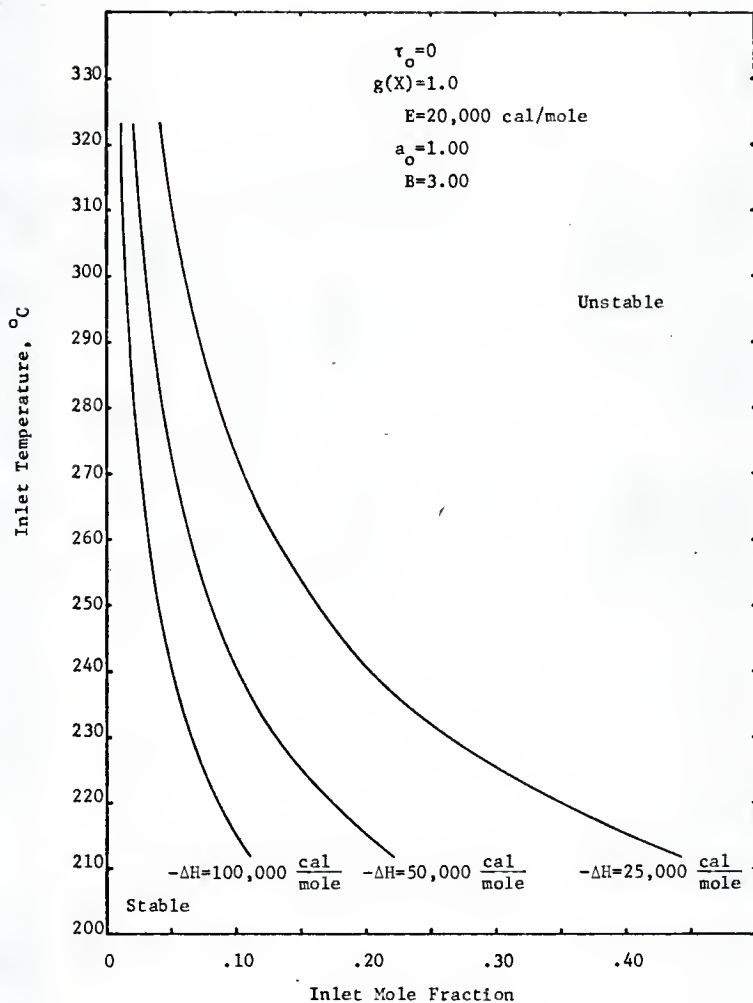


Fig. 40. Critical inlet temperature operating policy for  $B = 3.00$

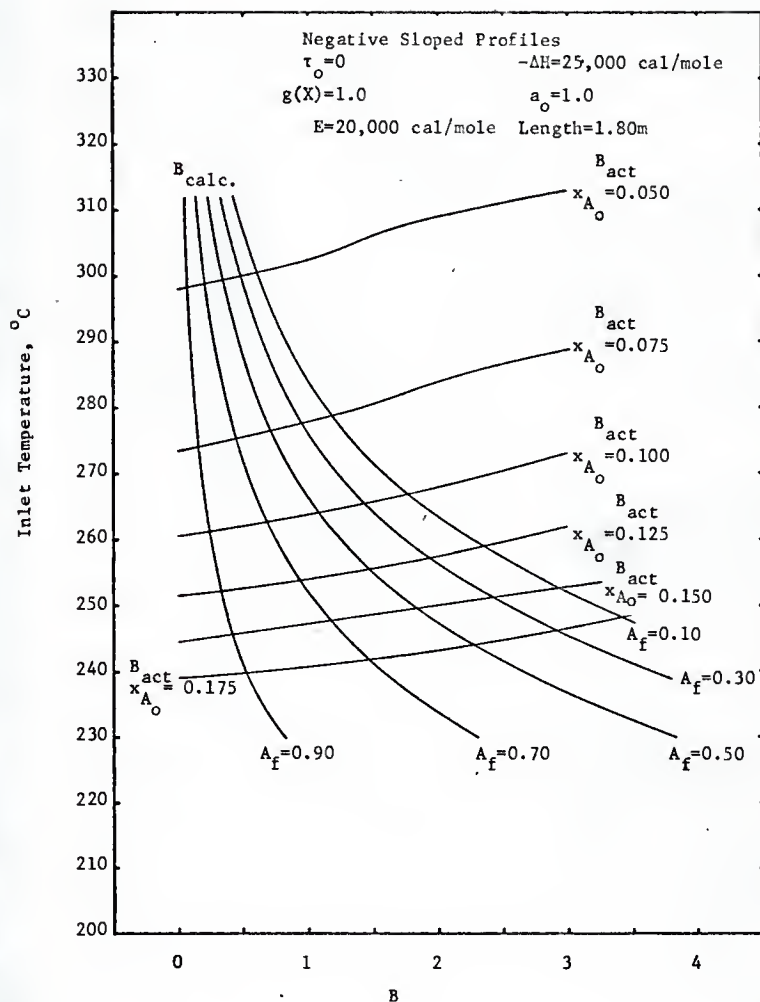


Fig. 41. Critical inlet temperature versus  $B_{\text{act}}$  and  $B_{\text{calc}}$

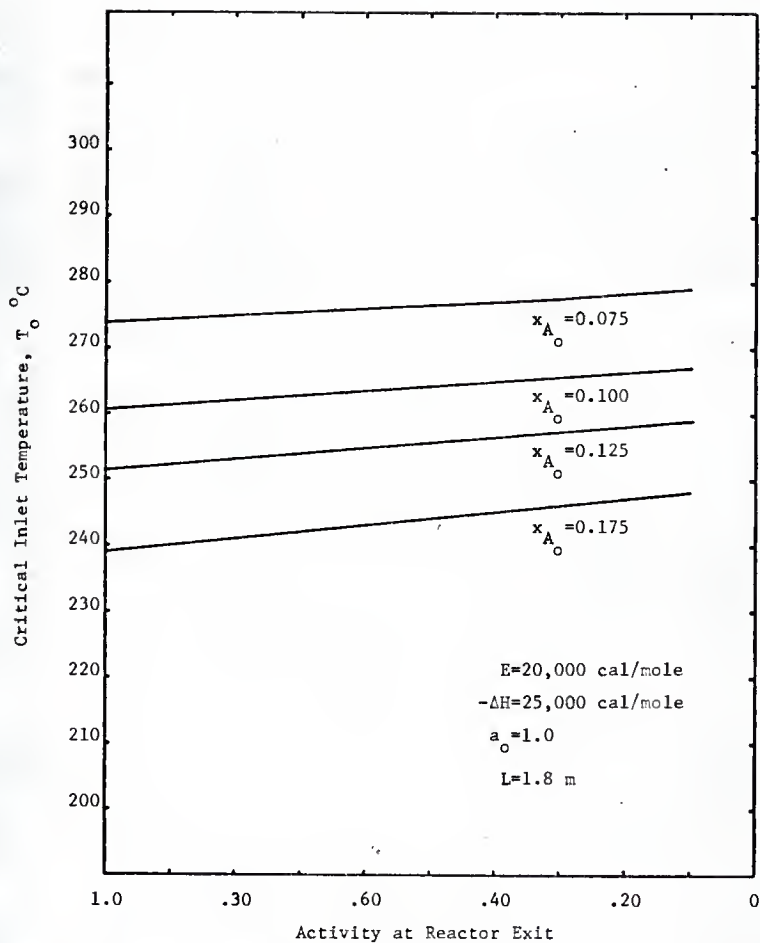


Fig. 42. Effect of the exit activity condition on the critical inlet temperature for  $-\Delta H = 25,000 \text{ cal/mole}$

of 25,000 calories per mole. Similar figures were constructed for heats of reaction of 50,000 and 100,000 calories per mole with an activation energy of 20,000 calories per mole. The operating policies for these cases are shown in Figures 43 and 44 for the indicated parameter values. It is of interest to note that the critical value of the inlet temperature approximates a linear increase with the decrease of the exit activity in these figures.

As in the previous section the results of the stability limited operational policies were applied to the example reactor system. Figures 45, 46 and 47 show typical temperature and conversion profiles for the parameter combinations indicated. In these figures the hotspot temperature occurs closer to the reactor entrance than it did when uniform activity profiles were used. It was also observed that as the heat of reaction was increased the hotspot moved toward the exit of the reactor. The magnitude of the temperature difference,  $T - T_0$ , remained unchanged as the heat of reaction was varied. It was again found that the magnitude of  $(T - T_0)$  increased as the inlet mole fraction was decreased, but the increase was not as great as it was for the uniform activity profiles.

The effect on the conversion in the example reactor system when negative sloped activity profiles were used is shown in Figures 48, 49 and 50. These figures correspond to an activation energy of 20,000 calories per mole and heats of reaction of 25,000, 50,000 and 100,000 calories per mole respectively. It is apparent from the figures that increased conversion can not be obtained with negative sloped activity profiles. Further the figures show that as poisoning decreases the activity it is not possible to increase the inlet temperature enough to counteract the loss of activity. The result is a loss

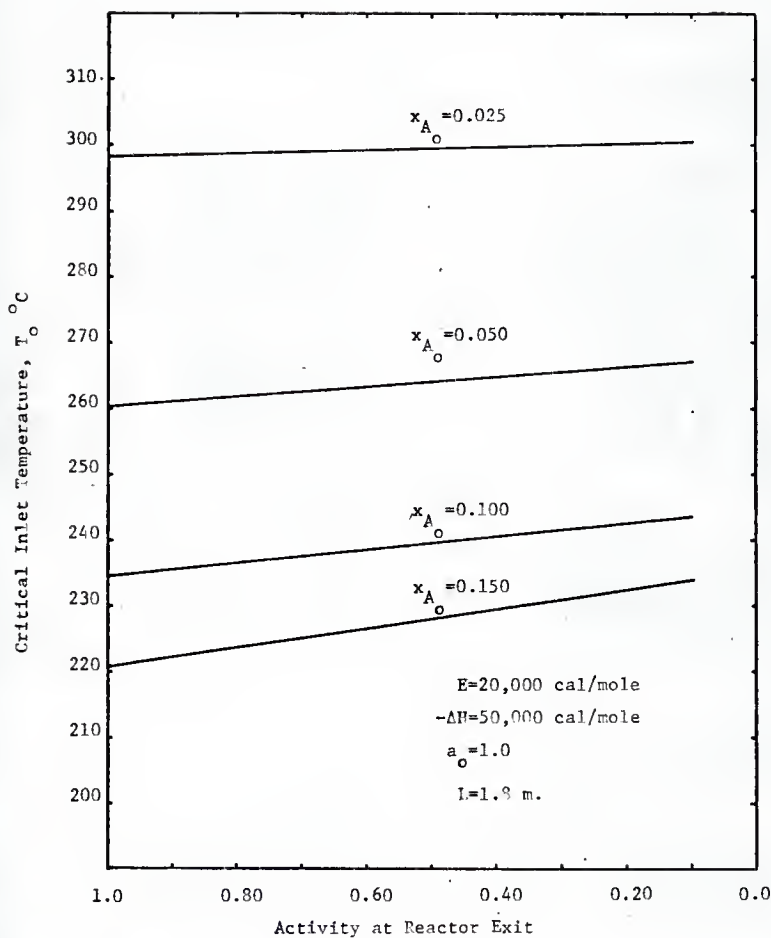


Fig. 43. Effect of the exit activity condition of the critical inlet temperature for  $-\Delta H = 50,000$  cal/mole



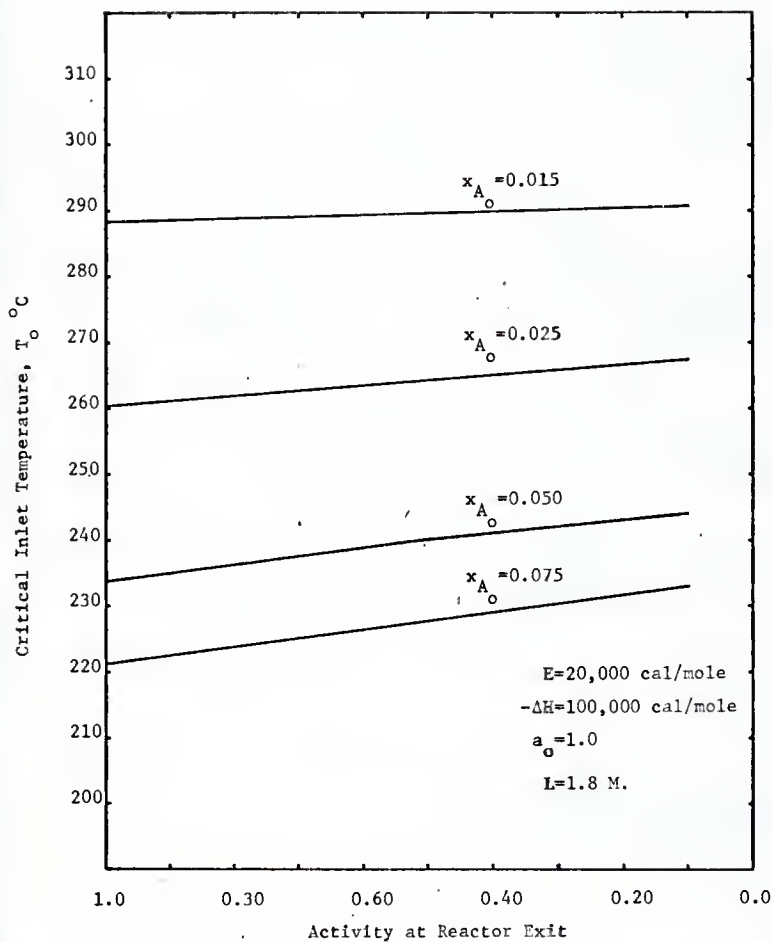


Fig. 44. Effect of the exit activity condition on the critical inlet temperature for  $-\Delta H = 100,000$  cal/mole

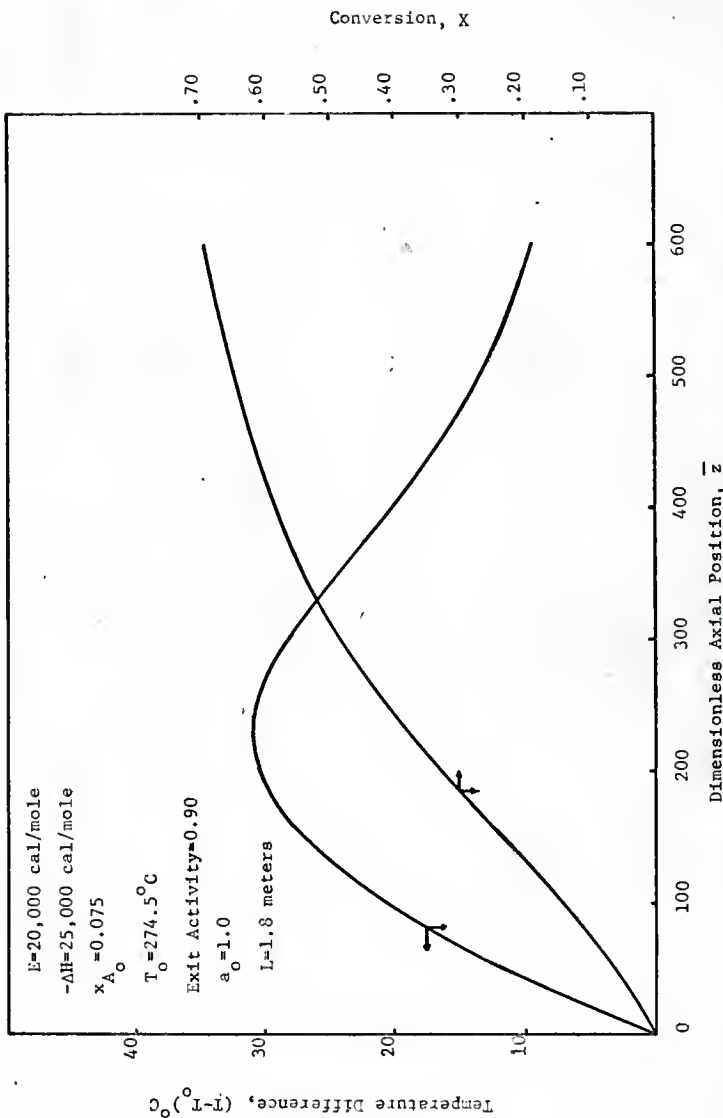


Fig. 45. Typical temperature and conversion profiles for an exit activity of 0.90.

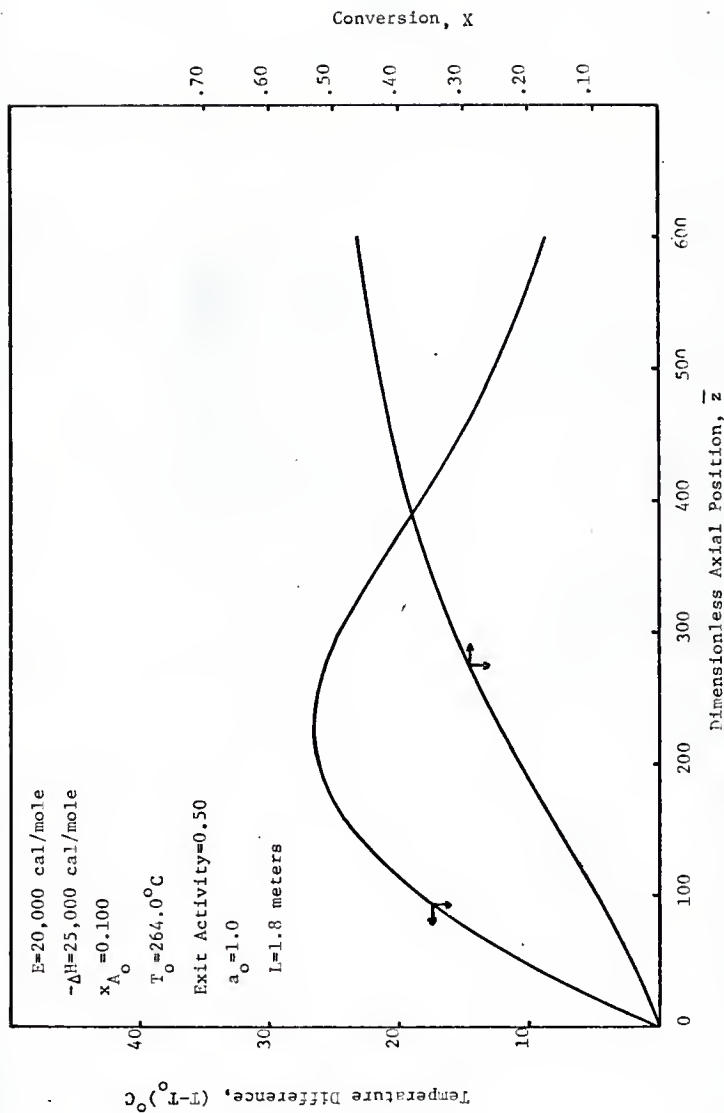


Fig. 46. Typical temperature and conversion profiles for an exit activity of 0.50

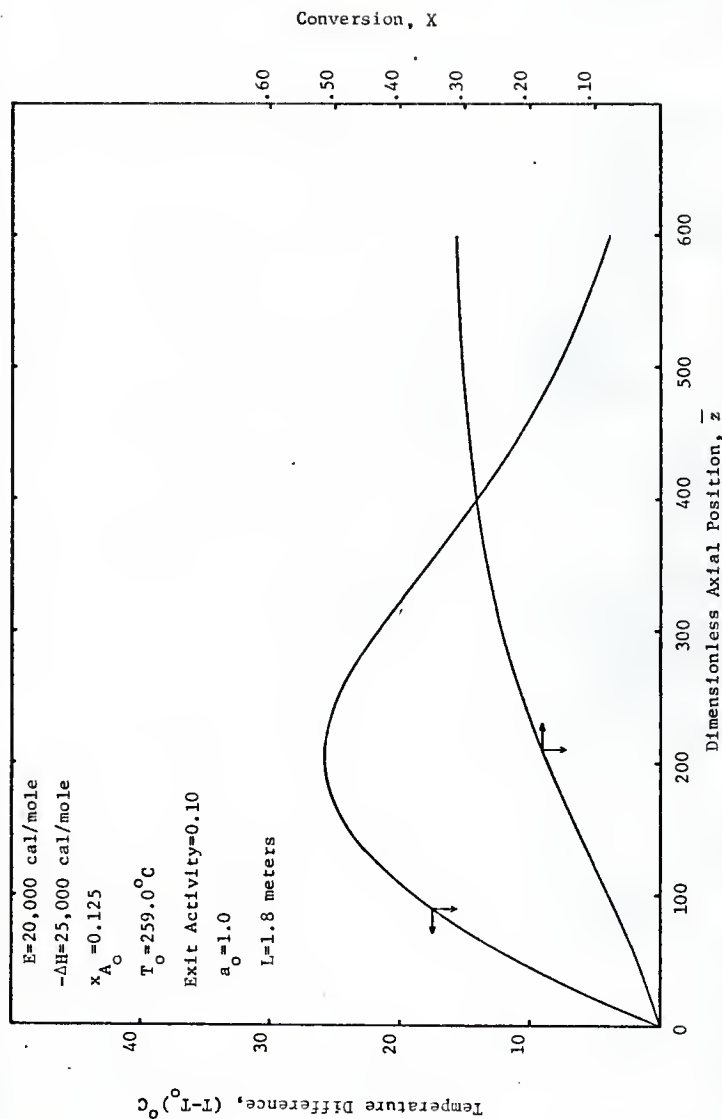


Fig. 47. Typical temperature and conversion profiles for an exit activity of 0.10

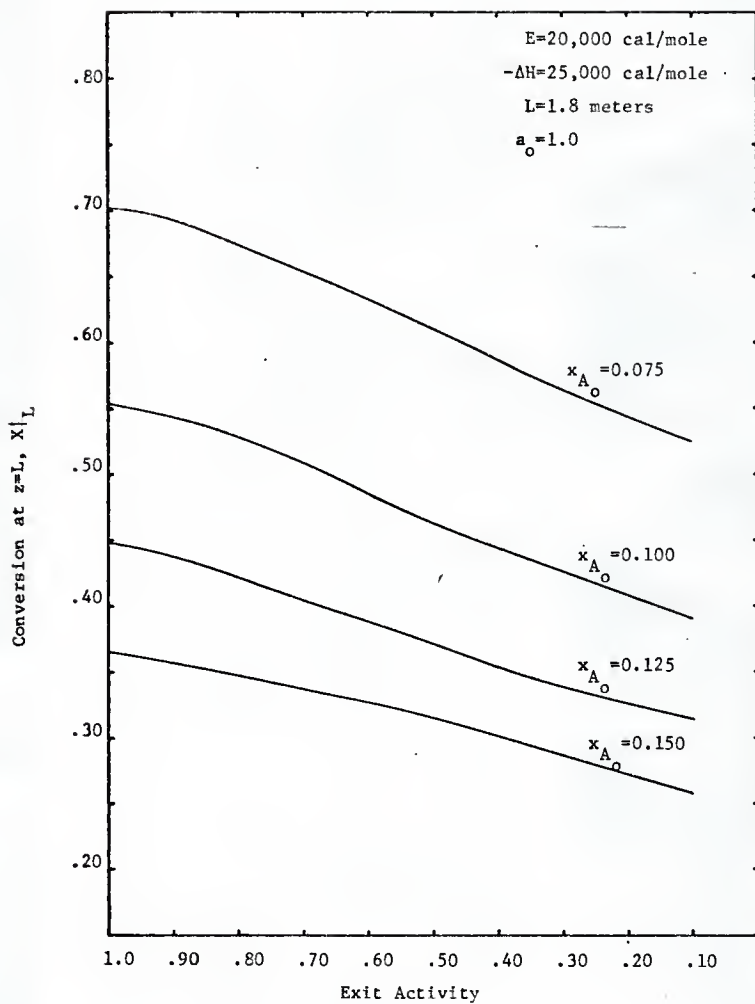


Fig. 48. Effect of the exit activity condition on the conversion at  $z = L$  for  $-\Delta H = 25,000$  cal/mole

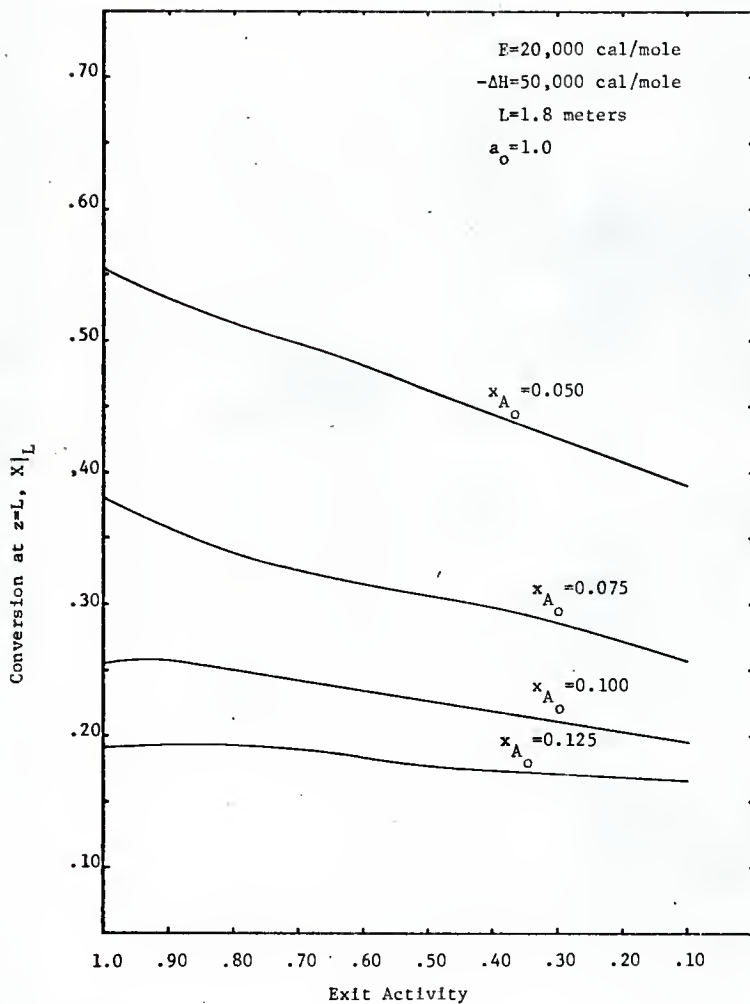


Fig. 49. Effect of the exit activity condition on the conversion at  $z = L$   
for  $-\Delta H = 50,000$  cal/mole

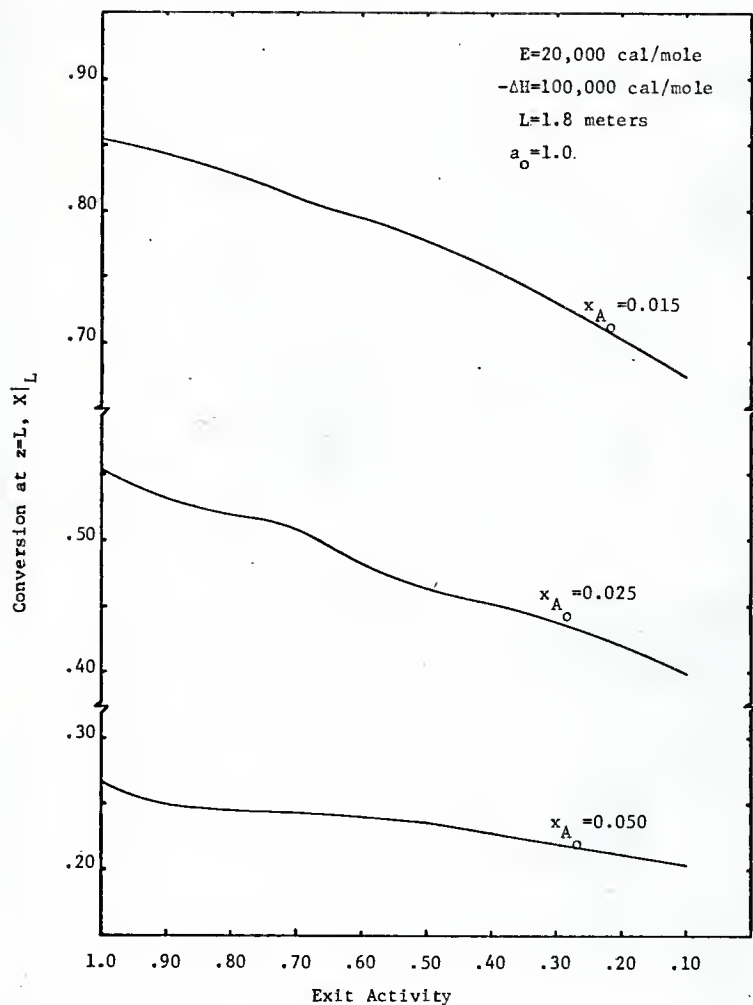


Fig. 50. Effect of the exit activity condition on the conversion at  $z = L$  for  $-\Delta H = 100,000$  cal/mole

of conversion because of poisoning even when operating at the stability limit of the reactor. More will be said about the apparent reasons for the decrease in conversion in Section VI. It can be concluded at this point, however, that for a physical system which could be approximated by a linear negative sloped activity profile, the operating policy generated above would generally not be acceptable. The above results suggest frequent regeneration of the catalyst before severe poisoning is incurred. Such a policy would depend on economic factors associated with each particular case and is not in the scope of this work.

Figure 51 shows that although the stability criterion is conservative it predicts the critical value of the inlet temperature to within a 5 to 10 °C range of the actual critical value. It is felt that Figure 51 and similar such cases validate the trial and error procedure used in determining the critical operating policy for the inlet temperature.



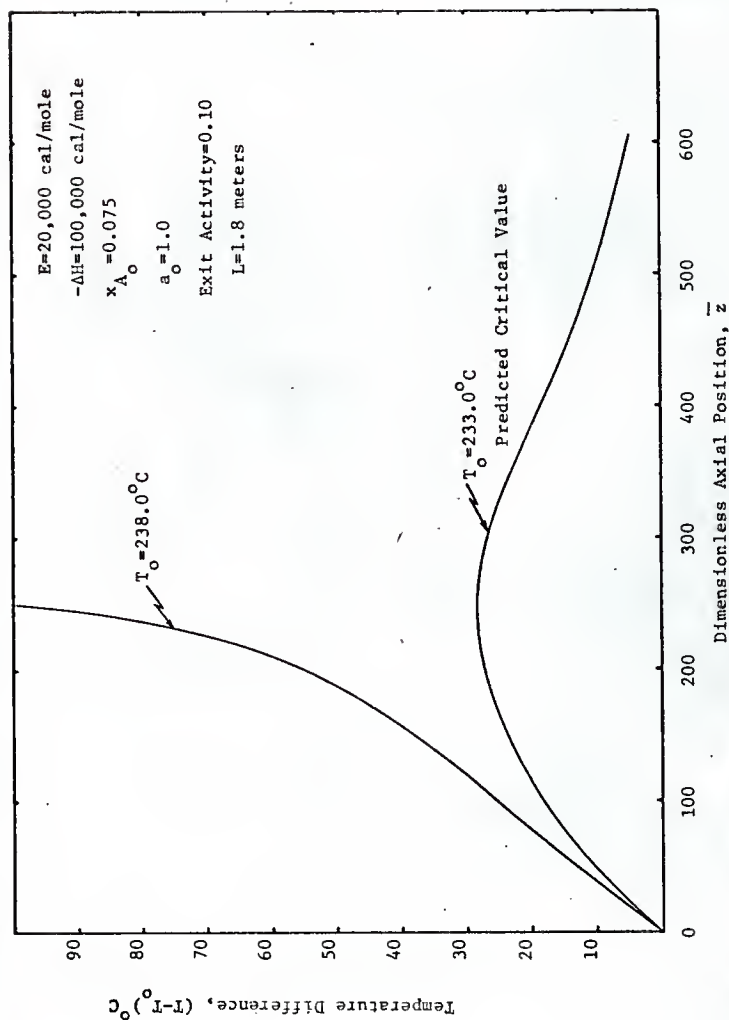


Fig. 51. An example of reactor runaway for  $T_{0\text{CRIT}} + 5.0^\circ\text{C}$

## V. Positive Sloped Activity Profiles

In this section positive activity profiles are treated in a manner similar to that used in the preceding section for the negatively sloped activity profiles. An operational policy for the stability limited inlet temperature was developed from the stability envelopes and then applied to the example reactor system. Representative results are presented in graphical form.

### V.1 Results for Positive Sloped Activity Profiles

Reactor systems in which catalyst deactivation occurs as the result of a poisoning reaction in parallel with the main reaction will generally experience a greater degree of catalyst poisoning near the reactor inlet. This will also be the case when a poison is introduced with the reactants.

The procedures used in determining the stability limited inlet temperature operating policy are identical to those of the previous section with two changes. One of these concerns the conditions set for the activity at the reactor inlet and exit. The relative activity at the reactor exit was assumed to be unity for all cases considered. Relative activities of 0.70, 0.30 and 0.10 were investigated for the inlet activity condition.

The second change appears in the form of a constraint on  $\tau$  which it was found necessary to impose when numerically integrating Equations 4.1 and 4.2. For the negative sloped activity profiles, the dimensionless temperature,  $\tau$ , experienced a maximum during the early part of the activity profile. When the inlet activity was decreased considerably, however, it was found for a great many combinations of  $N$  and  $S$  that  $\tau$  possessed no real maximum. Rather,  $\tau$  continually increased along the activity profile. In these cases, the maximum value of  $\tau$  was taken to be its value when the

activity profile reached unity at the reactor exit. Physically this means that the reduced activity at the reactor inlet retarded the reaction rate to such an extent that no appreciable reaction occurred until the later stages of the activity profile.

Incorporating these two changes into the trial and error procedure described in Section IV, stability envelopes were constructed for values of  $B$  ranging from zero to minus five.  $B$  takes on minus values in these calculations to remain consistent with the defining equation, Equation 2.1, for the linear activity profiles. A series of stability envelopes was necessary for each inlet activity condition. The envelopes presented here are for  $a_0 = 0.30$ . Similar results were obtained for  $a_0 = 0.70$  and  $a_0 = 0.10$ , but have not been included.

Figures 52 and 53 are stability envelopes for  $B = -2.00$  and  $B = -4.00$  with  $a_0 = 0.30$ . It is readily apparent that the shape of these envelopes is somewhat different than those in the previous sections. This difference can be attributed to the constraint on  $\tau$  described above. To see this more clearly Figure 54 was constructed to show the relationship between the point at which  $\tau_{\max}$  was achieved and the ratio of  $N/S$  for the various values of  $S$ . In this figure  $\zeta = .35$  corresponds to the reactor length at which the activity reaches unity, i.e. the reactor exit. A real maximum for  $\tau$  occurs only on the portions of the  $S$ -curves which lie to the left of  $\zeta = .35$ . Any point on  $\zeta = .35$  corresponds to an artificial  $\tau_{\max}$  at the reactor exit. Thus in Figure 52 the stability envelope is forced into a convex curve by the extreme dependence on the reactor length exhibited by the  $S$ -curves for  $S=2, 4$ , and  $8$ . A similar phenomena exists for all the stability envelopes constructed with positive sloped activity profiles.

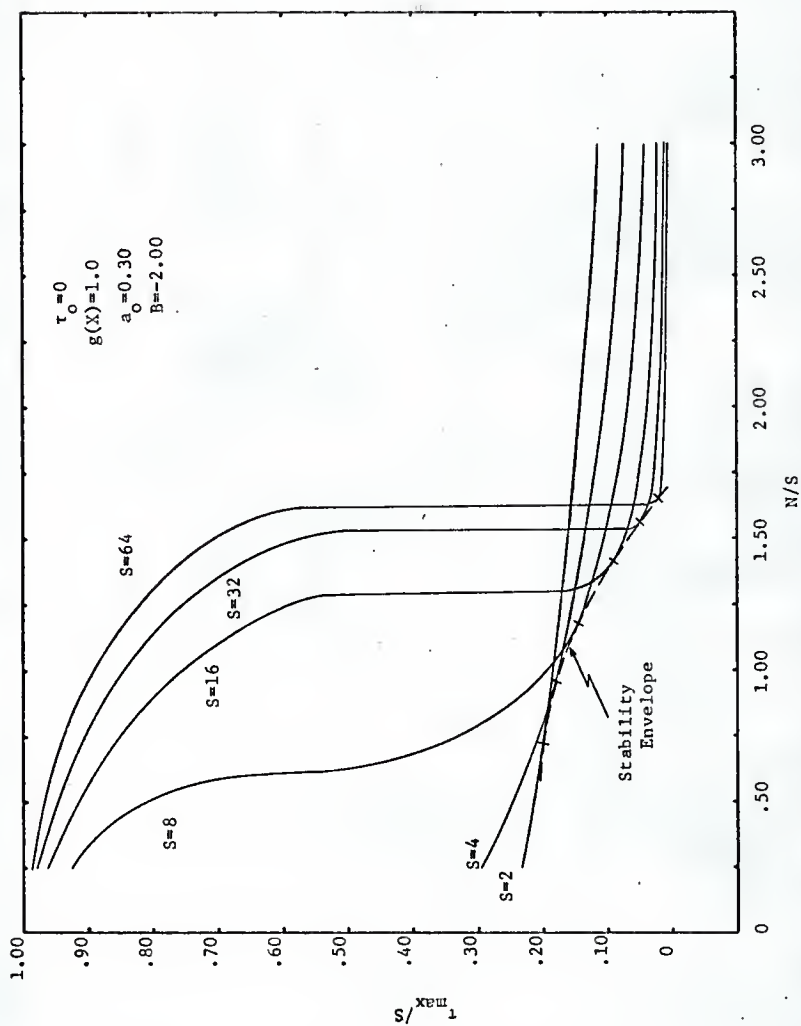


Fig. 52. Stability envelope for  $B = -2.00$  and  $a_0 = 0.30$

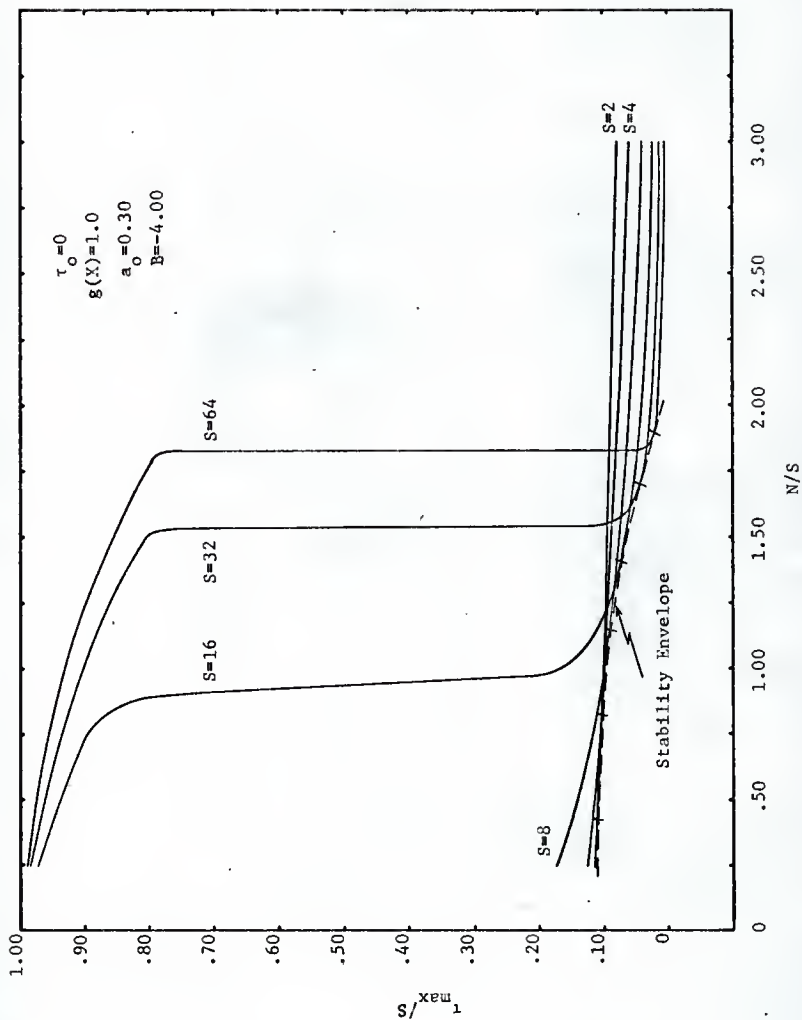


Fig. 53. Stability envelope for  $B = -4.00$  and  $a_o = 0.30$

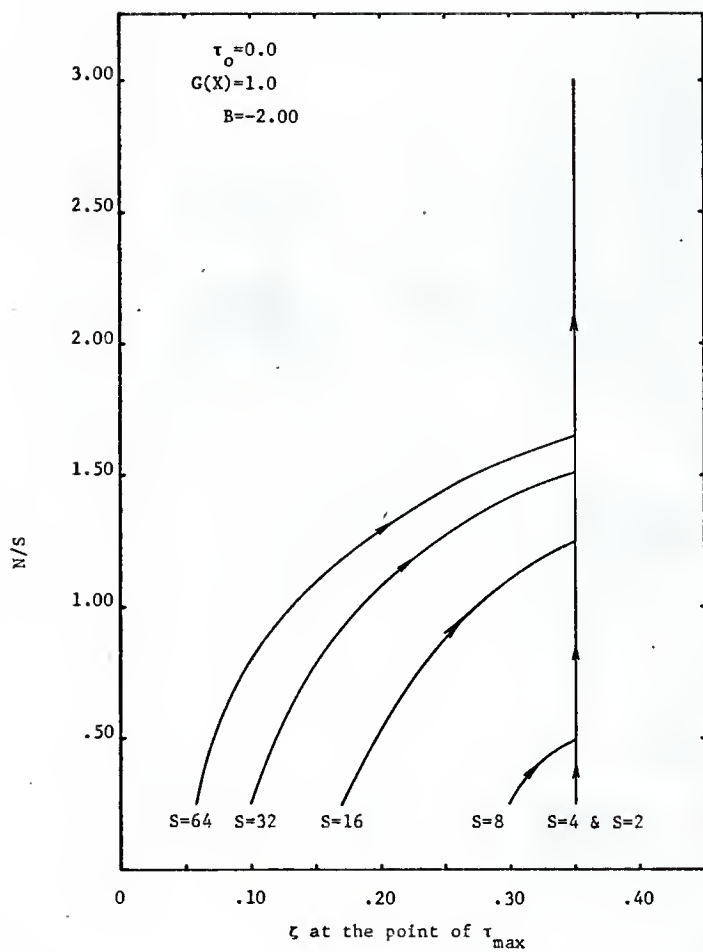


Fig. 54.  $\zeta$  at the point of  $\tau_{\max}$  for  $B = -2.00$  and  $a_o = 0.30$

The convex nature of the envelopes effects the stability criterion by making it more conservative in some regions and less conservative in others. In Figure 52 the points of tangency of the S-curves and the envelope for  $S \geq 16$  are positioned very near the extremely sensitive temperature region. The tangency points for  $S < 16$ , however, appear to have experienced an opposite effect, i.e. they have been shifted into an insensitive temperature region. In Figure 53 all points of tangency have been shifted to the right away from the very sensitive temperature regions of the S-curves. These effects are shown in Figure 55, the plot of the stability envelopes for the various values of B.

In Figure 55 the curve labeled  $B=0.0$  is the stability envelope which corresponds to the uniform activity profile with a relative activity of 1.0. The value of B decreases as the slope of the activity profiles increases in correspondence with Equation 2.1. As B decreases, the effect of the convex stability envelopes becomes increasingly more noticeable. The curves for  $B=-4.00$  and  $B=-5.00$  show the most severe effect. Each of these two curves intersects the other and the  $B=-2.00$  and  $B=-3.00$  curves at two different points. For values of  $S \leq 8$ , however, the validity of these curves must be questioned. This can be seen from Figure 53 where the points of tangency are arbitrary for  $S \leq 8$ . To exclude the possibility of large graphical errors, values for  $S < 8$  were not used in the remaining work.

Operating policies for the stability limited inlet temperatures were generated for the three conditions of the inlet activity in the usual manner. Combinations of an activation energy of 20,000 calories per mole with heats of reaction of 25,000, 50,000 and 100,000 calories per mole were used. Figure 56 shows the critical inlet temperature as a function of the inlet mole fraction for  $B=-2.00$  and  $a_0=0.30$ . This plot corresponds to Step 3

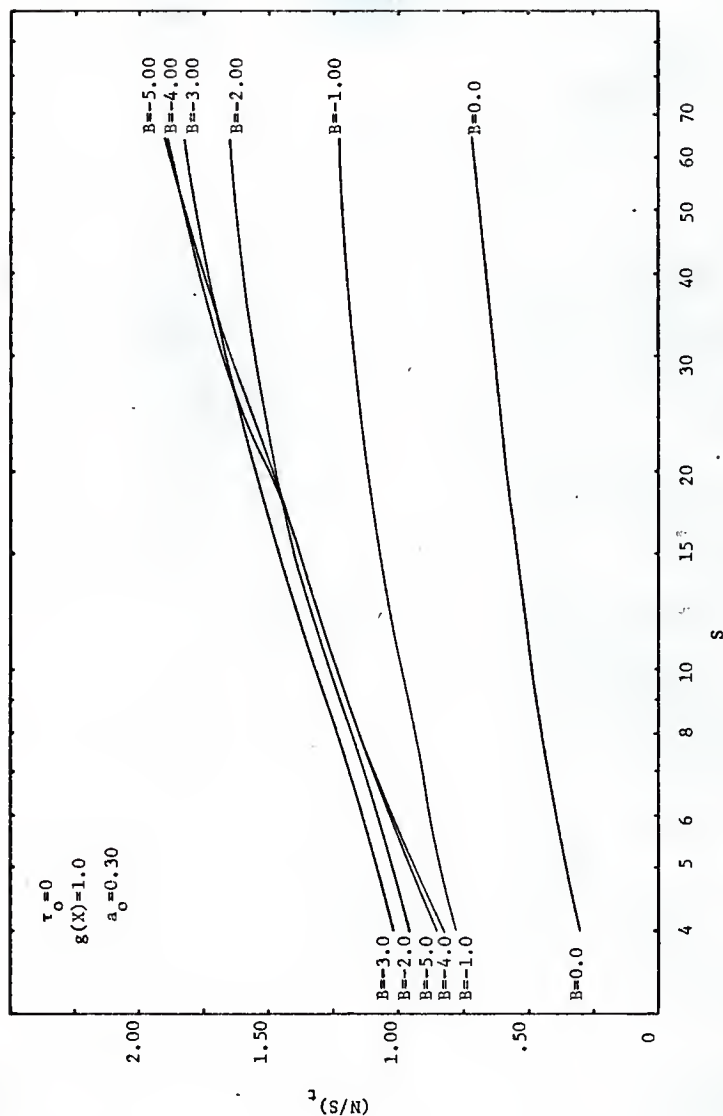


Fig. 55. Stability envelopes for positive sloped activity profiles with  $a_0 = 0.30$



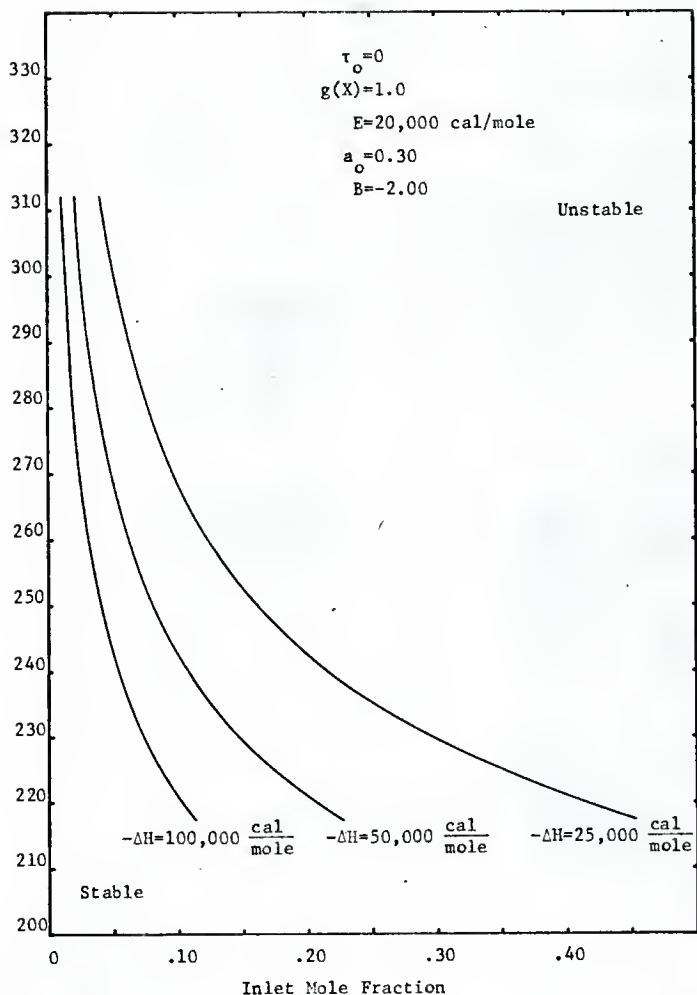


Fig. 56. Critical inlet temperature operating policy for  $B = -2.00$  and  $a_o = 0.30$

of the trial and error procedure in Section IV. Figure 57 shows the corresponding results for  $B=-4.00$  and  $a_0=0.30$ . Similar curves were constructed for all the other combinations of  $B$  and  $a_0$ , but have not been shown.

Using the results of the critical inlet temperature curves for a given inlet activity condition, the critical inlet temperatures were plotted as a function of  $B$  with the inlet mole fraction as a parameter. These are shown in Figure 58 for an inlet activity condition of 0.30 and a heat of reaction of 25,000 calories per mole. The points of intersection of these curves with the  $B_{calc}$  curve then define the critical inlet temperature operating policy for the given conditions of the inlet activity and heat of reaction. Similar figures were also constructed for the other combinations of the inlet activity and the heat of reaction, but are not shown. The curves in Figure 58 correspond to Steps 4 and 5 of the trial and error procedure.

The final critical inlet temperature operating policies were constructed using the points of intersection from Figure 58 and other similar figures. The operating policies are shown in Figures 59, 60 and 61 for heats of reaction of 25,000, 50,000 and 100,000 calories per mole. In these figures the critical inlet temperature has been plotted as a function of the inlet activity condition with the inlet mole fraction as a parameter.

In these figures it appears that the inlet temperature increase generally lies somewhere between an exponential and linear increase of the decreasing inlet activity. In Figure 59 the curve for an inlet mole fraction of 0.075 shows a considerably different behavior than the others because under the given conditions complete conversion of the reactant is attained

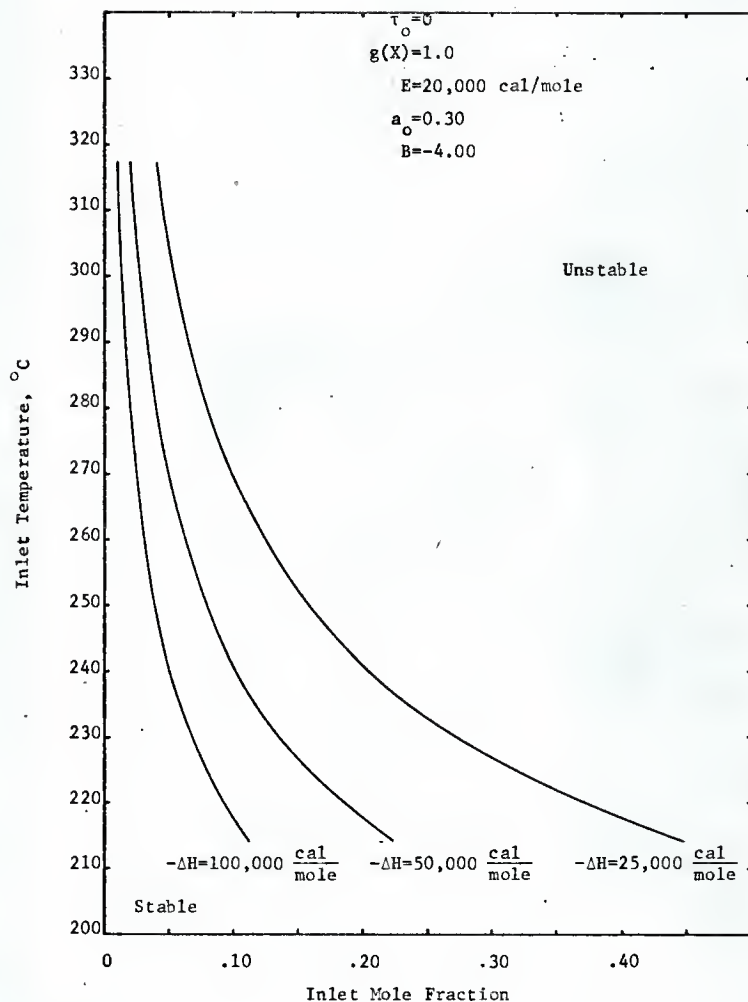


Fig. 57. Critical inlet temperature operating policy for  $B = -4.00$  and  $a_o = 0.30$

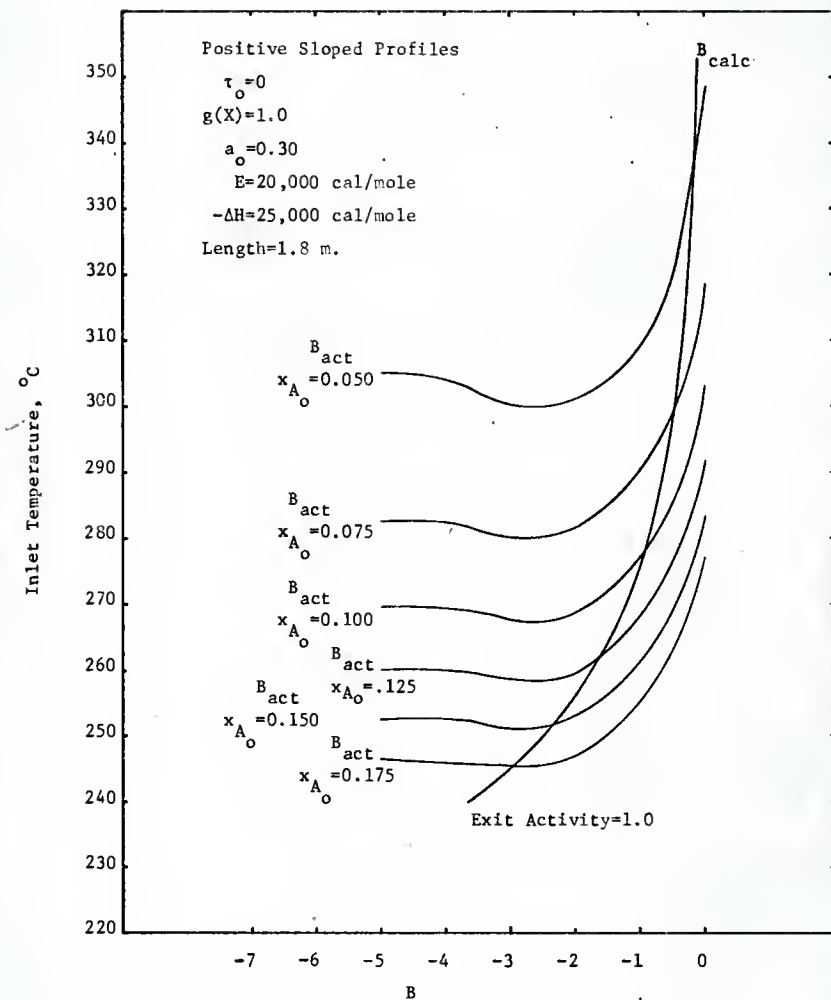


Fig. 58. Critical inlet temperature versus  $B_{act}$  and  $B_{calc}$  for  $a_o = 0.30$

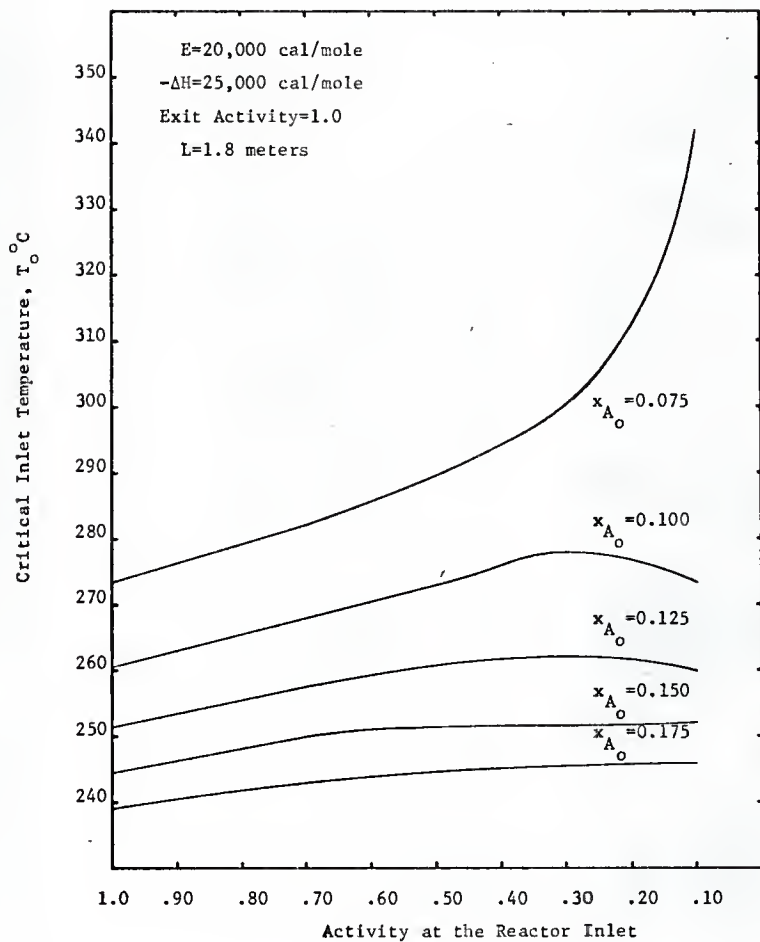


Fig. 59. Effect of the inlet activity condition on the critical inlet temperature for  $-\Delta H = 25,000$  cal/mole

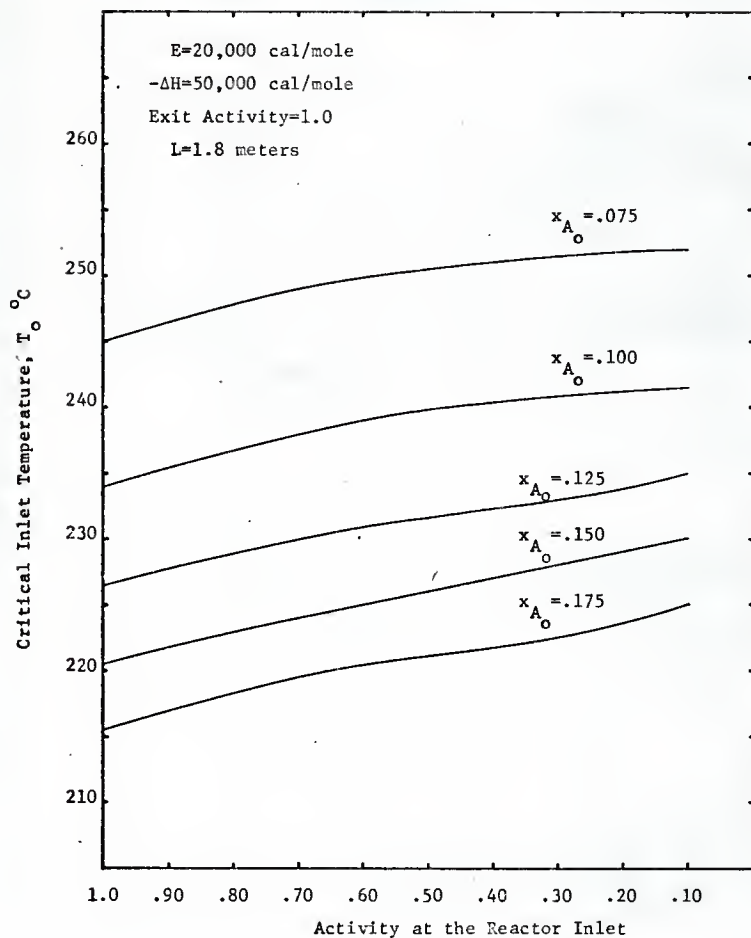


Fig. 60. Effect of the inlet activity condition on the critical inlet temperature for  $-\Delta H = 50,000$  cal/mole

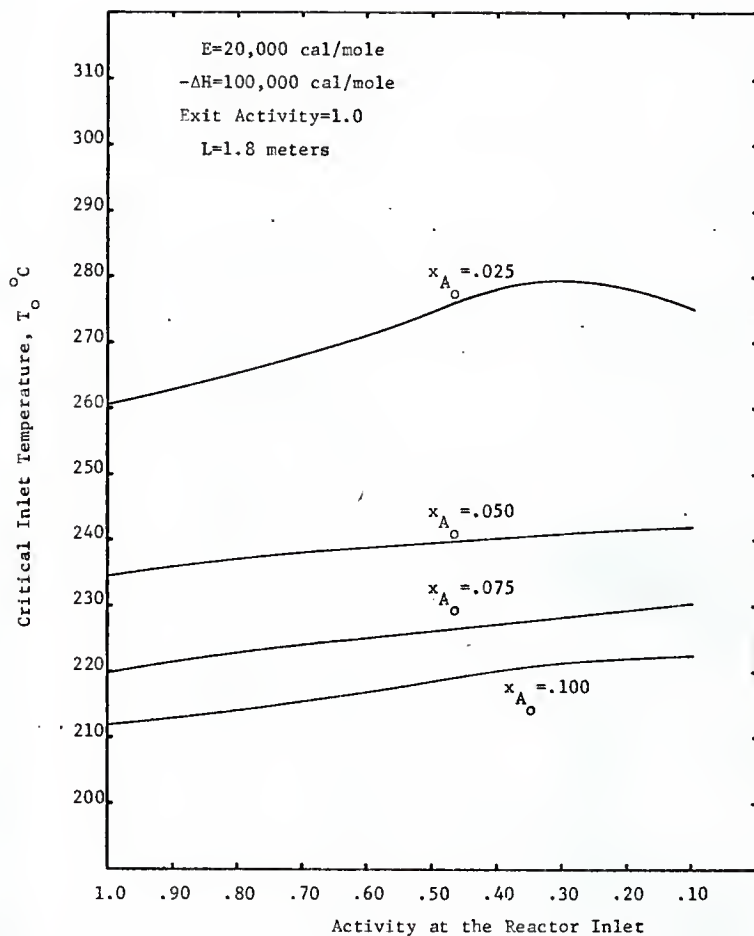


Fig. 61. Effect of the inlet activity condition on the critical inlet temperature for  $-\Delta H = 100,000$  cal/mole

before runaway can occur.

The operational policies were then applied to the example reactor system. Figures 62, 63 and 64 are typical temperature and conversion profiles which result from the operating policies for the indicated parameter combinations. Figures 63 and 64 in particular demonstrate the effect that the convex stability envelopes have on the operational policy. In Figure 64 the reaction rate is retarded at the reactor inlet to such a degree that no appreciable conversion takes place until near the exit. Both of the temperature profiles in Figures 63 and 64 increase continually until the reactor exit at  $\bar{z} = 600$  is reached. The temperature profile of Figure 64 also demonstrates another interesting point, that is, the temperature is beginning to increase very rapidly near the reactor exit. If the reactor was any longer the temperature might be expected to cause runaway because of this rapid increase. This type of behavior was observed in a number of cases with the inlet activity considerably less than unity. To further demonstrate this behavior and its effect on stability Figure 65 was plotted. Two things can be shown with this figure. First it shows that the stability criterion was able to predict the critical inlet temperature within a ten degree range of the actual value. Second it exemplified the above discussion in that the curve for  $T_0 = 255.5^\circ\text{C}$  could be treated as the critical profile for a reactor with a dimensionless length of approximately  $\bar{z} = 450$ . Any increase of reactor length would result in reactor runaway. It can be said then that temperature profiles of the type exhibited in Figure 64 are of an unstable nature, but reactor stability is maintained because the reacting mixture leaves the reactor before runaway can occur.

The conversions which were obtained at the reactor exit for the parameter



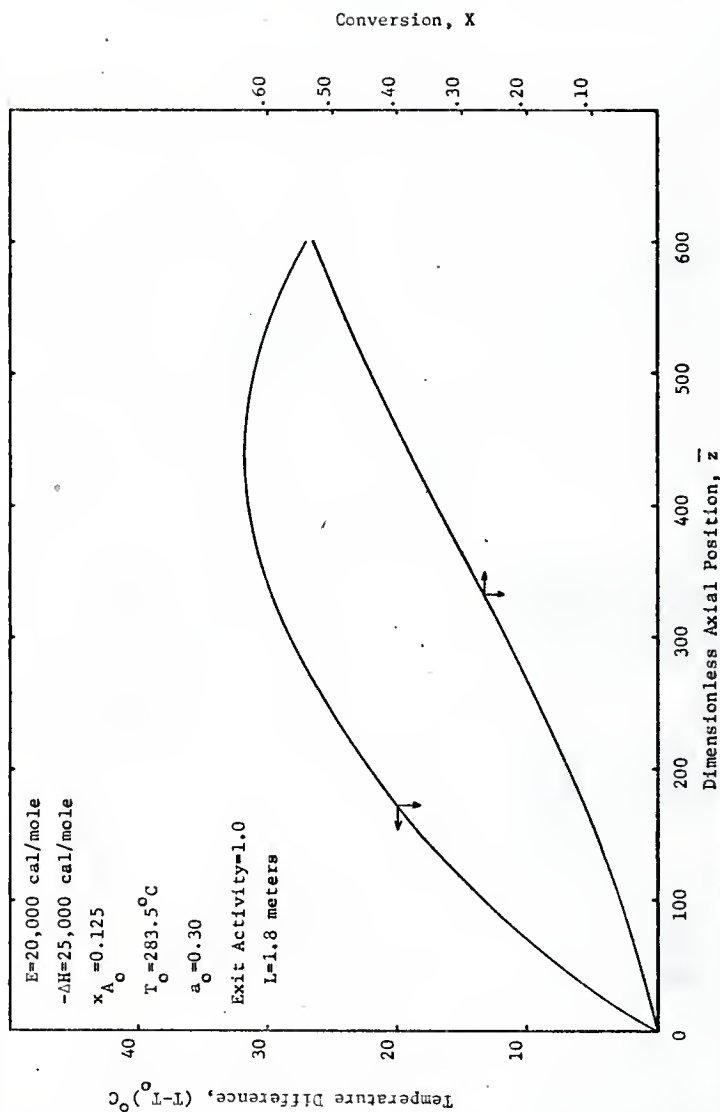


Fig. 62. Typical temperature and conversion profiles for  $a_0 = 0.30$

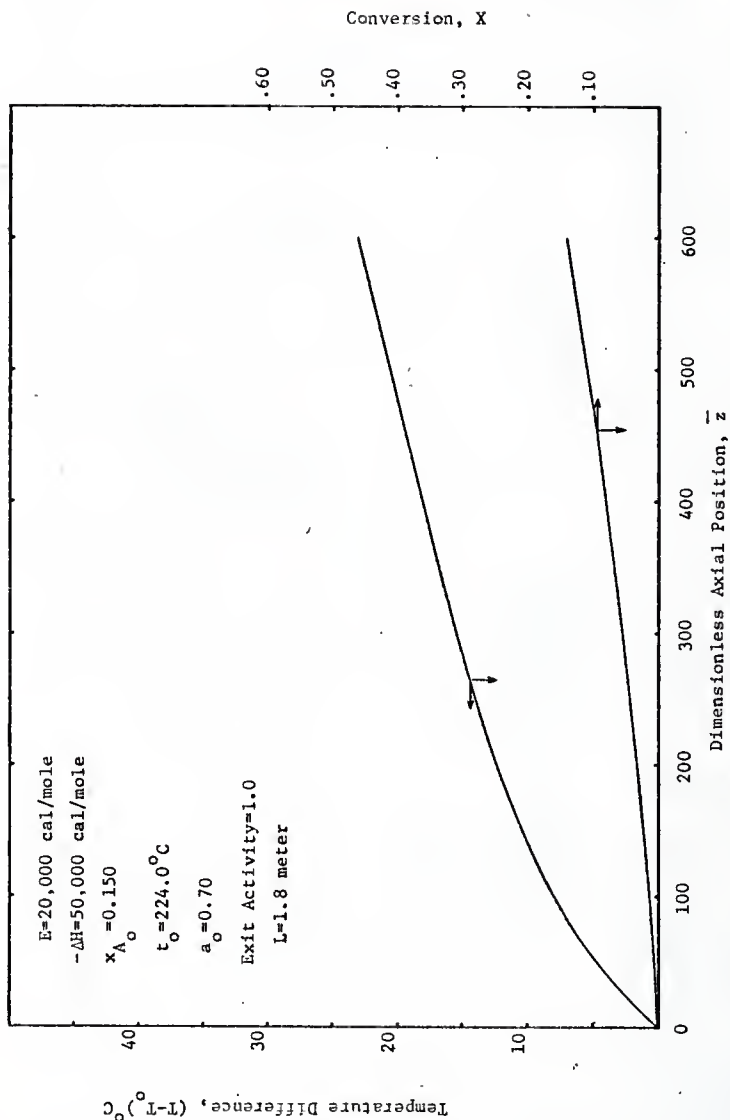


Fig. 63. Typical temperature and conversion profiles for  $a_0 = 0.70$

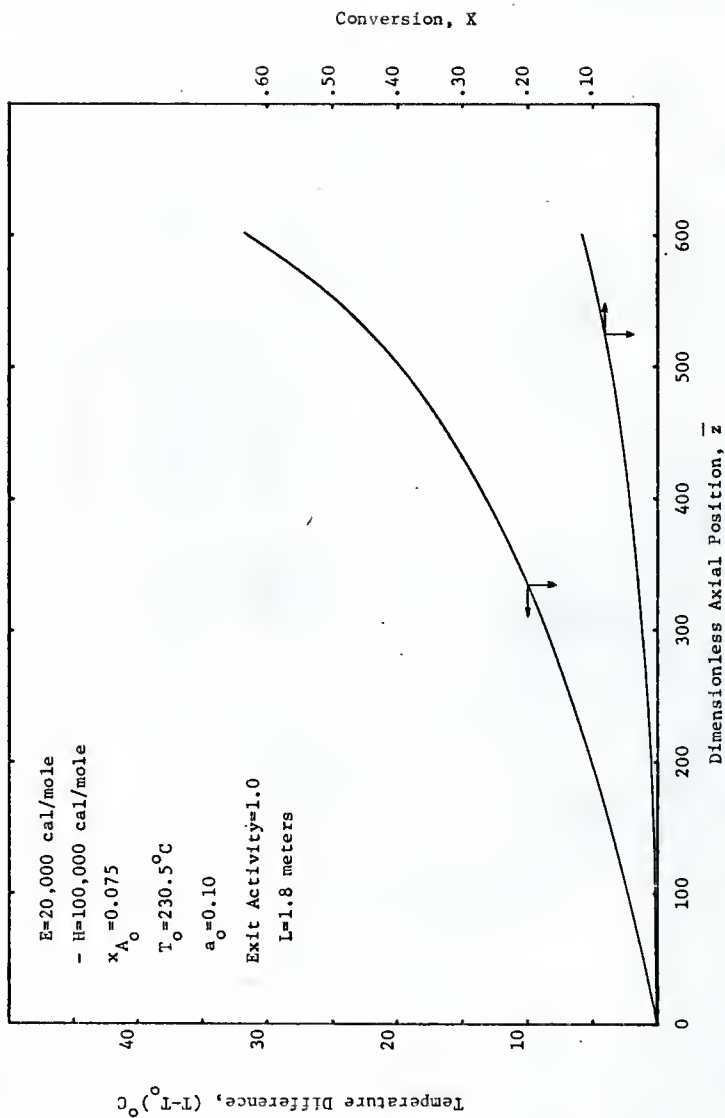


Fig. 64. Typical temperature and conversion profiles for  $a_0 = 0.10$

combinations investigated are shown in Figures 66, 67 and 68. It can be concluded from these figures that the operational policies could be used to maintain approximately the same level of conversion until poisoning has reduced the activity at the reactor inlet to somewhere between .70 and .50. When the inlet activity has dropped as low as 0.30 or 0.10 the reaction rate in the early parts of the reactor generally cannot be increased sufficiently to offset the deactivation without incurring reactor runaway.

Figure 66 exhibits curves with apparent optimum conversions. However, as in the uniform profile cases, it is felt there is not sufficient evidence available to warrant drawing conclusions concerning the possible optimum conditions.

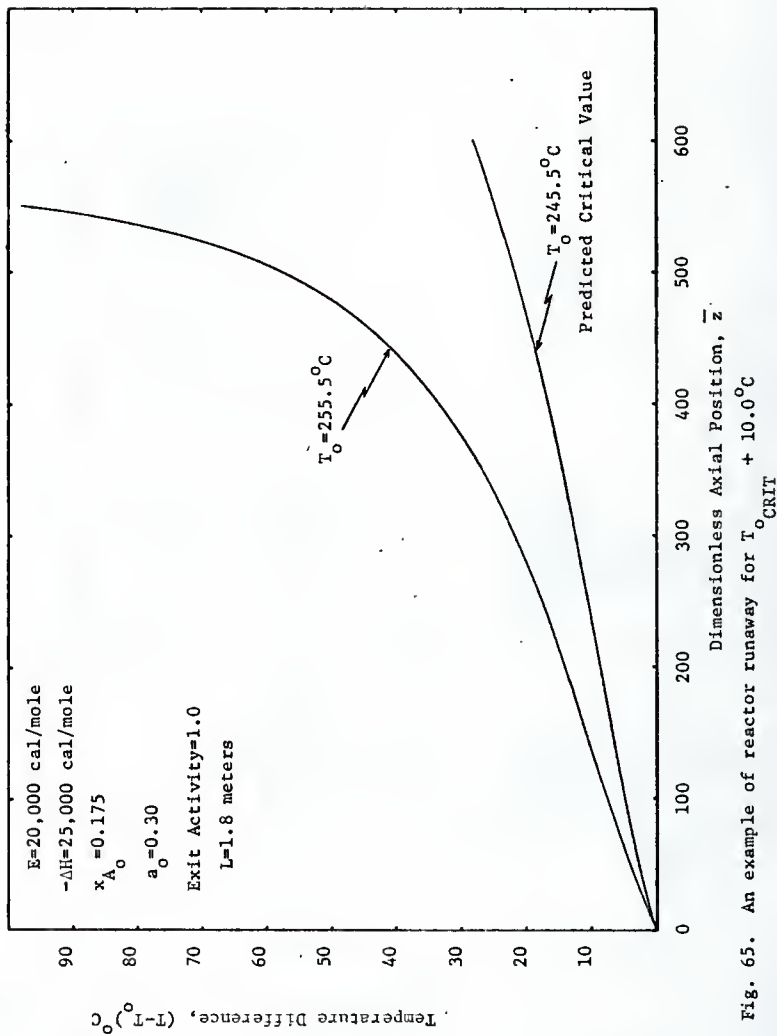


Fig. 65. An example of reactor runaway for  $T_{o,\text{CRIT}} + 10.0^\circ\text{C}$

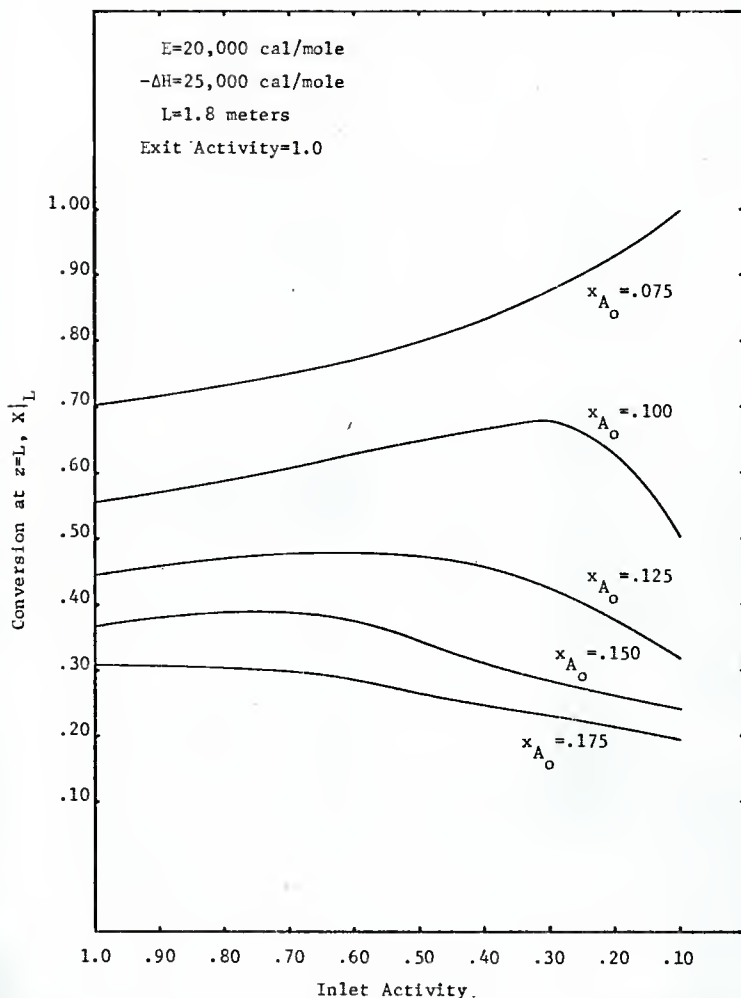


Fig. 66. Effect of the inlet activity condition on the conversion at  $z = L$  for  $-\Delta H = 25,000$  cal/mole

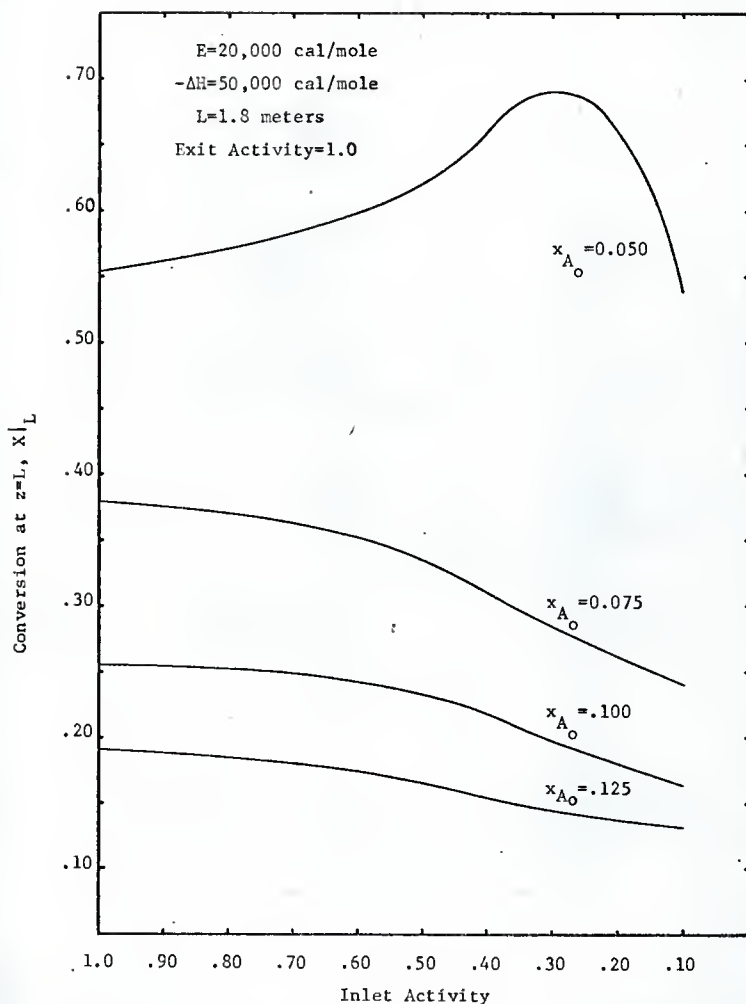


Fig. 67. Effect of the inlet activity condition on the conversion at  $z = L$  for  $-\Delta H = 50,000$  cal/mole

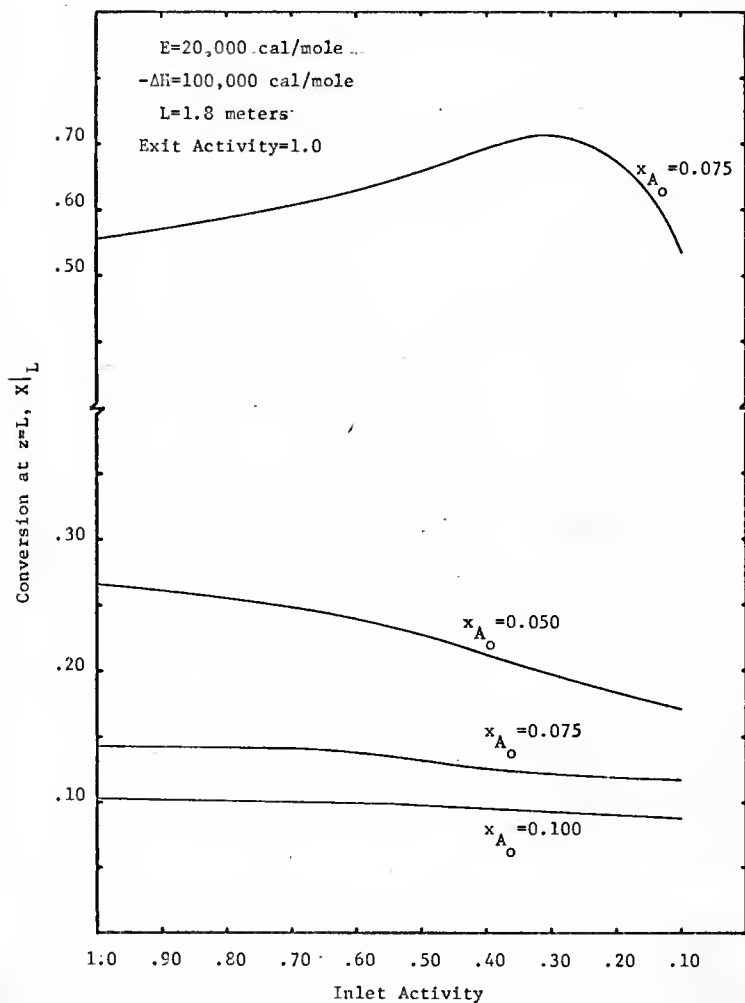


Fig. 68. Effect of the inlet activity condition on the conversion of  $z = L$  for  $-\Delta H = 100,000 \text{ cal/mole}$



## VI. Discussion of the Results

In the three previous sections the effect of activity on the inlet temperature operating policy, the temperature profiles, and the conversion for each of the three different types of activity profiles were presented. A comparison of the composite results can be employed to determine the effect that the type of activity profile has on the operating policy, the temperature profiles, and the conversion.

It can be assumed that the activity profiles result either from some form of poison deposition or from an artificially induced catalyst bed deactivation by using inerts in place of the catalyst particles (2,8).

It was shown for uniform activity profiles that the critical inlet temperature increases approximately exponentially with the catalyst deactivation. For the linear negative sloped activity profiles the critical inlet temperature increases linearly with the activity decrease at the reactor exit. The inlet temperature increase for the positive sloped activity profiles is also approximately linear, but with respect to the catalyst activity decrease at the reactor inlet. In Figure 69 the three inlet temperature policies were plotted as a function of the average catalyst activity in the reactor. For the two types of sloped profiles the rate of increase of the inlet temperature is considerably less than for the uniform activity profiles. The differences in the operating policies for the sloped profiles and the uniform profiles can be explained by the positioning of the catalyst particles having high relative activities. For negative sloped activity profiles the most active catalyst is concentrated near the reactor inlet. The critical inlet temperature cannot be increased as rapidly as for the uniform profiles because even as the exit activity condition decreases, the activity remains high in the early section of the reactor. Too rapid an

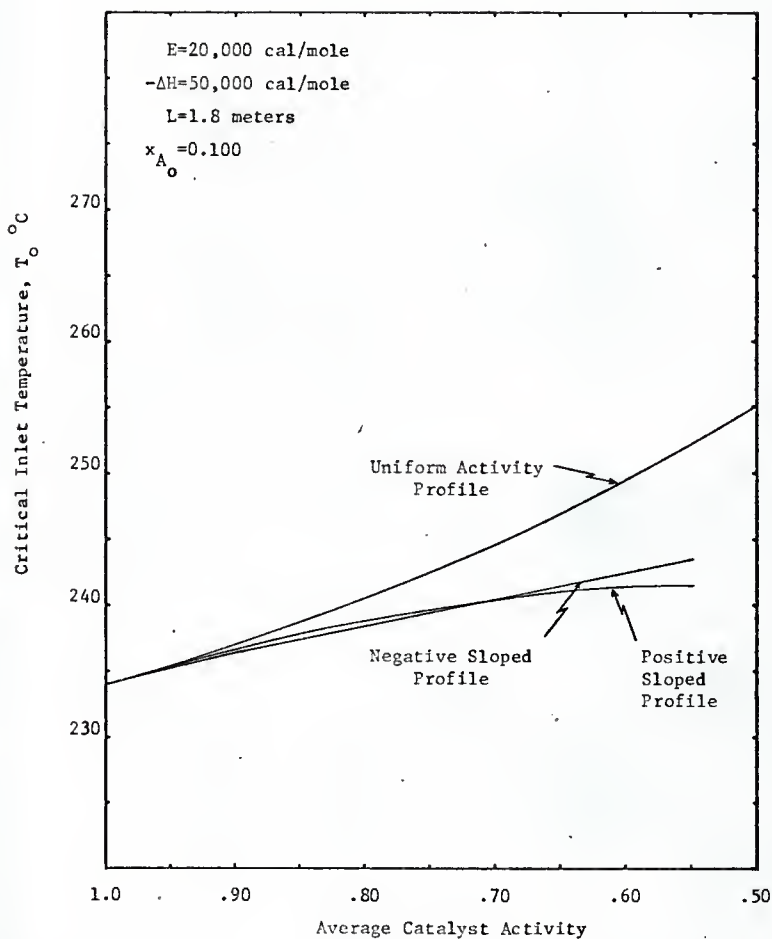


Fig. 69. Effect of the activity profile shape on the operating policy

increase in  $T_o$  would result in reactor runaway early in the reactor before it could be offset by the gradual decrease of activity along the reactor length.

A similar argument can be applied in the case of positive sloped profiles, but in a reverse order. In this case even as the inlet activity condition is decreased the activity near the exit remains high. Thus a rapid reaction rate at the reactor inlet must be sacrificed in order to maintain stability in the later sections of the catalyst bed.

In effect then, when sloped activity profiles are used a considerable portion of the catalyst bed is rendered inefficient in order to maintain stability. As the uniform activity profiles do not experience this effect the inlet temperature can be increased at a greater rate as the activity of the bed decreases.

As would be expected, the temperature and conversion profiles resulting from the example reactor system were greatly influenced by the type of activity profile which was used. If the axial position of the hotspot temperature is examined, it is found to depend significantly on the activity profile type. For the negative sloped profiles the hotspot occurs a short distance from the reactor inlet, the reason being readily apparent from the activity profile. Because the inlet activity is always unity, no matter what the exit condition, a rapid reaction rate occurs near the reactor inlet and then drops off rapidly as both the activity and the reactant concentration decrease.

For positive sloped activity profiles the axial position of the hotspot temperature, when it exists, is positioned near the reactor exit. In a number of cases it was forced completely out of the reactor. In the early sections of the reactor the reaction rate is retarded by the low activity

catalyst and a critical inlet temperature corresponding to an average activity considerably higher than the actual activity. Near the reactor exit, however, the reaction rate increases very rapidly, causing a similarly rapid temperature increase.

The axial positioning of the hotspot temperature for uniform activity profiles lies somewhere between the extremes corresponding to the sloped profiles. The temperature profiles are generally flatter because the influence of increasing or decreasing catalyst activity has been eliminated.

It is interesting to note that the maximum temperature differences,  $T_{\max} - T_0$ , which were observed are not noticeably affected by the shape of the activity profile. These temperature differences are limited by the stability criterion and would not be expected to show much dependence on the activity profile.

The axial conversion profiles are influenced in a manner similar to the temperature profiles. For negative sloped profiles the conversion increases more rapidly in the early sections of the reactor and then gradually levels off. For positive sloped profiles very little conversion occurs near the reactor inlet, but as the exit is approached it experiences a rapid increase. The conversion profiles for uniform activity fall somewhere between the two extremes.

The importance of the conversion, however, is its magnitude at the reactor exit and this magnitude is affected by the shape of the activity profile as shown in the three preceding sections. For both cases of sloped activity profiles using the critical inlet temperature operating policies, the conversion at the reactor exit decreases when the corresponding inlet or exit activity condition is much less than unity. These decreases are the result of two related principles, the stability limitation and the shape of

the temperature profiles imposed by the activity profiles. As discussed above, the stability limited operating policies for the inlet temperature is less than for uniform profiles. This was necessary to maintain reactor stability, but at the same time it produces inefficiency in sections of the catalyst bed where the activity is low. In the case of negative sloped profiles the temperature profiles drop off rapidly after experiencing a maximum early in the bed. This rapid decrease coupled with the low catalyst activity in the later bed sections results in little conversion in the last half of the reactor. For positive sloped profiles the first half of the reactor produces little conversion and the bulk of the reaction must take place near the reactor exit. The overall result is thus a loss of conversion at the reactor exit. For uniform activity profiles the temperature throughout the reactor is limited by the stability criterion, but there is no length effect to be considered with the activity. In these cases the temperature profile does not experience large regions of low temperatures. The temperature profile rises to a maximum, but the decrease after the hot-spot is quite slow. The average temperature over the length of the reactor is thus generally higher than when sloped activity profiles are used and this is reflected in higher conversions at the reactor exit.

In all the activity profiles used the critical inlet temperature predicted by the stability criterion was a conservative estimate of the actual critical value and generally was found to be within a 5 to 10°C range of the actual critical value. However, the values for the inlet temperatures should be considered as the best estimate of the actual critical values.

## VII. Conclusions

In conclusion a considerable amount of useful information concerning the influence of catalyst deactivation on reactor operation near the stability limit has been obtained.

A method was presented for developing an inlet temperature operating policy near the reactor runaway stability limit for catalyst beds experiencing deactivation. The method was shown to predict reasonable estimates of the critical inlet temperature within the limitations of a one-dimensional reactor model.

The operating policy developed for catalyst beds experiencing uniform deactivation showed that the inlet temperature could be increased sufficiently to maintain a comparable level of conversion and retain reactor stability. The operating policies for catalyst beds approximated by positive or negative sloped linear activity profiles showed that the inlet temperature could not be increased sufficiently to maintain a comparable level of conversion and still insure reactor stability. Thus it appears there would be no justification to artificially inducing either type of these profiles. However, further work needs to be completed in this area as the development of an optimum imposed activity profile still remains an important possibility.

## VIII. Nomenclature

The following nomenclature was used in the work of this thesis:

$A$  = reactor surface area per unit volume,  $m^2/m^3$

$a$  = relative catalyst activity, dimensionless

$B = \frac{mG}{k_e \gamma_{Tw}}$ , dimensionless parameter defined by Eqn 11.47

$B_1 = \frac{\rho_B d_p M_m}{G x_A}$ , dimensionless parameter defined by Eqn 11.36

$B_2 = \frac{1000(-\Delta H) d_p \rho_B}{G c_p}$ , dimensionless parameter defined by Eqn 11.37

$c_p$  = heat capacity of the fluid, cal./gm. $^{\circ}C$

$C$  = reactant concentration, for stability criterion, moles/ $m^3$

$C_A$  = concentration of reactant A, moles/ $cm^3$

$C_{A_0}$  = inlet concentration of reactant A, moles/ $cm^3$

$C_B$  = concentration of product B, moles/ $cm^3$

$C_O$  = inlet reactant concentration for stability criterion, moles/ $m^3$

$C_T$  = total concentration of entering stream, moles/ $cm^3$

$d_t$  = diameter of the reactor, m

$d_p$  = diameter of the catalyst particles, m

$E$  = activation energy, cal./mole

$F = \frac{4U d_p}{G c_p d_t}$ , dimensionless parameter defined by Eqn 11.38

$G$  = mass flow rate,  $\text{kg/m}^2\text{-hr.}$

$(-\Delta H)$  = heat of reaction,  $\text{cal./mole}$

$k$  = reaction rate constant in stability criterion,  $\text{moles/m}^3\text{-sec}$

$k_o$  = pre-exponential factor in stability criterion,  $\text{moles/m}^3\text{-sec}$

$k'$  = reaction rate constant in example model,  $\text{moles/(kgcat)-hr.}$

$k'_o$  = pre-exponential factor in example model,  $\text{moles/(kg-cat)-hr.}$

$L$  = length of the reactor,  $\text{m}$

$m$  = slope of the activity profile,  $\text{m}^{-1}$

$M_m$  = mean molecular weight,  $\text{gm/gm mole}$

$N = \frac{2U}{r_c k_e \gamma T_w}$ , dimensionless parameter defined by Eqn 11.6

$R'$  = gas law constant,  $\text{cal./gm mole-}^\circ\text{K}$

$R$  = reaction rate in stability criterion,  $\text{moles/m}^3\text{-hr.}$

$r$  = reactor radius,  $\text{m}$

$r_B$  = rate of formation of B,  $\text{moles/(kg cat)-hr.}$

$S = \frac{(-\Delta H) \gamma x_o}{c_p}$ , dimensionless parameter defined by Eqn 11.6

$T$  = fluid temperature,  $^\circ\text{C}$

$T_o$  = inlet fluid temperature,  $^\circ\text{C}$

$T_{\text{ref}}$  = reference temperature,  $^\circ\text{C}$



$T_w$  = reactor wall temperature,  $^{\circ}\text{C}$

$t = (T - T_w)$

$U$  = overall heat transfer coefficient,  $\text{kcal/m}^2\text{-hr-}^{\circ}\text{K}$

$V_z$  = axial fluid velocity,  $\text{m/hr.}$

$X$  = conversion of reactant A

$x_{A_0}$  = inlet mole fraction of reactant A

$x_0$  = inlet mole fraction of reactant in stability criterion

$z$  = axial direction

$\bar{z} = \frac{z}{d_p}$ , dimensionless axial direction

$f(C)$  = function of concentration in R.

$g(X)$  = function of concentration defined by Eqn 11.10 & 11.11

#### Greek Symbols:

$\alpha$  = reaction rate parameter in  $g(X)$  (see Table 2)

$\beta$  = reaction rate parameter in  $g(X)$  (see Table 2)

$\gamma$  = reaction rate parameter  $\approx \frac{E}{R'T_w^2}$

$\zeta$  = dimensionless length in stability criterion, Eqn 11.6

$\tau$  = dimensionless temperature in stability criterion, Eqn 11.6

$\rho_B$  = bulk catalyst density,  $\text{kg/m}^3$

$\rho_f$  = fluid density,  $\text{kg/m}^3$

Subscripts:

A = reactant A

A<sub>o</sub> = inlet condition with reference to A

B = product B

f = fluid

o = inlet condition

p = fluid or catalyst particle

t = reactor

w = wall

z = axial direction

## ACKNOWLEDGMENTS

The author wishes to express his sincere gratitude to Dr. John C. Matthews for his guidance and encouragement in this study. The author also wishes to thank his wife, Neva, for her efforts in typing the first draft of the thesis; NASA for its financial support; and the Kansas State University Computing Center for the aid of the IBM 360/50 computer.

## BIBLIOGRAPHY

1. Barkelew, C. H., "Stability of Chemical Reactors," Chem. Eng. Prog. Symposium Series, Vol. 55, No. 25, 37-46, (1959).
2. Froment, G. F., "Fixed Bed Catalytic Reactors - Current Design Status," I.&E.C., Vol. 59, 2, 18-27, (1967).
3. Van Heerden, C., "Autothermic Processes," I.&E.C., Vol. 45, 6, 1242-1247, (1953).
4. Wilhelm, R. H., Johnson, W. C., Acton, F. S., "Catalytic Converters," I.&E.C., Vol. 35, 5, 562-575, (1943).
5. Hoelscher, H. E., "Temperature Stability of Fixed-bed Catalytic Converters," Chem. Eng. Sci., Vol. 6, 183-189, (1957).
6. Froment, G. F., "Design of Fixed-bed Catalytic Reactors Based on Effective Transport Models," Chem. Eng. Sci., Vol. 17, 849-859, (1962).
7. Cullis, C. F., "Heterogeneous Catalytic Oxidation of Hydrocarbons," I.&E.C., Vol. 59, 12, 18-27, (1967).
8. Kominami, N., Shibata, A., Minekawa, S., "The Synthesis of Acrolein from Contact Oxidation - The Effect of Reacting Conditions," Kogyo Kagaku Fasshi, 65, 1510-1513, (1962).
9. Wilson, K. B., "Tubular Reactors, I," The Industrial Chemist, Feb., 93-100, (1947).
10. Boreskov, G. K., Slin'ko, M. G., "Simulation of Chemical Reactors," Theoretical Foundations of Chemical Engineering, Vol. 1, 1, 3-12, (1967).
11. Hlaváček, V., Marek, M., "Modelling of Chemical Reactors I," Collection Czechoslov. Chem. Commun., Vol. 32, 3291-3308, (1967).
12. Marek, M., Hlaváček, V., "Modelling of Chemical Reactors II," Collection Czechoslov. Chem. Commun., Vol. 32, 3309-3333, (1967).
13. Gee, R. E., Linton, W. H., Maier, R. E., Raines, J. W., "Use of Computers in Kinetic Calculations," Chem. Eng. Prog., Vol. 50, 10, 497-502, (1954).
14. Harriott, P., "Temperature Stability in Packed-Bed and Stirred Tank Reactors," Chem. Eng., 81-86, 5/29, (1961).
15. Bilous, O., Amundson, N. R., "Chemical Reactor Stability and Sensitivity," A.I.Ch.E. Journal, Vol. 1, 4, 513-521, (1955).

16. Bilous, O., Amundson, N. R., "Chemical Reactor Stability and Sensitivity, II," A.I.Ch.E. Journal, Vol. 2, 1, 117-126, (1956).
17. Liu, S. L., Amundson, N. R., "Stability of Adiabatic Packed Bed Reactors. An Elementary Treatment," I.&E.C. Fundamentals, Vol. 1, 3, 200-208, (1962).
18. Liu, S. L., Aris, R., Amundson, N. R., "Stability of Nonadiabatic Packed Bed Reactors," I.&E.C. Fundamentals, Vol. 2, 1, 13-20, (1963).
19. Liu, S. L., Amundson, N. R., "Stability of Adiabatic Packed-Bed Reactors," I.&E.C. Fundamentals, Vol. 2, 3, 183-189, (1963).
20. Butt, J. B., Rohan, D. M., "Analysis of Nonselective Poisoning and Its Influence on Reactor Behavior," Chem. Eng. Sci., Vol. 23, 489-501, (1968).
21. Padberg, G., Wicke, E., "Stabiles und instabiles Verhalten eines adiabatischen Rohrreaktors am Beispiel der katalytischen CO - Oxydation," Chem. Eng. Sci., Vol. 22, 7, 1035-1051, (1967).
22. Fraser, M. D., "Reactor Design by Analog Simulation," A.I.Ch.E. Meeting Presentation, Tampa, Florida, May 1968.
23. Beek, J., "Design of Packed Catalytic Reactors," Advances in Chemical Engineering, Vol. 3, 203-271, (1962).
24. Denbigh, K. G., Chemical Reactor Theory, Cambridge University Press, 1965.
25. Brian, P. L. T., Baddour, R. F., Eymery, J. P., "Transient Behavior of an Ammonia Synthesis Reactor," Chem. Eng. Sci., Vol. 20, 297-310, (1965).
26. Smith, J. M., Chemical Engineering Kinetics, McGraw-Hill, (1956).
27. Hill, F. B., Wilhelm, R. H., "Radiative and Conductive Heat Transfer in a Quiescent Gas-Solid Bed of Particles: Theory and Experiment," A.I.Ch.E. Journal, Vol. 5, 4, 486-495, (1959).
28. Schotte, W., "Thermal Conductivity of Packed Beds," A.I.Ch.E. Journal, Vol. 6, 1, 63-66, (1960).
29. Chen, J. C., Churchill, S. W., "Radiant Heat Transfer in Packed Beds," A.I.Ch.E. Journal, Vol. 9, 1, 35-41, (1963).
30. Moss, R. L., "The Structure and Activity of Heterogeneous Catalysts," The Chemical Engineer, No. 199, CE 114-CE141, June, (1968).
31. Emmett, P. H., Catalysis I - Fundamental Principles, Reinhold, (1954).

32. Alexander, W. A., Tollefson, E. L., "A Catalyst Mounting Technique for Close Temperature Control," The Canadian Journal of Chem. Eng., 346-348, Dec., (1965).
33. Hougen, O. A., Watson, K. M., Chemical Process Principles III Kinetics and Catalysis, Wiley, (1957).
34. Froment, G. F., Bischoff, K. B., "Non-Steady State Behavior of Fixed Bed Catalytic Reactors Due to Catalyst Fouling," Chem. Eng. Sci., Vol. 16, 189-201, (1961).
35. Frank-Kameneckij, D. A., Diffusion and Heat Exchange Chemical Kinetics, Princeton University Press, (1955).
36. Wen, C. Y., "Transient Activity and Replacement of Catalyst in Multi-stage Reactors," Canadian Journ. of Chem. Eng., 28-30, Feb. (1963).
37. Pozzi, A. L. and Rase, H. F., "Catalyst Fouling," I.&E.C., 1075-1080, Vol. 50, 7, (1958).

## XI. APPENDIX

## XI.1 Derivation of the Equations for the Modified Stability Criterion

For a one-dimensional steady state reactor model the differential material and energy balances can be given by the following equations:

$$\text{Material Balance: } G \frac{dc}{dz} = -R \quad 11.1$$

$$\text{Energy Balance: } c_p G \frac{dT}{dz} = (-\Delta H)R - AU(T - T_w) \quad 11.2$$

where  $R$  = reaction rate, moles/cm<sup>3</sup>-sec

$A$  = reactor surface area per unit volume

The reaction rate,  $R$ , can be defined as follows:

$$R = k_f(C)e^{\gamma T} \quad 11.3$$

This form is slightly different from the Arrhenius form and can be fitted to reaction-rate data almost as well. In Equation 11.3

$$\gamma \equiv E/R'T_w^2 \quad 11.4$$

$$k = k_o e^{-2\gamma T_w} \quad 11.5$$

The following transformations can now be defined:

$$C = C_o(1-X)$$

$$\tau = (T - T_w)\gamma$$

$$\zeta = \frac{z}{G/ke^{\gamma T_w}} \quad 11.6$$

$$N = \frac{2U}{rc_p ke^{\gamma T_w}}$$

$$S = \frac{(-\Delta H)C_o\gamma}{c_p}$$

with these transformations,

$$R = ax_o ke^{\gamma T_w(1-X)} g(X) e^{\tau} \quad 11.7$$

where  $x_o k$  has units of moles per cubic centimeter per second. Equations 11.1 and 11.2 then become

$$\frac{dX}{d\zeta} = \frac{ax_o ke^{\gamma T_w(1-X)} g(X) e^{\tau}}{x_o ke^{\gamma T_w}}$$

$$\frac{dX}{d\zeta} = a(1-X) g(X) e^{\tau} \quad 11.8$$

$$\frac{d\tau}{d\zeta} = \frac{\gamma(-\Delta H)x_o ke^{\gamma T_w(1-X)} g(X) e^{\tau} a}{c_p ke^{\gamma T_w}} - \frac{AU(T-T_w)\gamma}{c_p ke^{\gamma T_w}}$$

$$\frac{d\tau}{d\zeta} = Sa(1-X) g(X) e^{\tau} - N\tau \quad 11.9$$

where  $A$  has been set equal to  $2/r$ , its value for a tubular reactor. The function  $g(X)$  was introduced to allow for reactions which cannot be expressed as first-order reactions. The two forms for  $g(X)$  as suggested by Barkelew (1) are:

$$g(X) = (1+\alpha X) \quad 11.10$$

$$g(X) = (1+\beta X)^{-1} \quad 11.11$$

The length dependence in Equation 11.9 can be eliminated by multiplying by the reciprocal of Equation 11.8. This yields:

$$\frac{d\tau}{dX} = S - \frac{N\tau e^{-\tau}}{a(1-X)g(X)} \quad 11.12$$

$$\frac{d\zeta}{dX} = \frac{e^{-\tau}}{a(1-X)g(X)} \quad 11.13$$

Equation 11.12 can be used for the temperature stability study. If needed, the length corresponding to a particular  $\tau$  and  $X$  can be obtained from



Equation 11.13. The boundary conditions are:

$$\tau = 0$$

$$\text{at } X = 0$$

$$\zeta = 0$$

11.13a

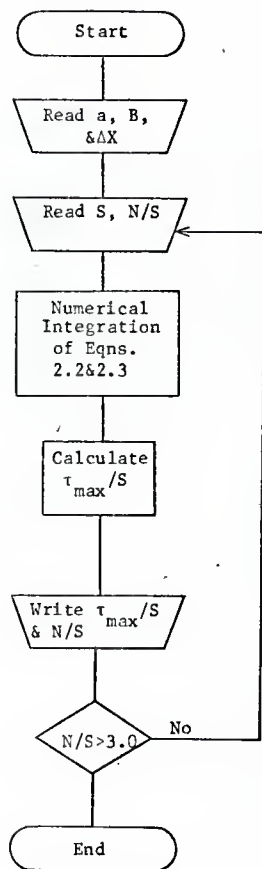


Fig. 70. Computer flow sheet for calculating the stability envelopes

## COMPUTER PROGRAM FOR CALCULATING THE STABILITY ENVELOPES

```

    DIMENSION FL(1500),X(1500),T(1500),A(1500)
1  FORMAT (3F10.5)
2  FORMAT (3F15.7)
3  FORMAT (1H0)
4  FORMAT (1H1)
5  FORMAT (3F10.3,3F14.4,F10.3,F12.4,F10.3)
6  FORMAT (7X,1HS,9X,1HN,7X,3HACT,9X,4HCONV,11X,3HTAU,
    114X,1HL,10X,3HN/S,7X,6HTMAX/S,3X,1HB)
8  FORMAT (I5,2F10.3)
9  FORMAT (5X,44HTHESE POINTS ARE FOR AN INLET VALUE OF
    1 AO = ,F8.5)
    READ (1,8) NN,DELX,AO
    WRITE (3,4)
    WRITE (3,3)
    WRITE (3,9) AO
    WRITE (3,3)
    WRITE (3,6)
    WRITE (3,3)
    K=1
10 CONTINUE
    READ (1,1) B,S,FN
    J=1
20 CONTINUE
    DO 25 I=1,NN
        FL(I)=0.0
        X(I)=0.0
        T(I)=0.0
        A(I)=0.0
25 CONTINUE
    I=1
    SN=FN/S
    A(1)=AO
30 CONTINUE
    DELL=(EXP(-T(I)))/((AO-B*FL(I))*(1.0-X(I))))*DELX
    DELT=(S-(FN*(T(I))*EXP(-T(I)))/((AO-B*FL(I))*(1.0-X(I))))*DELX
    FL(I+1)=FL(I)+DELL
    T(I+1)=T(I)+DELT
    X(I+1)=X(I)+DELT
    A(I+1)=AO-B*FL(I+1)
    IF (T(I+1)-T(I)) 51,40,40
40 CONTINUE
    IF (A(I+1)-1.000)45,45,55
45 CONTINUE

```

```

      I=I+1
      IF (I-NN) 50,55,55
50  CONTINUE
      GO TO 30
51  CONTINUE
      IF (J-2) 52,53,53
52  CONTINUE
      J=J+1
      GO TO 40
53  CONTINUE
      J=1
      TMOS=T(I)/S
      WRITE (3,5)S,FN,A(I),X(I),T(I),FL(I),SN,TMOS,B
      K=K+1
      I=I+1
55  CONTINUE
      TMOS=T(I)/S
      WRITE (3,5)S,FN,A(I),X(I),T(I),FL(I),SN,TMOS,B
      IF (K-35) 56,57,57
56  CONTINUE
      K=K+1
      GO TO 10
57  CONTINUE
      WRITE (3,4)
      WRITE (3,3)
      WRITE (3,9) A0
      WRITE (3,3)
      WRITE (3,6)
      WRITE (3,3)
      K=1
      GO TO 10
60  CONTINUE
      END

```

## XI.2 Equations for Determining the Stability Limited Inlet Temperature and Concentration

The critical values of the inlet temperature and concentration are determined from the semi-log plot of  $(N/S)_{\text{tang}}$  versus  $S$  in the following manner. The parameters  $N$  and  $S$  are the dimensionless groupings

$$N = \frac{2U}{rc_p k e^{\gamma T_w}} \quad 11.14$$

$$S = \frac{(-\Delta H)\gamma x_o}{c_p} \quad 11.15$$

By fixing values for all the variables except  $T_w$  and  $x_o$  in these two equations the critical values of  $T_w$  and  $x_o$  can be obtained. The steps are as follows:

1. Select a value for  $S$  and determine  $(N/S)_{\text{tang}}$  from the appropriate plot.
2. Fix the values for  $U$ ,  $r$ ,  $c_p$ ,  $E$ ,  $(-\Delta H)$ , and  $k$ .
3. Solve Equation 11.14 for  $T_w$ .
4. Solve Equation 11.15 for  $x_o$ .

Since it was assumed the inlet temperature was equal to the wall temperature, the desired results have been obtained.

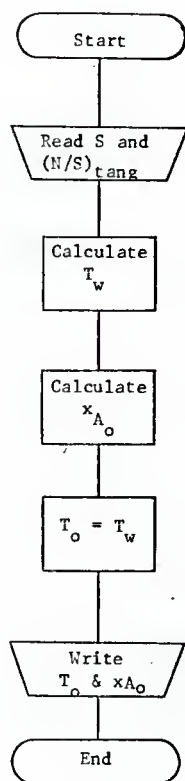


Fig. 71. Computer flow sheet for calculating the critical values of  $T_o$  and  $x_{A_o}$

COMPUTER PROGRAM FOR CALCULATING CRITICAL INLET TEMPERATURE AND MOLE FRACTIONS

```

1  FORMAT (2F10.2,F10.5)
4  FORMAT (F10.3,F9.5,F11.2,4F10.5)
6  FORMAT (20HUNIFORM ACTIVITY OF      ,F8.5)
7  FORMAT (F10.5)
   READ 7,AO
10 CONTINUE
   PUNCH 6,AO
15 CONTINUE
   READ 1, S,E,FNOS
   CF=7.38
   Q=25000.
   RPRIM=1.987
   FN=S*FNOS
   X=FN*(10.0**8.0)/(4.68*(5.00/1.80))
   FX=LOGF(X)
   TJ=(E/RPRIM)/FX
   TJC=TJ-273.00
   A=TJ*TJ
   CO1=(S*A*CF*RPRIM)/(Q*E)
   CO2=CO1/2.0
   CO3=CO2/2.0
   PUNCH 4,S,FNOS,E,TJC,CO1,CO2,CO3
20 CONTINUE
   GO TO 15
END

```

### X1.3 Derivation of the Equations for the Example Reactor System

For the first-order reaction



$r_B$ , the rate of formation of product B, has the units moles/(kg.cat)-hr and can be defined as follows:

$$r_B = \frac{1}{\rho_B} \frac{dC_B}{dt} \quad 11.16$$

where

$$\frac{dC_B}{dt} = k a C_A \quad 11.17$$

Using the definition of X,

$$X = \frac{C_{A_0} - C_A}{C_{A_0}} \quad 11.18$$

$r_B$  then becomes,

$$r_B = \frac{1}{\rho_B} k a C_{A_0} (1-X) \quad 11.19$$

Multiplication and division by the total concentration of the entering stream yields,

$$r_B = \frac{1}{\rho_B} C_T k a x_{A_0} (1-X) \quad 11.20$$

where  $x_{A_0}$  is the inlet mole fraction of reactant A.

Equation 11.20 can be written more conveniently as

$$r_B = k' a x_{A_0} (1-X) \quad 11.21$$

where

$$k' = \frac{1}{\rho_B} C_T k \quad 11.22$$



The Arrhenius equation then becomes

$$k' = k'_o \exp(-E/R'T) \quad 11.23$$

where

$$k'_o = \frac{1}{\rho_B} C_T k_o \quad 11.24$$

The steady-state molar balance for product B in a differential volume of the reactor can be written as follows

$$\left. \frac{\pi d_t^2}{4} \frac{G}{Mm} x_{A_o} X \right|_z - \left. \frac{\pi d_t^2}{4} \frac{G}{Mm} x_{A_o} X \right|_{z+\Delta z} + r_B \rho_B \frac{\pi d_t^2}{4} \Delta z = 0 \quad 11.25$$

where

$$G = \rho_f V_z \quad 11.26$$

Division by  $\pi d_t^2 \Delta z / 4$  and taking the limit as  $\Delta z$  goes to zero gives:

$$\frac{dX}{dz} = \frac{\rho_B Mm}{x_{A_o} G} r_B \quad 11.27$$

In a similar manner the steady-state energy balance on the differential reactor volume can be written as:

$$\left. \frac{\pi d_t^2}{4} G_c p (T - T_{ref}) \right|_z - \left. \frac{\pi d_t^2}{4} G_c p (T - T_{ref}) \right|_{z+\Delta z} - \pi d_t \Delta z U (T - T_w) + \frac{\pi d_t^2}{4} \rho_B r_B (-\Delta H) \Delta z = 0 \quad 11.28$$

where  $T_w$  is assumed constant over the length of the reactor.

Division by  $\pi d_t^2 \Delta z / 4$  and taking the limit as  $\Delta z$  goes to zero gives,

$$\frac{dT}{dz} = \frac{\rho_B (-\Delta H)}{G_c p} r_B - \frac{4U}{d_t G_c p} (T - T_w) \quad 11.29$$

Defining

$$t = T - T_w$$

then yields the following equation,

$$\frac{dt}{dz} = \frac{\rho_B (-\Delta H)}{Gc_p} r_B - \frac{4U}{d_t Gc_p} t \quad 11.30$$

Equations 11.27 and 11.30 can be made dimensionless by introducing the transformation

$$\bar{z} = \frac{z}{d_p} \quad 11.31$$

The dimensionless equations are

$$\frac{dX}{d\bar{z}} = \frac{\rho_B d_p M_m}{Gx_{A_o}} r_B \quad 11.32$$

$$\frac{dt}{d\bar{z}} = \frac{d_p \rho_B (-\Delta H)}{Gc_p} r_B - \frac{4U d_p}{d_t Gc_p} t \quad 11.33$$

The final form of the two equations is more conveniently written as

$$\frac{dX}{d\bar{z}} = B_1 r_B \quad 11.34$$

$$\frac{dt}{d\bar{z}} = B_2 r_B - (F)(t) \quad 11.35$$

where

$$B_1 = \frac{\rho_B d_p M_m}{Gx_{A_o}} \quad 11.36$$

$$B_2 = \frac{(1000.0) (-\Delta H) d_p \rho_B}{Gc_p} \quad 11.37$$

$$F = \frac{4Ud_p}{d_t Gc_p} \quad 11.38$$

Equations 11.34 through 11.38 correspond to equations 2.5 through 2.9 in Section II.5. The factor of 1000.0 in Equation 11.37 is an adjustment necessary for consistent units.

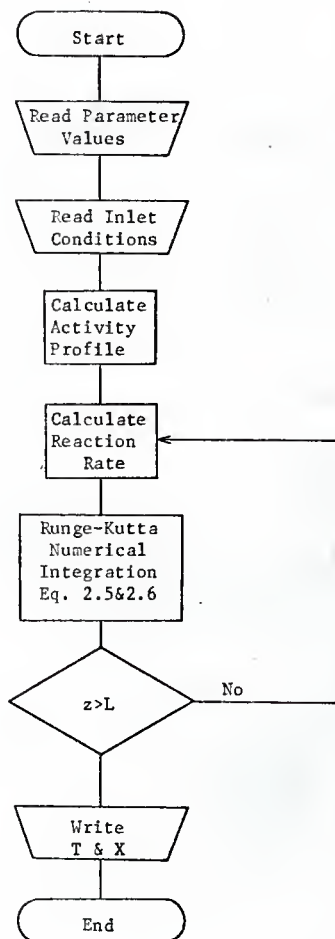


Fig. 72. Computer flow sheet for the example reactor system

## COMPUTER PROGRAM FOR THE EXAMPLE REACTOR SYSTEM

```

    DIMENSION Z(805),XX(805),TT(805),AT(805),A(805),Y(805)
1  FORMAT(3X,1H1,3X,12HDIMEN LENGTH,5X,8HACTIVITY,8X,4HCO
    1NV,9X,7HFLUID T,9X,6HWALL T,9X,4HCONV)
2  FORMAT (3F10.5)
3  FORMAT (15,5E15.5,F10.5)
5  FORMAT (1H0)
6  FORMAT (1H1)
7  FORMAT (F10.2,4F10.5)
9  FORMAT (2F10.5)
11 FORMAT(5X,7HPREX = ,F10.5,5X,4HU = ,F10.5,5X,5HDZ = ,F10.5)
12 FORMAT(5X,7HRHOB = ,F10.5,5X,5HDP = ,F10.5,5X,5HDT = ,F10.5)
13 FORMAT(5X,7HMW.W. = ,F10.5,5X,9HHT CAP = ,F10.5,5X,12HFLO
    1 RATE = , F10.5)
14 FORMAT(5X,5HAO = ,F10.5,5X,5HAF = ,F10.5,5X,4HH = ,F10.3,
    1 5X,4HE = ,F10.3)
15 FORMAT(5X,13HINLET TEMP = ,F10.5,5X,12HWALL TEMP = ,F10.5,
    1 5X,18HINLET MOLE FRAC = ,F10.5)
    READ (1,2) PREX,U,H
    READ (1,2) RHOB,DP,DT
    READ (1,2) FMM,CP,PI
    READ (1,9) G,DZ
8  CONTINUE
    READ (1,7) E,AA,AF,FNAO,TO
    K=1
    M=1
    B1=(RHOB*DP*FMM)/(G*FNAO)
    B2=(DP*RHOB*H*1000.)/(G*CP)
    FM=(4.0*U*DP)/(DT*G*CP)
    TW=TO
25 CONTINUE
    ASLOP= (AA-AF)/600.0
    DO 20 I=1,200
        Z(I)=0.0
        XX(I)=0.0
        TT(I)=0.0
        AT(I)=0.0
        Y(I)=0.0
        A(I)=AA-ASLOP*Z(I)
20 CONTINUE
    WRITE (3,6)
    WRITE (3,5)
    WRITE (3,11) PREX,U,DZ
    WRITE (3,12) RHOB,DP,DT
    WRITE (3,13) FMM,CP,G
    WRITE (3,14) AA,AF,H,E
    WRITE (3,15) TO,TW,FNAO
    WRITE (3,5)
    WRITE (3,1)
    WRITE (3,5)

```

```

I=1
TT(1)= TO-TW
30 CONTINUE
T=TT(I)
X=XX(I)
J=0
35 CONTINUE
J=J+1
TTT=T+TW+273.
FLN1=-(E/(1.98*(TTT)))+PREX
FKK1=EXP(FLN1)
RB=FKK1*FNA0*(1.0-X)
GO TO (40,41,42,43),J
C RUNGE-KUTTA NUMERICAL INTEGRATION
40 FK1=B1*A(I)*RB*DZ
FL1=(B2*A(I)*RB-FM*T)*DZ
X=XX(I)+FK1/2.0
T=TT(I)+FL1/2.0
GO TO 35
41 FK2= B1*A(I)*RB*DZ
FL2=(B2*A(I)*RB-FM*T)*DZ
X=XX(I)+FK2/2.0
T=TT(I)+FL2/2.0
GO TO 35
42 FK3= B1*A(I)*RB*DZ
FL3=(B2*Z(I)*RB-FM*T)*DZ
X=XX(I)+FK3
T=TT(I)+FL3
GO TO 35
43 FK4=B1*A(I)*RB*DZ
FL4=(B2*A(I)*RB-FM*T)*DZ
DXX=(1./6.)*(FK1+2.0*FK2+2.0*FK3+FK4)
DTT=(1./6.)*(FL1+2.0*FL2+2.0*FL3+FL4)
XX(I+1)=XX(I)+DXX
TT(I+1)=TT(I)+DTT
AT(I+1)=TT(I+1)+TW-TO
Y(I+1)=XX(I+1)
Z(I+1)=Z(I)+DZ
I=I+1
A(I)=AA-ASLOP*Z(I)
IF (M-5) 60,61,61
61 WRITE (3,3) I,Z(I),A(I),XX(I),TT(I),AT(I),Y(I)
M=M+1
60 CONTINUE
M=M+1
IF (I-161) 45,45,50
45 CONTINUE
GO TO 30
50 CONTINUE
53 CONTINUE
GO TO 8
70 CONTINUE
END

```

#### XI.4 Derivation of the Stability Criterion Equations for Linear Catalyst Activity Profiles

The steady-state mass and energy balance equations are:

$$G \frac{dc}{dz} = -R \quad 11.39$$

$$c_p G \frac{dT}{dz} = (-\Delta H)R - AU(T - T_w) \quad 11.40$$

The transformations given by Equation 11.6 can be used with

$$R = x_0 k e^{\gamma T_w (1-X)} g(X) a(z) \quad 11.41$$

to transform Equations 11.39 and 11.40 into

$$\frac{d\zeta}{dX} = \frac{e^{-\tau}}{(1-X)a(z)} \quad 11.42$$

$$\frac{d\tau}{dX} = S - \frac{N\tau e^{-\tau}}{(1-X)a(z)} \quad 11.43$$

In these equations  $g(X)=1$  corresponding to a first-order reaction. The inlet conditions are

$$\begin{aligned} \tau &= 0 \\ \zeta &= 0 \end{aligned} \quad \text{at } X = 0 \quad 11.43a$$

The catalyst activity is now a function of the reactor length. For a linear profile

$$a(z) = a_0 - mz \quad 11.44$$

where  $a_0$  is the activity at the reactor inlet and  $m$  is the slope of the linear profile. In dimensionless form Equation 11.44 becomes

$$a(\zeta) = a_0 - \frac{mG}{k e^{\gamma T_w}} \zeta \quad 11.45$$

or

$$a(\zeta) = a_o - B\zeta \quad 11.46$$

where

$$B = \frac{mG}{k_e \gamma T_w} \quad 11.47$$

is a dimensionless parameter. Equations 11.42 and 11.43 then become

$$\frac{d\zeta}{dX} = \frac{e^{-\tau}}{(1-X)(a_o - B\zeta)} \quad 11.48$$

$$\frac{d\tau}{dX} = S - \frac{Nre^{-\tau}}{(1-X)(a_o - B\zeta)} \quad 11.49$$

Equations 11.48 and 11.49 must be integrated simultaneously because of the coupling introduced by the length dependence of the activity. In addition B is a new parameter which must be varied in conjunction with N and S. B cannot be calculated since  $T_w$  is not known. The case where the activity was assumed to be uniform throughout the reactor bed is a specific case of this general form where  $B=0$ .

Since there are three parameters to vary, a slightly different procedure was necessary to determine the critical values of the inlet temperature and inlet mole fraction. The procedure can be outlined as follows:

1. Construct "stability envelopes" for several values of B.
2. Plot the  $(N/S)_{\text{tang}}$  versus S curves for each value of B.
3. From the plots of Step 2 calculate and plot the values of the critical inlet temperature versus the critical inlet concentration.
4. Plot the inlet temperature versus B with the inlet concentration as a parameter.
5. For the desired activity slope, m, in Equation 11.47, a value can be calculated for B as a function of the inlet temperature.



6. Plot the values for B calculated in Step 5 on the plot of Step 4. The point of intersection of the two curves is then the desired critical value of B, inlet temperature, and inlet mole fraction.

The introduction of the additional parameter greatly increases the amount of work required to obtain the critical  $T_o$  and  $x_{A_o}$  values.

It is also possible to treat other forms of the activity profile in a similar manner.

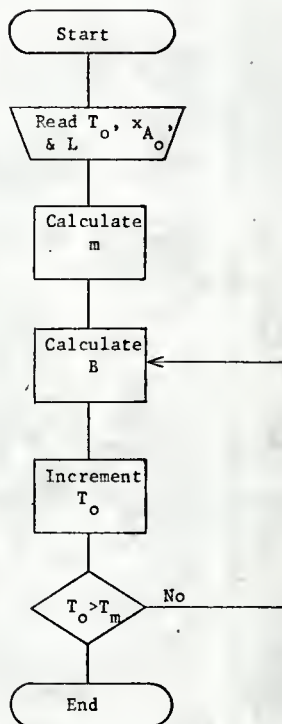


Fig. 73. Computer flow sheet for determining the value of the parameter  $B$

## COMPUTER PROGRAM FOR DETERMINING THE VALUE OF PARAMETER B

```

1  FORMAT (3F10.3)
2  FORMAT (5F10.5)
5  FORMAT (5X,4HG = ,E12.5,15HMOLES/SQ CM SEC)
6  FORMAT (5X,10HK PRIME = ,F10.3,16HMOLES/CUB CM SEC)
7  FORMAT (5X,9HLENGTH = ,F10.3,2HCM)
8  FORMAT (2F7.3,2F10.2,F10.4,F10.3,F8.2,F10.4)
9  FORMAT (2F15.2,F15.5)
10 CONTINUE
    READ 1,G1,FKP,FL
    READ 9,E,H,R
    AMW=29.48
    C=(G1*1000.)/(AMW*3600.*10000.)
15 CONTINUE
    PUNCH 5,G
    PUNCH 6,FKP
    PUNCH 7,FL
20 CONTINUE
    READ 2,AO,AF,XAO,TO,BA
    FM=(AO-AF)/FL
    TTT=TO+273.0
    GAMMA=-E/(R*TTT)
    BC=(FM*G)/(FKP*EXP(GAMMA)) ,
    PUNCH 8,AO,AF,H,E,XAO,TO,BA,BC
25 CONTINUE
    GO TO 20
END

```

THE EFFECT OF CATALYST ACTIVITY ON  
STABILITY LIMITED PACKED BED REACTORS

by

KERRY FRED WILLIAMS

B. S., Kansas State University, 1966

---

AN ABSTRACT OF A MASTER'S THESIS

submitted in partial fulfillment of the

requirements for the degree

MASTER OF SCIENCE

Department of Chemical Engineering

KANSAS STATE UNIVERSITY  
Manhattan, Kansas

1969

## ABSTRACT

In this thesis a method is presented for determining the stability limited inlet temperature operating policy for a packed tubular reactor experiencing catalyst deactivation. The catalyst deactivation can be considered to be the result of poison deposition or as having been induced by artificial means. Three types of axial activity profiles were considered: uniform activity throughout the bed, negative sloped activity profiles, and positive sloped activity profiles. An operating policy was determined for each of these. An example reactor system was used to investigate the operating policies and determine the effect which catalyst deactivation has on the conversion at the reactor exit and the axial temperature profiles within the reactor. The operating policies and typical conversion and temperature results are presented graphically.